12-2016

The Durability of Single, Dual, and Multiphase Titanate Ceramic Waste Forms for Nuclear Waste Immobilization

Devin H. Harkins
Clemson University

THE DURABILITY OF SINGLE, DUAL, AND MULTIPHASE TITANATE CERAMIC WASTE FORMS FOR NUCLEAR WASTE IMMOBILIZATION

A Thesis
Presented to
the Graduate School of
Clemson University

In Partial Fulfillment
of the Requirements for the Degree
Master of Science
Materials Science & Engineering

---

by
Devin J. H. Harkins
December 2016

Accepted by:
Dr. Kyle S. Brinkman, Committee Chair
Dr. Marian S. Kennedy
Dr. Fei Peng

ABSTRACT

A significant amount of the energy used in the United States comes from nuclear power, which produces a large amount of waste materials. Recycling nuclear waste is possible, but requires a way to permanently fix the unusable radionuclides remaining from the recycling process in a stable, leach resistant structure. Multiphase titanate ceramic waste forms are one promising option under consideration. However, there is insufficient work on the long term corrosion of the individual phases, as well as the multiphase systems of these ceramics.

These multiphase titanate ceramic waste forms have three targeted phases: hollandite, pyrochlore, and zirconolite. Hollandite is a promising candidate for the incorporation of Cs, while pyrochlore is readily formed with lanthanides, such as Nd, the most prevalent lanthanide in the waste stream. The third targeted phase, zirconolite, is for the incorporation of zirconium and the actinides. This work looks into the formation of single phase systems of lanthanide titanates, formation of dual phase systems of Ga doped Ba hollandites and Nd titanate, durability of single phase hollandites and multiphase model systems using Vapor Hydration Testing (ASTM C 1663-09), dissolution of dual phase systems of Ga doped Ba hollandites and Nd titanate using Product Consistency Testing (ASTM C 1285-02), as well investigating how grain size affects amount of alterative phases formed using Vapor Hydration Testing.

The dual phase systems of hollandites and Nd titanate show significant amounts of secondary phases forming, heavily influenced by the composition of hollandite used in the systems. The most significant phase present was $BaNd_2Ti_5O_{14}$. This phase proves to be problematic due to the degradation to the hollandite structure.

Using Vapor Hydration Testing to investigate single and multiphase systems presented many some possible alteration phases that could occur in the long term aging of these ceramics. Most notably, Cs rich phases were found in nearly every system, meaning that different hollandites produced similar phases.

Using Product Consistency Testing to investigate dissolution in dual phase systems of hollandites and Nd titanate led to the conclusion that as the volume fraction of hollandite increases, so does the stability of the hollandite in the systems.

ACKNOWLEDGEMENTS

While the completion of this thesis resulted from my own work and dedication over the past two years, it was enabled through the support of many people who need to be acknowledged.

I would like to begin by first thanking my advisor, Dr. Kyle S. Brinkman, for sharing his knowledge and providing guidance over the last two years. You were always kind and patient, while also knowing how to motivate me when needed. For that, I will always be thankful.

In addition to my advisor, I must also acknowledge my committee members Dr. Marian (Molly) S. Kennedy and Dr. Fei Peng. Dr. Kennedy always pushed me to do my best and to also better myself, in both my undergraduate and graduate careers*. I will always be grateful for your guidance and encouragement*. Dr. Fei Peng was both an outstanding teacher and provided great technical suggestions for my research path. *I will always be thankful to you Dr. Peng*.

I would next like to acknowledge all my past and present research group members who I had the pleasure of working with and getting to know. They included Dr. Siwei Wang, Dr. Yun Xu, Dr. Cong Ren, Dr. Tao Hong, Mr. Robert Grote, Mr. Mingyang Zhao, and Mr.Changlong Li. To this group: *I am thankful for the time I had with each and every one of you.*

I need to acknowledge Dr. Jake Amoroso and the rest of our collaborators at Savannah River National Laboratory for their guidance, access to characterization equipment and fabrication of the melted multiphase samples. I would also like to thank Ms. Yamei Liu, and her advisor Dr. Jian He, for help with Spark Plasma Sintering samples. Thanks to Dr. Ramesh Chandra Biswal for help with densification of dual phase samples. Thanks to AMRL for help and access to SEM/EDS and the diamond saw. Finally, I need to thank the entire Materials Sciences and Engineering department (faculty, staff, and students) for the wonderful research environment.

Finally, I owe much gratitude to my family. My wife, Jessica Harkins, has given me her unconditional love and support. *You are the reason that this is possible.* We have three beautiful children Lily, John, and Liam. *You are all the driving motivation to get me out of bed and give it all that I have got.* Lastly, I must thank my parents and the rest of my family who pushed me to achieve my goals.

TABLE OF CONTENTS

Page

Table of Contents (Continued) Page

LIST OF TABLES

List of Tables (Continued) Page

LIST OF FIGURES

List of Figures (Continued) Page

List of Figures (Continued) Page

List of Figures (Continued) Page

ABBREVIATIONS

Abbreviation	Meaning
TRUEX	transuranic extraction
TALSPEAK	Trivalent Actinide-Lanthanide Separations by Phosphorus-reagent Extraction from Aqueous Complexes
VHT	Vapor Hydration Testing
SEM	Scanning Electron Microscopy
EDS	Energy Dispersive Spectroscopy
XRD	X-ray Diffraction
SYNROC	“Synthetic Rock;” Term given to certain mixtures of titanate ceramics meant for safely storing radioactive waste
PCT	Product Consistency Testing
ICP-MS	Inductively coupled plasma mass spectroscopy
SPS	Spark Plasma Sintering
SYNROC	multiphase titanate ceramic wasteform containing specific amounts of hollandite, zirconolite, and perovskite that also contains metal alloys

Chapter 1. Introduction

1.1 Background

Increased attention has been given to the development of materials that serve as alternatives to glass waste forms currently being employed for nuclear waste immobilization. In the United States approximately 20% of the energy produced is nuclear, with 100 working nuclear power plants. In South Carolina, there are four working nuclear plants, producing about 55% of the state's net energy[1]. With a significant portion of the United States' energy coming from nuclear energy, it is important to minimize waste. There are two different types of nuclear waste: defense waste and commercial waste. Defense waste is waste remaining from atomic energy defense, while commercial is nuclear waste produced from nuclear fission reactors. The Nuclear Waste Institute states the nuclear industry produces approximately 2,000 tons of used nuclear fuel each year[2], and this number could be reduced.

According to Lerner[3] at Argonne National Laboratory, used nuclear fuel rods could be recycled and separated into useable fuel and unusable waste. There are a few processes that have been investigated for recycling used nuclear fuel, however the TRUEX-TALSPEAK are both industrially used and being considered for by the U.S. Department of Energy[4]. Transuranic Extraction (TRUEX) is a process that involves extracting the lanthanides and minor actinides, while the Trivalent Actinide-Lanthanide Separations by Phosphorus-reagent Extraction from Aqueous Complexes (TALSPEAK) process separates the methods minor actinides from the lanthanides. These processes are one of the most promising methods of recycling used nuclear fuel, however this would require a durable waste form to immobilize the remaining unusable waste material.

Currently, nuclear waste is stored in glass waste forms where the radionuclides are suspended in a glass matrix. One issue with the currently employed glass waste forms is the questionable long term durability in repositories, showing leaching of radionuclides[5,6], which is caused by unfavorable crystallization that forms nepheline and spinel during processing[7]. These crystallized phases weaken the glass network, leading to increased leaching. To combat this problem, this work looks to investigating a multiphase crystalline ceramic waste form, where radionuclides are incorporated into the crystal structures, which can be placed in a geological repository and remain for long periods of time with minimum leaching. One promising ceramic waste form is a durable multiphase titanate ceramic composed of zirconolite, hollandite, and perovskite/pyrochlore, and rutile. Some secondary phases have been also known to occur. These phases are capable of incorporating a large variety of the elements present in nuclear waste, and may be more stable in many harsh environments, compared to glass, because they are naturally forming crystalline structures. Zirconolite is targeted to incorporate the zirconium transition metal and actinides, hollandite is targeted to incorporate cesium, strontium, and possibly other alkalis, and pyrochlore/perovskite is used to incorporate the rare earths.[8,9,10,11]

There are uncertainties in the understanding of the corrosion of the multiphase ceramic waste forms and their resistivity to leaching in an aqueous environment. Work has been done on single phase corrosion of titanate ceramic using various corrosion tests, as well as some work on multiphase titanate ceramics. However, no work has been done examining the interactions between just two different phases at a time. In order to understand the corrosion of these multiphase titanate ceramic waste forms there must be a clear understanding of single, dual, and multiphase titanate ceramics and how each phase competes with one another during formation.

This information coupled with knowledge of the resistivity to aqueous leaching and corrosion of each phase individually, in pairs, and as multiphase ceramics could provide understanding of the corrosion mechanics of these waste forms.

1.2 Single Phases

Multiphase titanate ceramic waste forms consist of three targeted phase: pyrochlore/perovskite, hollandite, and zirconolite. These three targeted phases are for the incorporation of different radionuclides in the waste stream, which are gone into detail in this section.

A. Pyrochlores/Perovskites

Pyrochlore is one of the target phases of the multiphase crystalline ceramic waste forms that is used to incorporate lanthanides[9]. The general formula of pyrochlore is $A_2B_2O_7$, where A^{+3} is a lanthanide(La, Pr, Ce, Eu, Nd, Sm, Gd, Dy, Yb, Y)[11,12] and B^{+4} is tetravalent titanium. These pyrochlores have been easily formed using many different methods such as solid-state synthesis[13], coprecipitation[14], melt[9], hydrothermal[15], and even as a single crystal[16,]. Pyrochlores are essentially an anion-deficient fluorite lattice where $1/8^{th}$ of the anions are systematically absent[17].

Perovskites, with general formula ABO_3, are also a possible target phase of multiphase crystalline ceramic waste forms. Actinides can be immobilized in the perovskite structure, similar to pyrochlores[8,10]. Perovskite or pyrochlore formation is dictated by the partial pressure of oxygen utilized during synthesis. If calcination occurs in an oxygen rich environment, the resulting structure is pyrochlore[14], however, calcination in an atmosphere with a low partial pressure of oxygen will cause the tetravalent titanium to reduce to titanium(III) forming perovskite[18].

B. Hollandite

Hollandite, specifically barium hollandite, is another target phase of multiphase crystalline ceramic waste forms for the incorporation of cesium, as well as strontium and other alkalis[9,11,19]. Barium hollandite ($(Ba_xCs_y)(M, Ti)_8 O_{16}$ where M= (Al, Mn, Fe, Ga, Cr, Sc, Mg)$^{+3}$ is a prime candidate for incorporation of cesium and barium ions due to the ability to substitute cesium in place of barium and trap electrons during decay[19]. However, new research shows that pure cesium hollandite can be achieved with no barium in the structure[20].

C. Zirconolite

Zirconolite is the third targeted phase of multiphase crystalline ceramic waste forms, specifically for incorporation of zirconium and tetravalent actinides[9,21]. Zirconolite ($CaZrTi_2O_7$) can substitute actinides into calcium and zirconium sites making it able to incorporate a variety of radionuclides. Zirconolite is a derivative of the pyrochlore structure and therefor also acts as a secondary host for rare earth elements and tetravalent actinides[9,21,22]. Kesson et al[21] extensively studied the solid solution characteristics of zirconolite an incorporated many different ions from the nuclear waste stream into the structure of zirconolite successfully. What makes zirconolite so stable is that only about a 50% occupancy of Ti-sites need to be occupied by Ti^{+4} to keep the zirconolite structure. The Ca-site does not appear to destabilize the zirconolite structure if occupied by elements other than calcium, as long as they are close in size[21].

1.3 Multiphase Ceramic Waste forms

The three popular phases, previously discussed, of multiphase ceramic waste forms have the ability to stabilize almost all high level radioactive wastes[10]. Many previous researchers have done

work on multiphase ceramic waste forms[8,9,10,11,22,23] , however, detailed studies of phase stability between pyrochlore, hollandite, and zirconolite are required to ensure proper incorporating of radionuclides[24] as well as focusing on the durability and leachability of the multiphase ceramic waste forms.

A problem that commonly occurs during processing of the multiphase crystalline ceramic waste forms is the formation of non-desirable secondary phases. Smith et al[8], while performing SEM on samples of SYNROC, one type of multiphase titanate ceramic waste form, discovered multiple other phases such as intermetallic alloy particles, grains of calcium aluminum titanate, titanium aluminate, and others[8]. Understanding the relationships between phases could help to minimize the formation of these secondary phases.

1.4 Experimental Procedures

A. Vapor Hydration Testing

Vapor Hydration testing (VHT) is a method to study the corrosion and alteration of waste glass and ceramics by mimicking the humid environment where waste forms are stored[25,26]. Monolithic samples are suspended inside of 304L stainless steel vessel by platinum wire that is tied to stainless steel stand that is placed in the vessel, seen in Figure 1-1. An amount of water is added, depending on the volume of the vessel and temperature the test is performed at, to achieve 100% humidity inside of the reaction vessel. This humidity inside of the chamber causes a thin layer of water to condense on the surface of the sample(s) giving the potential to react to them, depicted in Figure 1-2. There is no standard time or temperature for the test to be carried out at, periods of up to seven years[26] and temperatures anywhere from 40 °C[27] to 300 °C[28] have been reported. There are also many reported ways to examine the specimens after vapor hydration testing such

as EDS, optical microscopy, SEM, and XRD[25,26,29]. For SEM and EDS, the sample are marked for locating the same locations before and after testing. It has also been reported to use multiple samples of the same glass specimen in the same container[25]. All of these variations in test procedure make different specimens hard to compare, however the purpose of VHT is to generate larger alteration layers and more secondary phase formation[30] giving more insight into the long term corrosion of crystalline ceramic waste forms

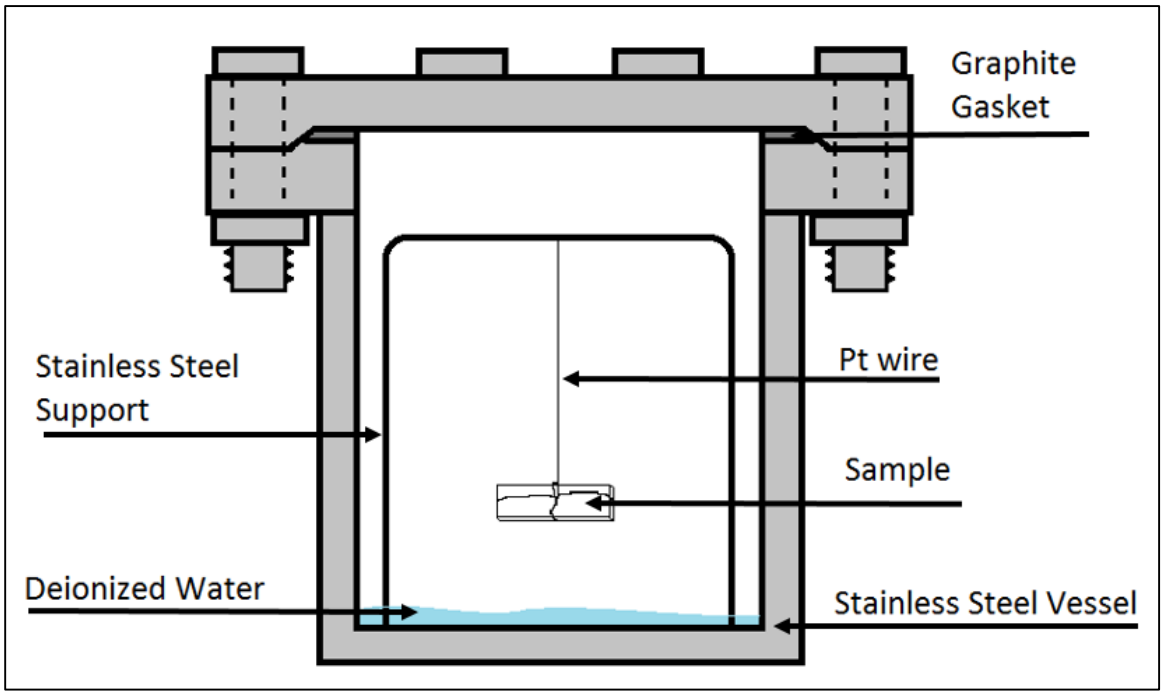

Figure 1-1. Depiction of the experimental setup for vapor hydration testing.

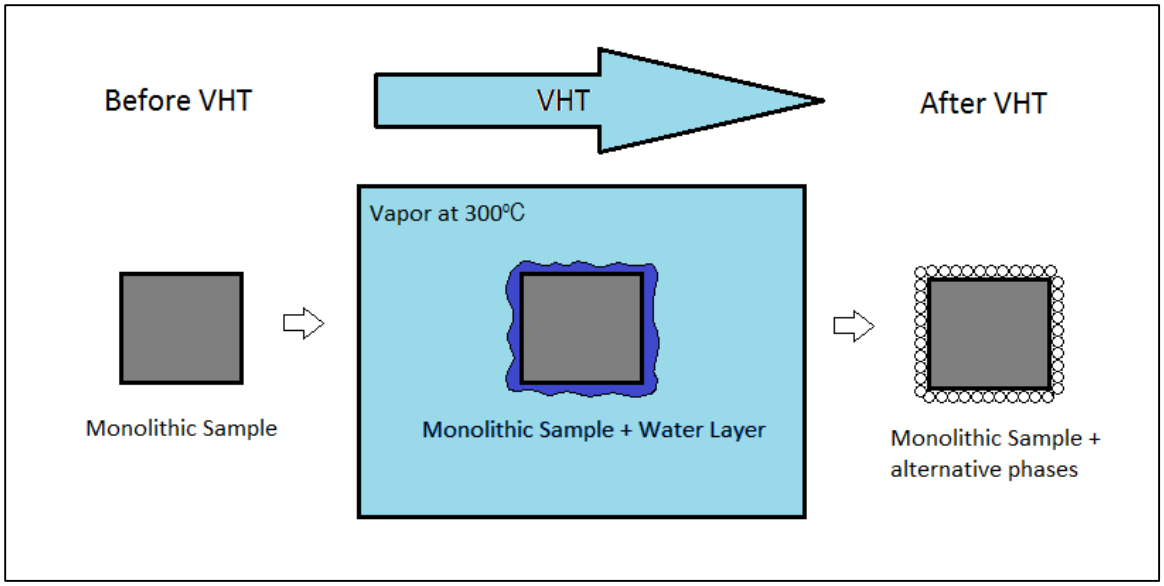

Figure 1-2. Cartoon of VHT showing the formation of thin water layer that occurs while testing and alternative phases that are remaining.

Ceramics

Buck et al[22] performed vapor hydration testing on Pu-bearing zirconolite-rich SYNROC for 35 days at 200 °C and examined the surface alteration using TEM, reproduced in Figure 1-3. There appeared to be a 100-200nm thick alteration layer on the surface of the ceramic. This layer suggests that dissolution occurred and this alteration layer was found to be high in Pu, but this is not believed to have come from the zirconolite phase in the SYNROC. Secondary phases present, including an iron rich material containing Pu were found to have precipitated on the zirconolite surface- no corrosion of the zirconolite parent phase was found.

Bourcier[31] reported VHT tests on zirconolite ceramics. Tests were performed at 200 °C and the results showed an alteration zone that contained small amounts of phosphates and iron oxides, which were presumed to be impurities in the ceramic, seen in Figure 1-4.

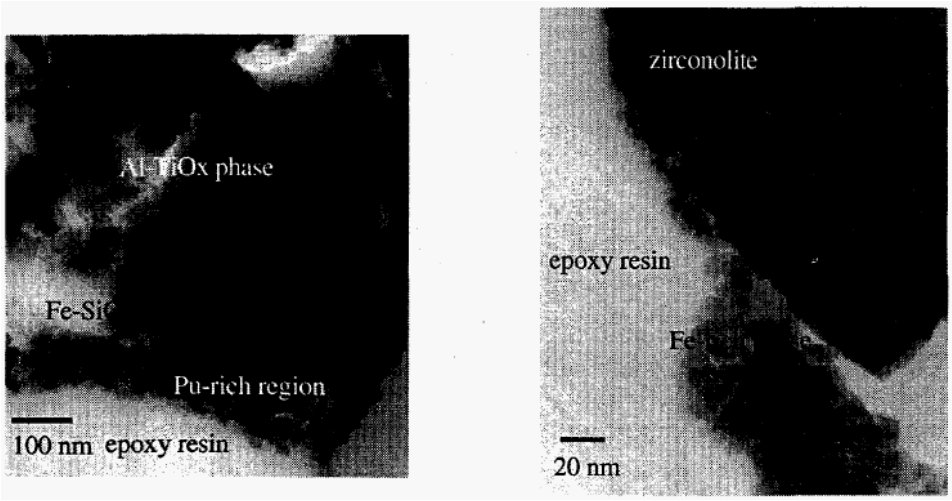

Figure 1-3. TEM micrographs of Al-Bearing Titanate (left) and Zirconolite crystal (right), both showing surface alteration[22]. Reproduced Without Permission.

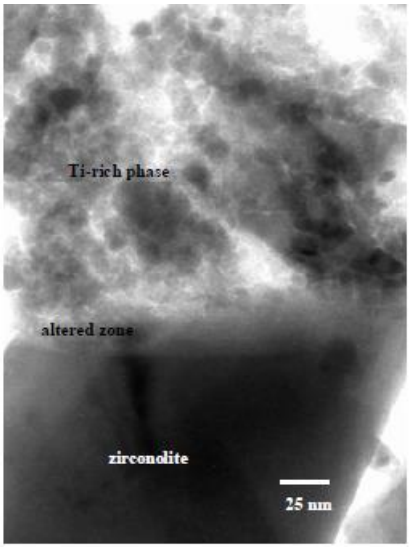

Figure 1-4. Ti-enriched layer in contact with a corroded zirconolite surface from a 200 °C VHT[31]. Reproduced Without Permission.

Glasses

In comparison, waste glasses examined after VHT exhibit a larger alteration area in a less amount of time. Neeway et al[29] performed vapor hydration tests on French reference nuclear waste glass SON68 using temperatures from 90 °C to 200 °C as well as varying time periods from 57 days to

512 days. On one of the samples, the researchers performed EDS topography, where an aluminum and silicone layer formed as well as a gel layer consisting of alteration products, seen in Figure 1-5.

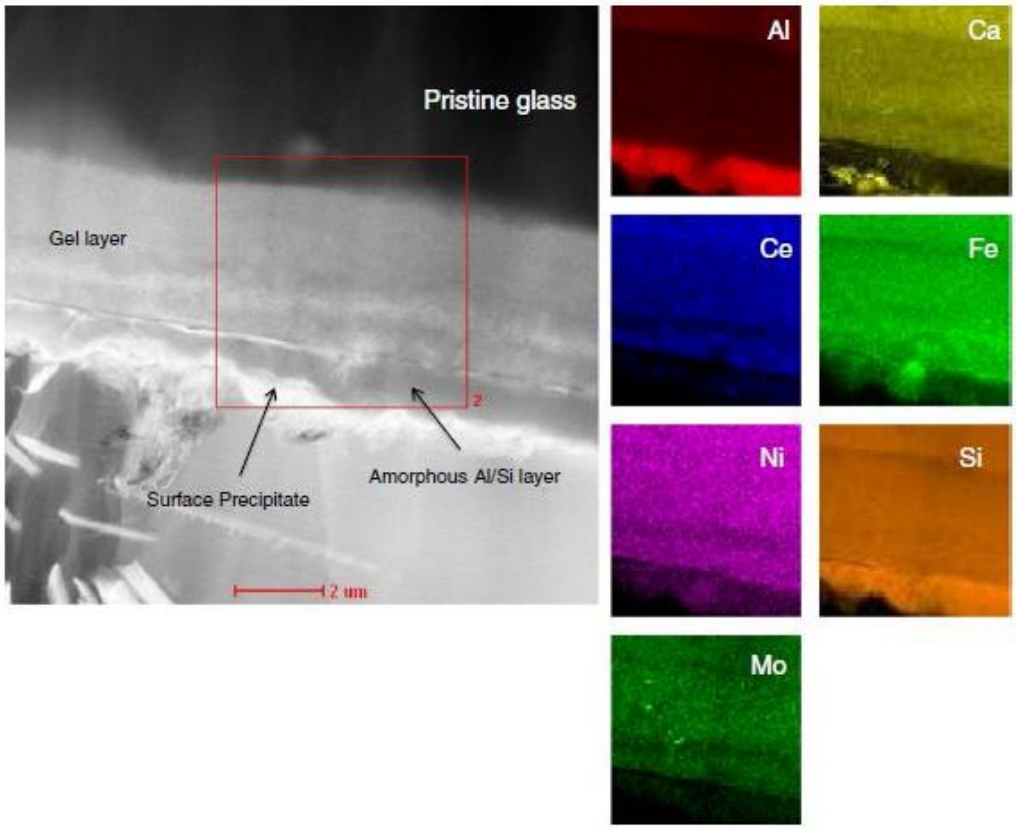

Figure 1-5. Profile of the layers formed after VHT on SON68 waste glass after held for 99 days at 175 °C and a relative humidity of 92%[29]. Reproduced Without Permission.

At present, a comparison of VHT for SYNROC versus waste glass is difficult to a lack of available data. While VHT has been done many times on waste glasses, there has been very little performed on SYNROC and its constituent phases. Each of the individual phases need to be extensively examined for corrosion, as well as bulk samples of SYNROC to determine what possible alteration and secondary phase formation could be expected in long term corrosion. The lack of existing

literature motivates systematic studies on single, dual, and multiphase samples as a function of composition and microstructure.

B. Product Consistency Testing

The Product Consistency Test (PCT) is a method to examine the quantitative dissolution of elements over time. The samples are typically crushed into a fine powder, with a known particle size, and placed inside of a 304L stainless steel reaction vessel along with demineralized water, depicted in Figure 1-6. There is a standard PCT-A and a non-standard PCT-B test. PCT-A is done specifically at 90 °C for exactly seven days with a water/sample mass ratio of 10:1. While the PCT-B test has no set time, temperature, or any other controlled variables[32]. Once the tests are run for set time period, the leachate is collected and analyzed using ICP-MS.

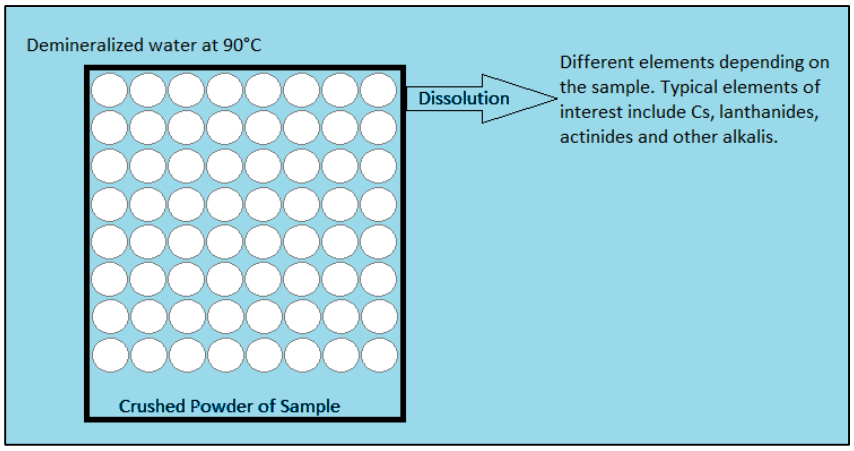

Figure 1-6. Cartoon depiction of PCT testing showing elemental dissolution over time.

Single Phase Testing

Carter et al[33] performed PCT-B testing on single phase hollandites, specifically Al and Mg hollandites. Instead of rinsing the 100-200 mesh particles with deionized water, cyclohexane was

used to prevent preleaching of Cs. These samples were then leached in 10 ml of deionized water for seven days.

James et al[34] performed PCT-B on U-containing pyrochlores, specifically, $Ca_{1.25}U_{0.75}$ Ti_2O_7 and $Ca_{1.40}U_{0.7}Ti_{1.90}O_7$. The PCT-B protocol involved using crushed samples of 100-200 mesh, then washing the particles in cyclohexane. The testing was carried out by 1 g of powder to 10 mL of DI water at 90 °C for 7 days. The normalized concentration of U leached over the seven day period was found to be $2.5*10^{-5}$ g/L for $Ca_{1.25}U_{0.75}$ Ti_2O_7 and $1.2*10^{-5}$ g/L for $Ca_{1.40}U_{0.7}Ti_{1.90}O_7$. James et al state that these concentrations are significantly less than synthetic brannerite (UTi_2O_6), which is another possible phase for the immobilization of U in SYNROC.

Multiphase Testing

Brinkman et al[35] and Billings et al[36] used PCT-B to examine Cs leeching in deionized water out of multiple different multiphase SYNROC formulations. Structural and chemical analysis of the materials systems indicated preferential Cs-Mo association and the absence of a Cs-containing hollandite phase. This resulted in poor aqueous durability and motivated improved formulations for Cs-containing hollandites that are compatible with a melt and crystallization process[11, 37–39]. These multiphase sample compositions can be seen, along with the normalized concentration of Cs, in Table 1-1.

Ringwood et al[10] also examined Cs leeching in a SYNROC multiphase sample, however instead of normalized mass loss rates being reported, plateau leech rates were reported which were said to be achieved in approximately three weeks for samples. This makes it difficult to compare with other reported mass loss rates since there is no exact time period reported.

Crum et al[40] used PCT-B testing to examine Cs leeching on glass ceramic composites for 3 and 28 days. The three glass ceramic composites had varying compositions and had similar leach rates, seen in Table 1-1. The Cs showed preferential portioning into the glass phase of the multiphase.

Table 1-1. PCT-B Results for elemental loss in powdered samples all performed in Deionized Water. Concentrations labeled with *1 next to them are Normalized Mass loss (g/m^2).

Element	Compound	Structure	Temperature (°C)	Time (d)	Normalized Concentration (g/L)	Reference
Cs	Single Phase Hollandite	Al-18 Hollandite	90	7	6.20E-01	41
		Al-12 Hollandite	90	7	5.20E-01	
		Mg-18 Hollandite	90	7	1.30E+00	
		Mg-12 Hollandite	90	7	2.80E+00	
Cs	Glass Ceramic Composite	5.86% MoO_3	90	3	1.40E-01	40
		6.25% MoO_3	90	3	1.50E-01	
		6.94% MoO_3	90	3	2.70E-01	
		5.86% MoO_3	90	28	1.90E-01	
		6.25% MoO_3	90	28	1.30E-01	
		6.94% MoO_3	90	28	1.80E-01	
Cs	Multiphase Ceramic	CSLNTM-02	90	7	2.88E+00 *1	35
		CSLNTM-06	90	7	3.34E+00 *1	
		CSLNTM-11	90	7	9.62E+00 *1	
Cs	Multiphase Ceramic	CS/LN-03	90	7	4.41E+01	36
		CS/LN-04	90	7	3.24E+01	
		CS/LN-05	90	7	4.48E+01	
		CS/LN/TM Mo-02	90	7	3.80E+01	
		CS/LN/TM Mo-03	90	7	2.81E+01	
		CS/LN/TM Mo-04	90	7	2.37E+01	
		CS/LN/TM Mo-05	90	7	2.51E+01	
U	Pyrochlore	$Ca_{1.25}U_{0.75}Ti_2O_7$	90	7	2.50E-05	34
		$Ca_{1.20}U_{0.70}Ti_2O_8$	90	7	1.20E-05	

1.5 Experimental Summary

Outlined in Figure 1-7, this work will begin with single phase studies of lanthanide titanates, specifically Nd and La titanates and Ce brannerite. Next, dual phase studies of these lanthanide titanates and Ga doped Ba hollandites were fabricated and characterized, followed by dissolution testing using PCT. Finally, durability studies were conducted on multiphase model systems, as well as some single and dual phase samples for comparison, using VHT.

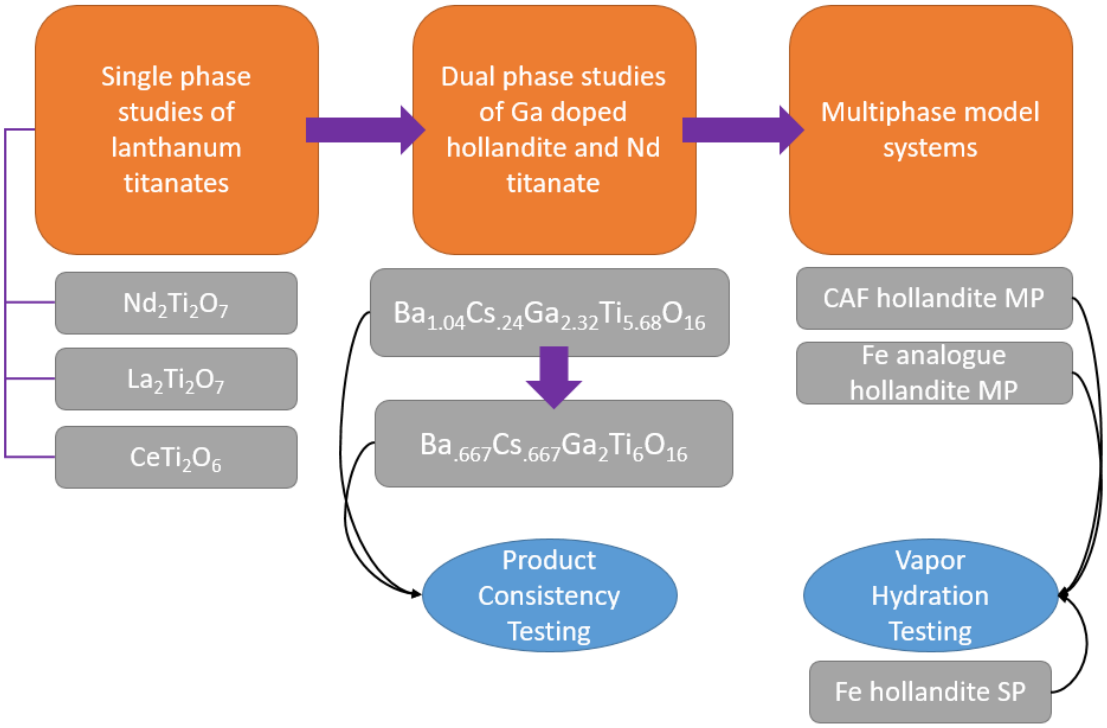

Figure 1-7. Map of experiments beginning with single phase fabrication to durability testing.

Chapter 2. Synthesis/Processing

2.1 Single Phase Studies of Lanthanide Titanates

Single phase titanate structures were fabricated in order to provide a baseline comparison for model multiphase systems. The three lanthanides neodymium, lanthanum, and cerium were selected for this study first because they are the three most prevalent lanthanides in the waste stream[11]. Neodymium (III) oxide (Nd_2O_3), lanthanum oxide (La_2O_3), and cerium (II) oxide (CeO_2) were individually mixed into batches with titanium oxide and ethanol. The batches were then ball milled five times for one minute intervals. The batches were strained and removed from the ball mill containers using more ethanol and then allowed to dry in an oven at 90 °C for 24 hours. After drying, the batches were pulverized with a pestle and mortar and pressed into pellets. Approximately three, two gram pellets were made from each batch. Each pellet was calcined for four hours at 1000 °C, 1200 °C, and 1400 °C, as shown in Table 2-1.

Table 2-1. Temperatures of calcination for the single phase systems

	Titanates		
	Neodymium	**Cerium**	**Lanthanum**
Hours	**4 h**	**4 h**	**4 h**
Temperature	1000 °C	1000 °C	1000 °C
	1200 °C	1200 °C	1200 °C
	1400 °C	1400 °C	1400 °C

After calcination, the pellets were pulverized with a pestle and mortar. Next, powder X-ray diffraction (XRD) was ran on the samples using Cu radiation. The samples were then examined using SEM and EDS analysis.

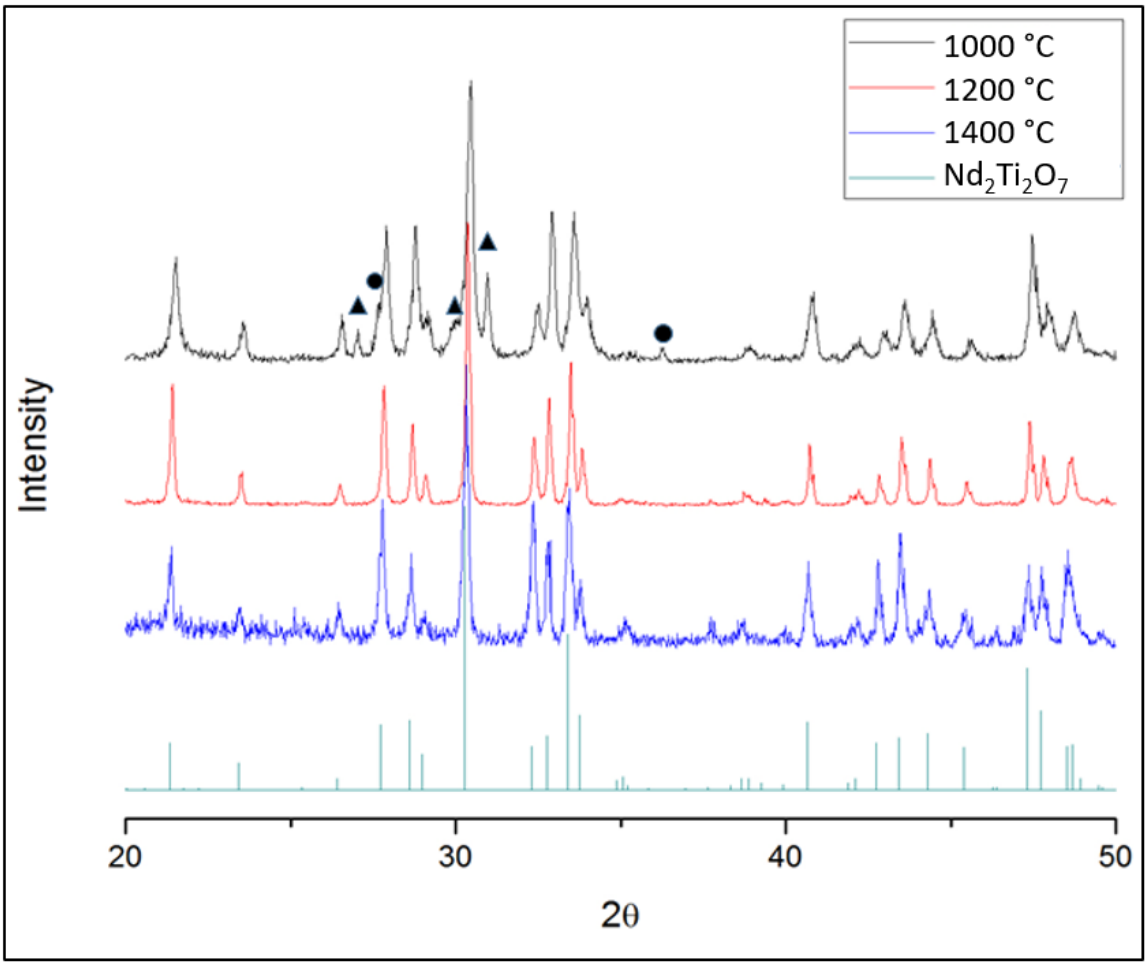

Figure 2-1. XRD spectra for neodymium titanate samples that were calcined at 1000 °C, 1200 °C, and 1400 °C compared to ICSD database file 4133 for a monoclinic neodymium titanate. ▲ Nd_2O_3 (ICSD 32514); ● TiO_2 (ICSD 64987).

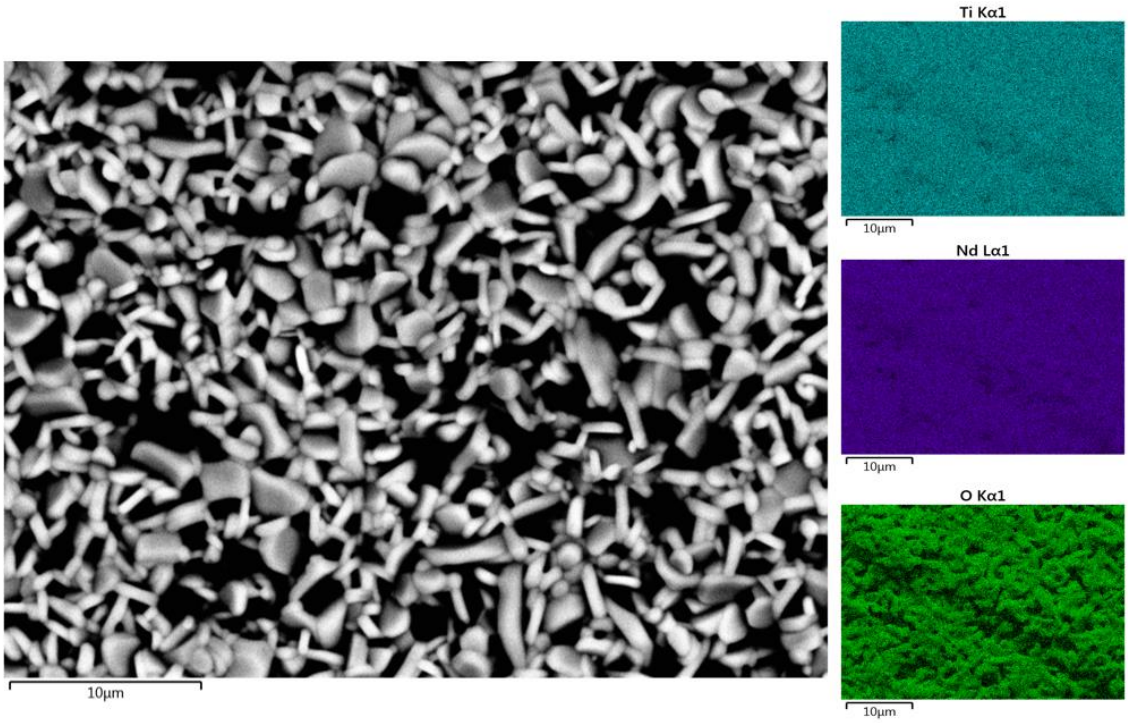

Figure 2-2. SEM image and EDS elemental analysis on Nd titanate formed at 1200 °C.

Table 2-2. Summary Table of the phases found for each sample at each temperature (*Crystalline phases determined by XRD results and EDX elemental analysis)

Oxide mixed with TiO_2	Temperature (°C)	Phase*
Nd_2O_3	1000	Nd titanate +Nd_2O_3+TiO_2
	1200	Nd titanate
	1400	Nd titanate
La_2O_3	1000	La titanate +Nd_2O_3+TiO_2
	1200	La titanate
	1400	La titanate
CeO_2	1000	CeO_2+TiO_2
	1200	CeO_2+TiO_2
	1400	Melted

In Figure 2-1, the XRD spectra for the neodymium titanate samples that were calcined at 1000 °C, 1200 °C, and 1400 °C are shown compared to a Nd titanate from the ICSD file 4133. The SEM image and EDS analysis is shown in Figure 2-2 for Nd titanate calcined at 1200 °C, showing a pure phase Nd titanate was achieved. In Table 2-2 is a summary Table of all the samples of Nd, La, and Ce phases confirmed using XRD, SEM, and EDS.

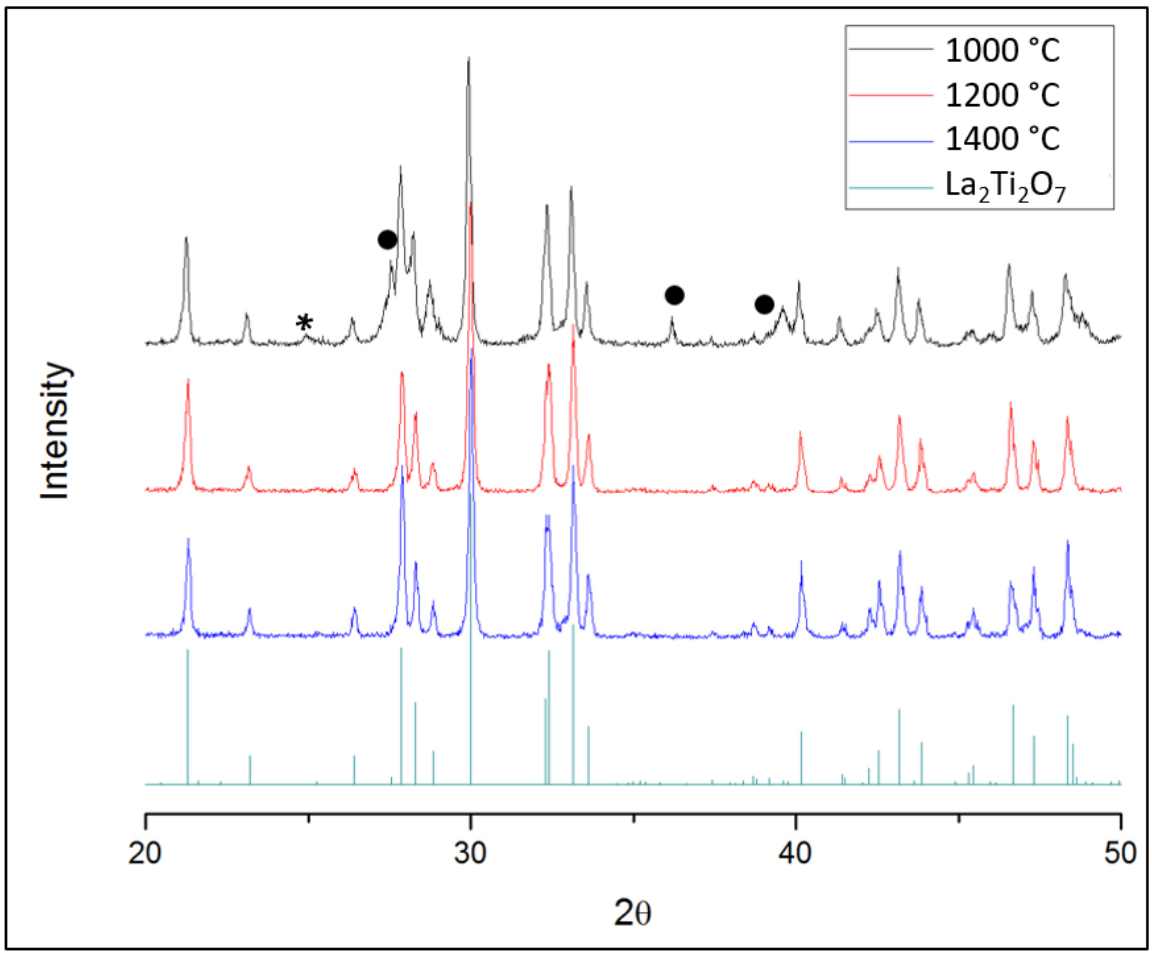

Figure 2-3. XRD spectra for lanthanum titanate samples that were calcined at 1000 °C, 1200 °C, and 1400 °C compared to ICSD database file 1950 for lanthanum titanate. ● TiO_2 (ICSD 64987). Peak labeled with a * is an unidentified peak.

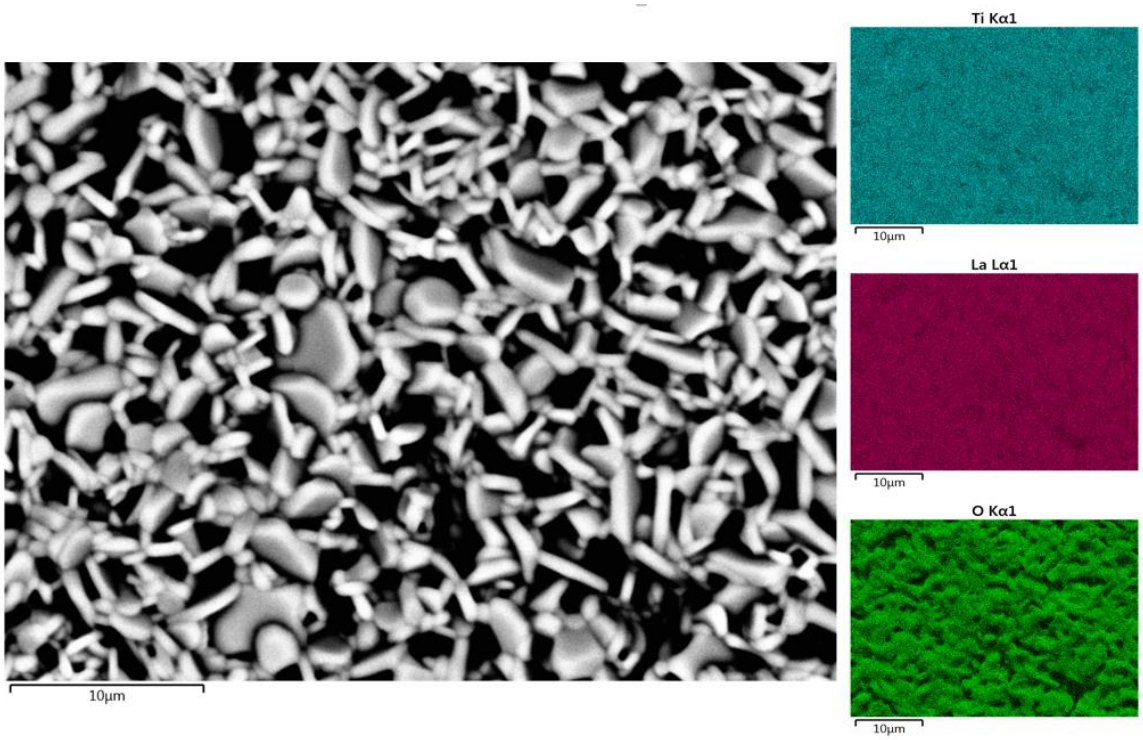

Figure 2-4. SEM image and EDS elemental analysis on La titanate formed at 1200 °C.

Lanthanum titanate samples calcined at 1000 °C, 1200 °C, and 1400 °C are shown in Figure 2-3 compared to the XRD spectra of La titanate (ICSD # 1950). As seen the 1000 °C sample is not a pure phase titanate with some TiO_2 peaks present, however at temps above this a pure phase is achieved, supported by SEM and EDS data seen in Figure 2-4. These results are similar to what was seen while forming Nd titanate, which was expected with both having a +3 valence.

Cerium, however, is slightly different because at room temperature cerium has +4 charge instead of +3 like neodymium and lanthanum. This causes the cerium(IV) oxide and titanium(IV) oxide to form $CeTi_2O_6$ instead around 1350 °C[42–44]. Samples were calcined at 1000 °C, 1200 °C, and 1400 °C to begin. The samples calcined at 1000 °C and 1200 °C were both matched to the starting materials CeO_2 and TiO_2 with the Jade database, shown in Table 2-2, and the 1400 °C sample melted.

However, another sample calcined at 1350 °C for four hours, the XRD pattern shown in Figure 2-5, was matched to uranium brannerite, UTi_2O_6 (ICSD # 201342). Ce is a well-known substitute for U, proving that a cerium brannerite was achieved. However, some TiO_2 and CeO_2 precursors remained in the sample.

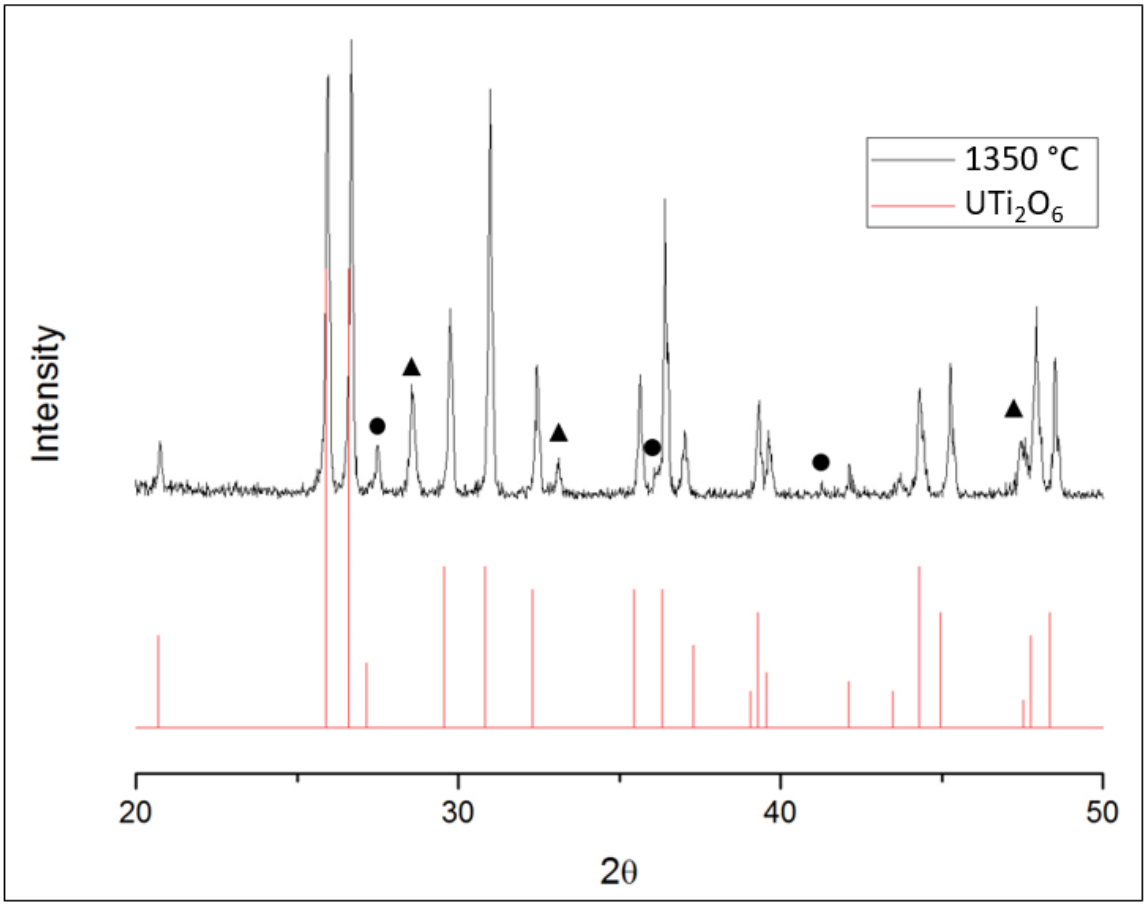

Figure 2-5. The sample of CeO_2 and TiO_2 that was calcined at 1350C for four hours and is matched to a Brannerite crystal structure ICSD file 201342. ▲ CeO_2 (ICSD 32514); ● TiO_2 (ICSD 64987).

However, when processed under reducing conditions, Ce titanates can become more unpredictable. Ce and Ti both being able to have a valence of +3 or +4 making multiple possible phases that can form, such as Ce_2TiO_5, $Ce_2Ti_2O_7$ or related structure $Ce_4Ti_9O_{24}$[42].

Some lanthanides, such as Ce, with a +4 valence that have the potential to form a number of different phases, depending on processing conditions, causes some uncertainties in the stability of multiphase ceramic waste forms. At most temperatures, in air, Ce^{+4} is most stable as CeO_2 unless rapidly cooled or at certain temperature ranges[42–44]. Elements like Ce make processing multiphase ceramic waste forms with vast variety of elements difficult to prepare, study, and compare.

2.2 Dual Phase studies of Lanthanide titanates and Ga doped Ba Hollandite

One of the large gaps in the available literature on crystalline ceramic waste forms is the stability during processing and storage, including how each phase reacts individual with another. To examine how model binary phases interact, a Ga doped Ba hollandite was mixed with three different lanthanide titanates and heated to see if a reaction would occur. The Ba hollandite chosen was a common Ba/Cs ration that is found in literature[19], $Ba_{1.04}Cs_{.24}Ga_{2.32}Ti_{5.68}O_{16}$. This hollandite was mixed in a 50/50 volume ratio with three different lanthanide titanates: neodymium, lanthanum, and cerium. The mixtures were heated in a furnace for four hours and characterized using XRD and SEM. The hollandite and lanthanides were fabricated by an oxide route and calcined to achieve single phase materials.

For comparison, the same experiment was repeated, but instead of crystalline hollandite and lanthanide titanate the precursors (Nd_2O_3, TiO_2, $BaCO_3$, etc.) to them were used in the same stoichiometric portions and 50/50 volume fraction. These were heated to see if the same crystalline phases could be achieved. This comparison of starting phases is important for crystalline ceramic waste forms because some waste forms are with crystalline materials and densified, while others with start with slurries of oxides or nitrates and then melt.

Table 2-3. Crystalline vs. Raw Powder systems of Ga doped Ba hollandite and lanthanide titanate mixtures.

Ba hollandite +	1200 °C Cry.	1300 °C Cry.	1400+ °C Cry.	1200 °C Raw Powders	1300 °C Raw Powders	1400+ °C Raw Powders
$Nd_2Ti_2O_7$	X	X	Melted	X	X	Melted
$La_2Ti_2O_7$	X	X	Melted	X	X	Melted
$CeTi_2O_6$	X	X	Melted	X	X	Melted

Shown in Table 2-3, all the samples melted at 1400 °C, which could possibly due to eutectics forming in the dual phase system. The Ga doped hollandite has a melting temperature around 1415 °C. Next, to examine whether the reaction was complete after four hours, one sample of each the crystalline phases and raw powder precursors was heated to 1300 °C for 12 hours.

Figure 2-6 shows the XRD results for the crystalline Nd titanate and Ga doped Ba hollandite mixtures after heating. It should be noted that the sample was processed at 1300 °C for four hours has an XRD spectra that was matched to large aluminum peaks. This is an experimental artifact from x-rays hitting the aluminum sample pan and should be ignored. Otherwise, the two samples processed at 1300 °C are almost identical and indicate the phase assemblage of matched phases $BaNd_2Ti_5O_{14}$ (Jade PDF #33-0166), $Nd_2Ti_2O_7$ (ICSD# 4133), $Ba_{1.143}Fe_{2.286}Ti_{5.71}O_{16}$ Hollandite (ICSD# 68730), and $Nd_4Ti_9O_{24}$ (ICSD# 72316). The system that was heated to 1350 °C is a sample from the PCT section discussed later in the chapter, which shows identical peaks to the 1300 °C systems. The last sample, 4 hours at 1200 °C, show similar phases as well, however the Nd titanate and hollandite peaks seem to be more dominate than the other phases found in the 1300 °C samples.

To confirm the XRD spectra matches, shown in Figure 2-7 is SEM and EDS of the dual phase systems were performed, serves as an example of how all systems phases where confirmed. In this particular system, which corresponds to ND-BH-CRYS-1350 in Figure 2-6, hollandite, Nd titanate, and $BaNd_2Ti_5O_{14}$ can be seen along with what appears to be a small amount of a Ga rich phase. The phase labeled 1 is identified as hollandite, where phase 2 is identified as Nd titanate, however it is not only $Nd_2Ti_2O_7$, but appears to be a mixture of $Nd_2Ti_2O_7$ and $Nd_4Ti_9O_{24}$, and phase 3 is identified as $BaNd_2Ti_5O_{14}$. These phases were determined with the aid of a location specific EDS tool on the SEM that gives an atomic percentage in a location from counts in the EDS.

To begin, the $Nd_2Ti_2O_7$ and $Nd_4Ti_9O_{24}$ mixture explains where the Nd is coming from to form the $BaNd_2Ti_5O_{14}$. As the $BaNd_2Ti_5O_{14}$ is formed the Nd is taken from the Nd titanate structure causing the shift from $Nd_2Ti_2O_7$ to $Nd_4Ti_9O_{24}$, which is an orthorhombic structure. Also, as $BaNd_2Ti_5O_{14}$ is formed and the hollandite structure is broken down, the Ga and Cs are left in another separate titanate. This did not show up on the XRD results, which could possibly be due to only being a small amount of the sample so the reflections are so weak they do not appear on the spectra, or it could possibly share peaks with other phases in the sample. It should also be noted that the Ti and Ba energies overlap, so the Ba map is identical to the Ti.

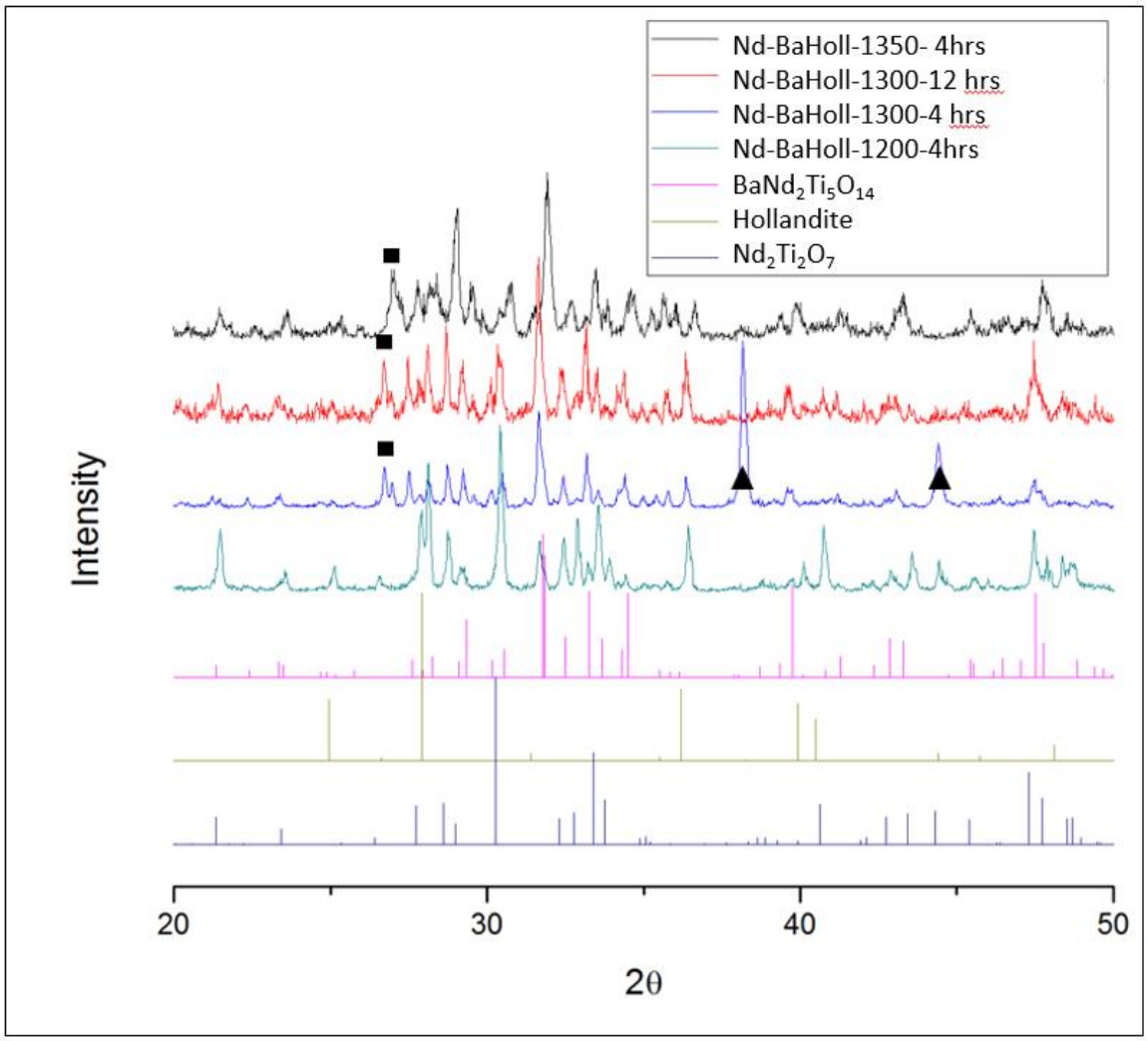

Figure 2-6. XRD patterns for Nd titanate and Ga doped Ba hollandite formed using crystallized precursors. ▲ Aluminum (ICSD # 64700); ■ $Nd_4Ti_9O_{24}$ (ICSD# 72316).

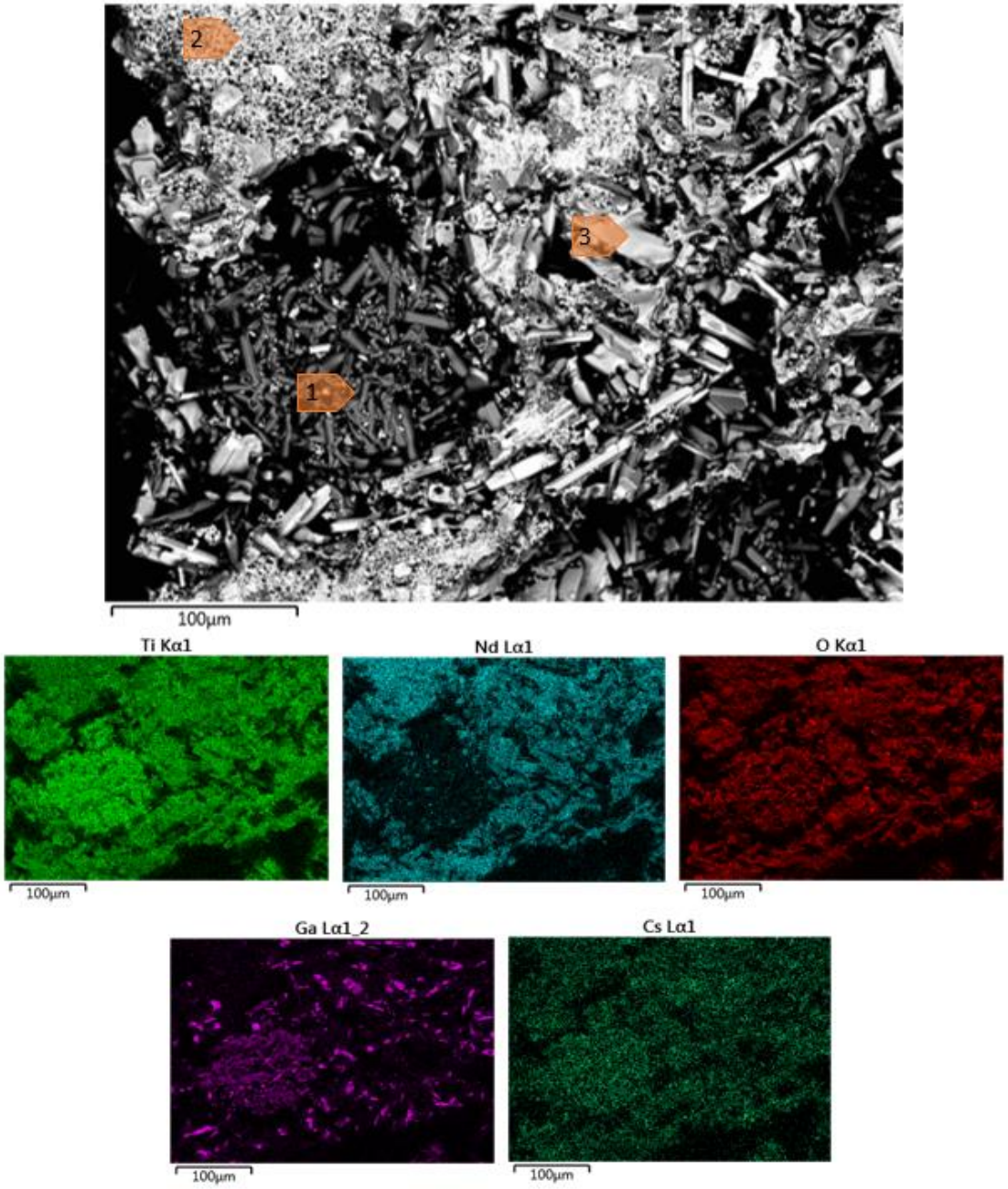

Figure 2-7. SEM and EDS images of a sample of dual phase Nd titanate and Ga doped Ba hollandite mixed in a 50/50 volume fraction, using the crystalline phases as the precursors, and then sintered at 1350 °C for 4 hours. Phase 1 is identified as hollandite, phase 2 being a mixture of $Nd_2Ti_2O_7$ and $Nd_4Ti_9O_{24}$, and phase 3 identified as $BaNd_2Ti_5O_{14}$.

Shown in Figure 2-8 are the XRD results for the raw powders of Nd titanate and Ga doped Ba Hollandite mixtures after heating. Starting with the precursors of the two crystalline phases seemed to make no difference for the formation of phases as the phases formed at each temperature and time is identical to the results from the crystalline mixtures.

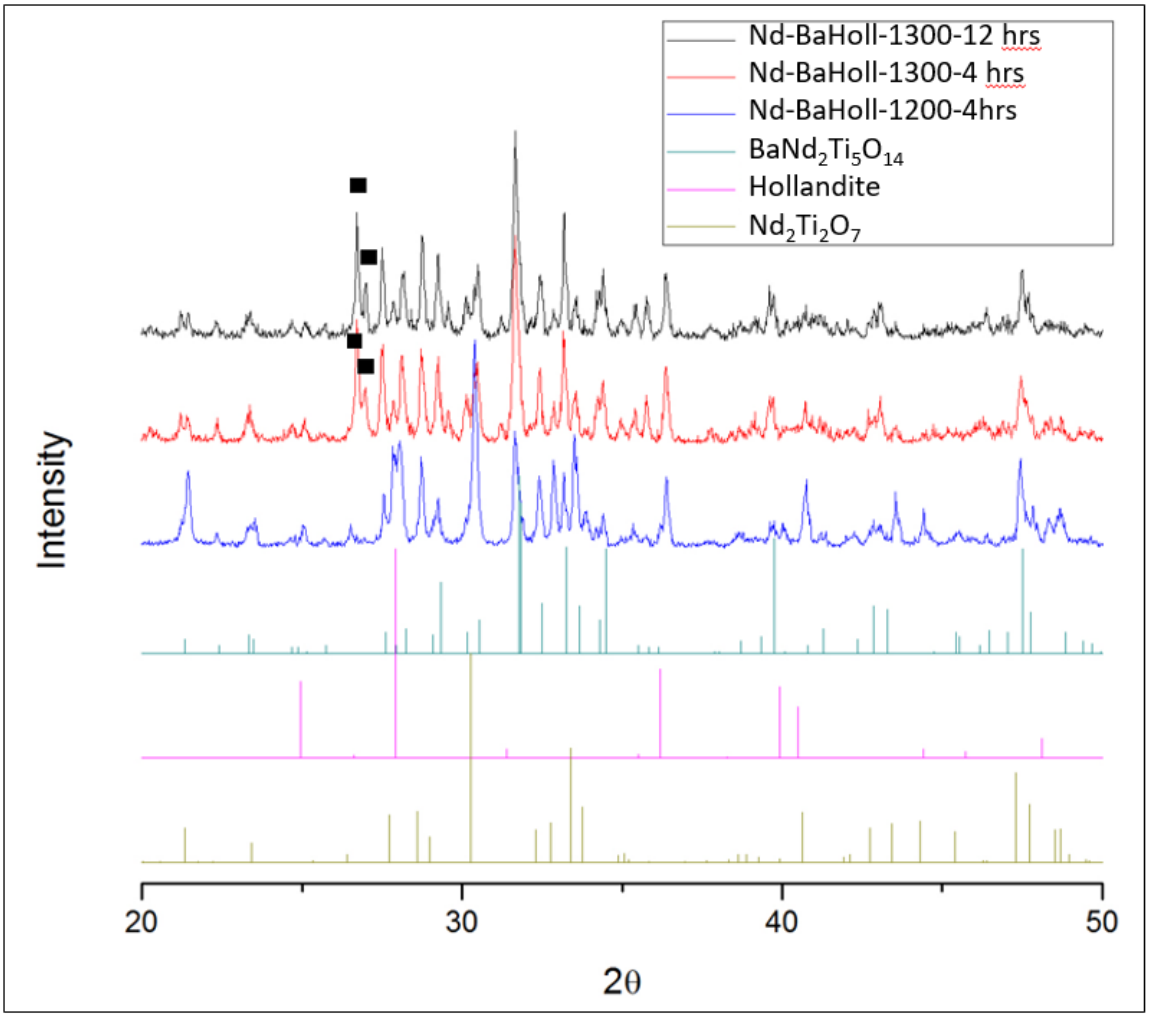

Figure 2-8. XRD spectra comparison for raw powder precursors of neodymium titanate and barium hollandite. ■ $Nd_4Ti_9O_{24}$ (ICSD# 72316).

Table 2-4 is summary Table on all of the raw powder precursors and crystallized samples and the phases that were found using XRD. Seen in Figure 2-9, the crystallized precursors of lanthanum

titanate and barium hollandite had no reaction at 1200 °C. At 1300 °C, a new phase was formed, $La_{0.66}TiO_{2.993}$ (found in Jade database, card # 26-0827), which is an orthorhombic perovskite structure. This would imply that that the titanium went under a reduction from Ti^{4+} to Ti^{3+} and the monoclinic titanate structure transitioned to a perovskite structure.

The raw powder precursor samples, however, had many different phases form at both 1200 °C and 1300 °C. Shown in Figure 2-10, at 1200 °C similar phase that formed in the Nd samples are present, $La_2Ti_2O_7$, hollandite, and the same $BaNd_2Ti_5O_{14}$ (Jade PDF #33-0166). However, at 1300 °C the same perovskite phase from the crystalline precursor samples begins to form, meaning that the reduction of the Ti occurred in this sample as well. Other phases accompany the La perovskite in the 1300 °C raw powder precursor sample, including $La_2Ti_2O_7$, hollandite, $BaNd_2Ti_5O_{14}$, and some $Nd_4Ti_9O_{24}$.

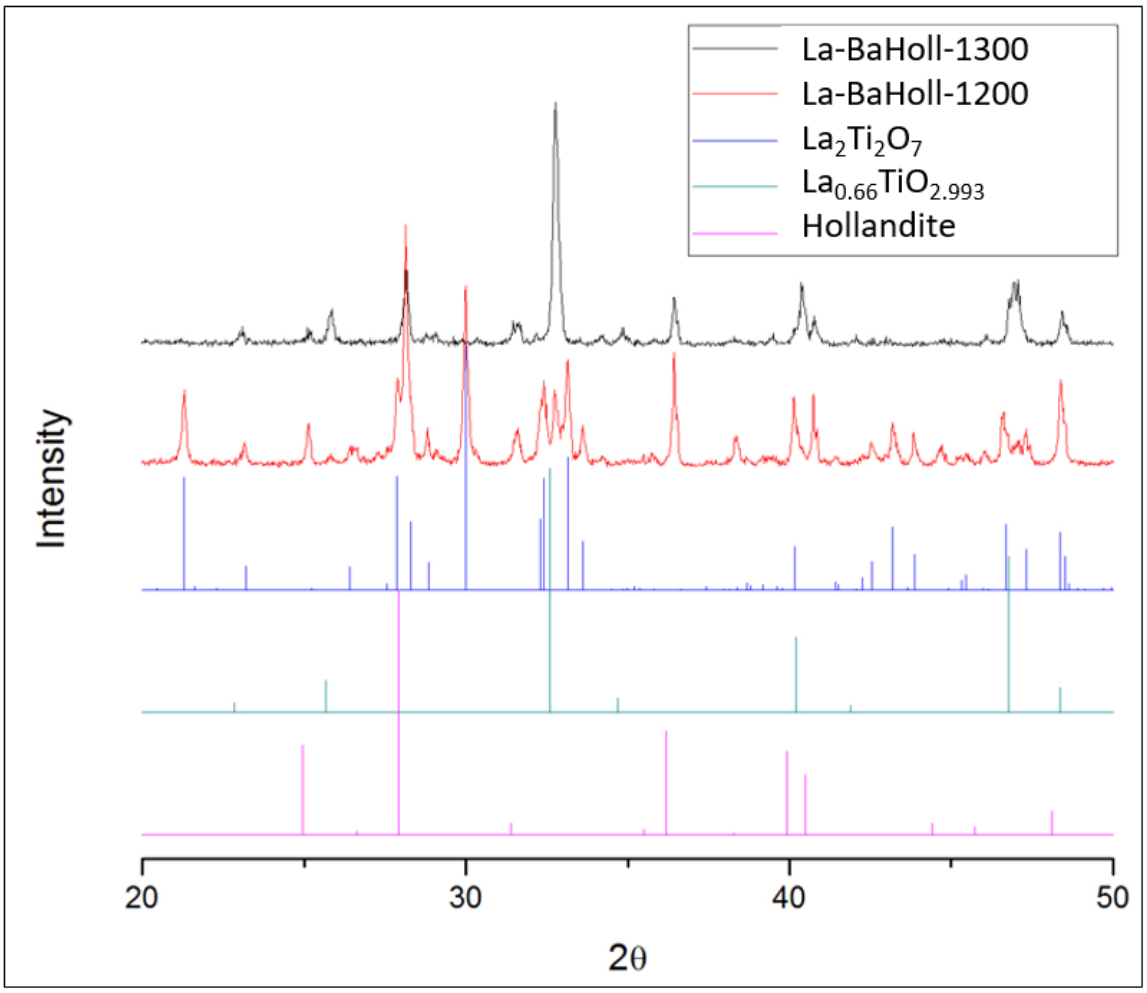

Figure 2-9. XRD spectra for crystalline powders of lanthanum titanate and barium hollandite compared to $La_2Ti_2O_7$ (ICSD # 1950), $Ba_{1.143}Fe_{2.286}Ti_{5.71}O_{16}$ hollandite (ICSD# 68730), and $La_{0.66}TiO_{2.993}$ (Jade database, card # 26-0827).

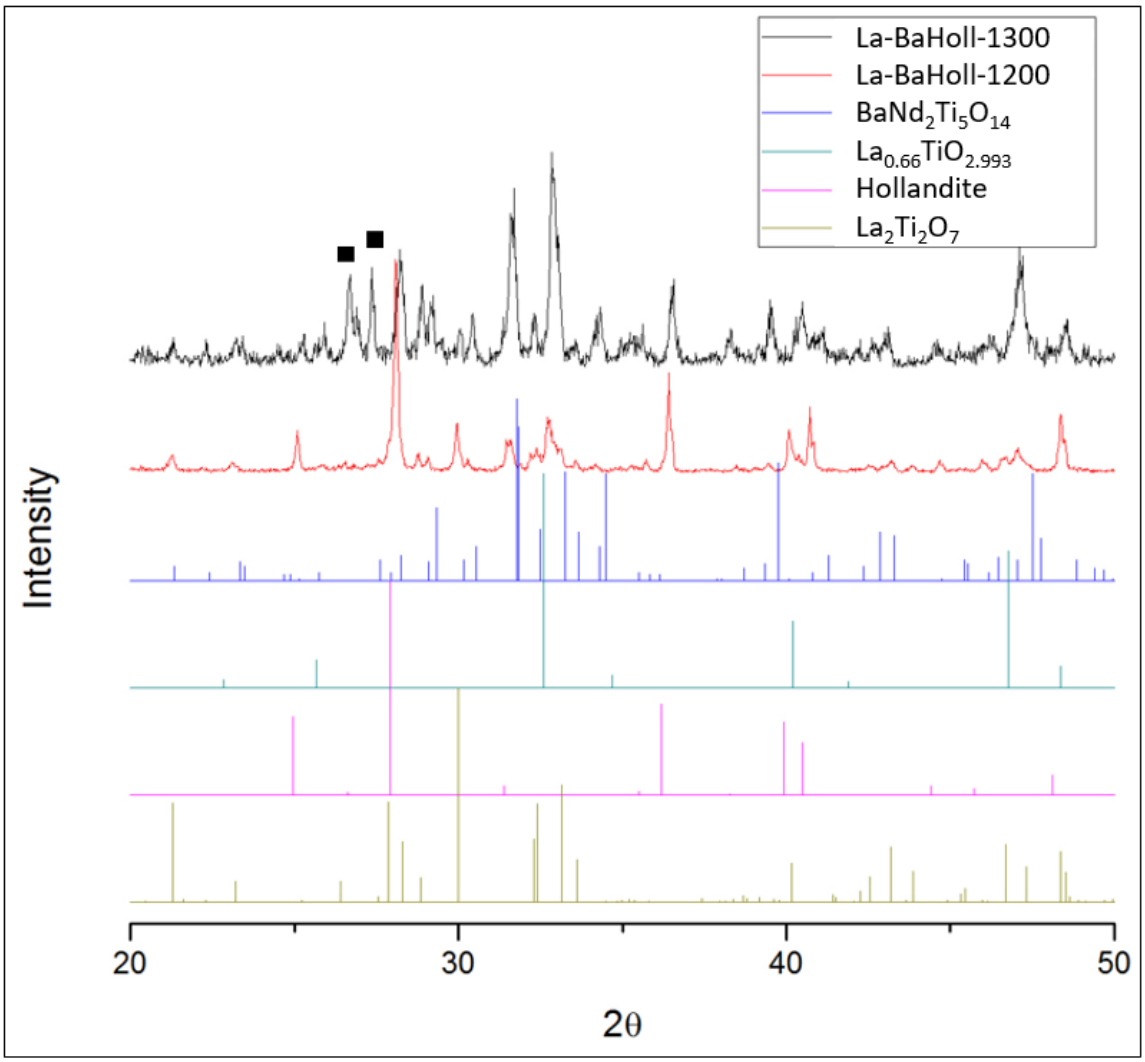

Figure 2-10. XRD spectra for raw powder precursors of lanthanum titanate and barium hollandite compared to $La_2Ti_2O_7$ (ICSD # 1950), $Ba_{1.143}Fe_{2.286}Ti_{5.71}O_{16}$ Hollandite (ICSD# 68730), $BaNd_2Ti_5O_{14}$ (Jade PDF #33-0166), $Nd_4Ti_9O_{24}$ (ICSD# 72316), and $La_{0.66}TiO_{2.993}$ (Jade database, card # 26-0827). ■ $Nd_4Ti_9O_{24}$ (ICSD# 72316).

The cerium brannerite mixed with hollandite had no reaction, whether the starting materials were crystalline or not. The raw powder samples formed hollandite, CeO_2, and TiO_2. While the crystalline cerium brannerite and barium hollandite remained as brannerite and hollandite.

Table 2-4. Summary Table of the dual composition phase results matched using XRD spectra.

-All samples mixed with Hollandite					
Titanate Used	CRYS or RAW	Temperature (°C)	Time (hours)	Matched Phases	
$Nd_2Ti_2O_7$	CRYS	1200	4	All contained: $BaNd_2Ti_5O_{14}$, Hollandite, $Nd_2Ti_2O_7$	
	CRYS	1300	4		$Nd_4Ti_9O_{24}$
	CRYS	1300	12		$Nd_4Ti_9O_{24}$
	CRYS	1350	4		$Nd_4Ti_9O_{24}$
	RAW	1200	4		
	RAW	1300	4		$Nd_4Ti_9O_{24}$
	RAW	1300	12		$Nd_4Ti_9O_{24}$
$La_2Ti_2O_7$	CRYS	1200	4	$La_2Ti_2O_7$, Hollandite	
	CRYS	1300	4	Hollandite, $La_{0.66}TiO_{2.993}$	
	RAW	1200	4	Hollandite, $La_2Ti_2O_7$, $BaNd_2Ti_5O_{14}$	
	RAW	1300	4	$BaNd_2Ti_5O_{14}$, $Nd_4Ti_9O_{24}$, Hollandite, $La_2Ti_2O_7$, $La_{0.66}TiO_{2.993}$	
$CeTi_2O_6$	CRYS	1200	4	Hollandite, Brannerite	
	CRYS	1300	4		
	RAW	1200	4	Hollandite, CeO_2, TiO_2	
	RAW	1300	4		

In summary, there were some new phases that form in these dual phase systems. Nd titanate and Ga doped Ba hollandite systems, accompanied by Nd titanate and hollandite, all formed a $BaNd_2Ti_5O_{14}$ phase, some systems accompanied with a $Nd_4Ti_9O_{24}$ phase. As the hollandite structure is broken down and $BaNd_2Ti_5O_{14}$ is formed, which caused $Nd_2Ti_2O_7$ to transition to $Nd_4Ti_9O_{24}$, as well as a possible Ga and Cs titanate to form.

In the lanthanum titanate and Ga doped Ba hollandite systems the samples starting with the raw precursors formed identical phases to the Nd titanate samples, but in the systems using the crystalline phases as precursors, the La titanate underwent a reduction to a La perovskite. This is not an unfavorable phase in multiphase systems, however, if something is reducing, than something has to be oxidizing which could have a large impact on a multiphase system.

In the Ce titanate and Ga doped Ba hollandite systems, no reaction was seen regardless of the precursors.

Dual Phase samples for PCT testing

As previously stated, Nd was chosen to fabricate the lanthanide titanate to continue with further testing because it is the most prominent lanthanide in the waste stream. To begin sample preparation for PCT testing, a dilatometer was used on the dual phase system of Nd titanate and $Ba_{1.04}Cs_{.24}Ga_{2.32}Ti_{5.68}O_{16}$ hollandite to obtain a curve that related temperature to density. This was done in order to calculate what sintering temperature is required to achieve sample density above 80%. PCT requires approximately 15 g of each sample to run the test in triplicate. PCT samples consisted of single phase hollandite and Nd titanate, along with mixtures in varying volume fractions, as seen in Table 2-5. The dual phase samples were mixed thoroughly by ball milling in ethanol for 24 hours. The mixtures were strained and the milling balls and milling container were rinsed with ethanol to collect all of the mixture and then dried in an oven at 90 °C for 24 hours to remove the ethanol. These powders were pulverized and pressed into pellets and then sintered. The single phase hollandite and all the dual mixtures were sintered at 1350 °C to have little variation in processing. The single phase Nd titanate, however, required a higher sintering temperature and was sintered at 1400 °C.

Table 2-5. List of samples prepared for PCT testing.

Samples	Phase type	Chemical Formula	Volume Fraction H/P	Sample Name
Ga Hollandite 1	Single	$Ba_{1.04}Cs_{0.24}Ga_{2.32}Ti_{5.68}O_{16}$	100/0	H1
Ga Hollandite 2	Single	$Ba_{.667}Cs_{.667}Ga_2Ti_6O_{16}$	100/0	H2
Nd Titanate	Single	$Nd_2Ti_2O_7$	0/100	P1
Ga Hollandite + Nd Titanate		$Ba_{1.04}Cs_{0.24}Ga_{2.32}Ti_{5.68}O_{16}$+ $Nd_2Ti_2O_7$	70/30	HP1
		$Ba_{1.04}Cs_{0.24}Ga_{2.32}Ti_{5.68}O_{16}$+ $Nd_2Ti_2O_7$	50/50	HP2
		$Ba_{1.04}Cs_{0.24}Ga_{2.32}Ti_{5.68}O_{16}$+ $Nd_2Ti_2O_7$	30/70	HP3
		$Ba_{.667}Cs_{.667}Ga_2Ti_6O_{16}$+ $Nd_2Ti_2O_7$	70/30	HP4
		$Ba_{.667}Cs_{.667}Ga_2Ti_6O_{16}$+ $Nd_2Ti_2O_7$	50/50	HP5
		$Ba_{.667}Cs_{.667}Ga_2Ti_6O_{16}$+ $Nd_2Ti_2O_7$	30/70	HP6

As discussed previously, it is clear the dual phase systems are not staying dual phase systems, but instead splitting into multiphase systems. The second hollandite used in the dual systems being used for PCT testing, $Ba_{.667}Cs_{.667}Ga_2Ti_6O_{16}$, has also been examined using XRD to determine if other phases formed upon heating. It does appear that similar phase, such as $Nd_2Ti_2O_7$, hollandite, $BaNd_2Ti_5O_{14}$, and possible $Nd_4Ti_9O_{24}$, do form upon heating the crystalline phases together at 1350 °C and the amount of phases were estimated using Jade software and will be discussed later in the section 2.3.

To perform PCT testing, the samples had to be crushed into a powder with a particle size distribution +100/-200. First, a mechanical crusher to break up the pellets of each dual phase sample was used, followed by running the broken down pellets through sieves to achieve the desired particle size distribution. This process was repeated until approximately 5 g of desired particle size powder was obtained. Then the powders were run through five rinses with DI water followed by three rinses with ethanol to remove any powder that may be too fine that possibly did not go through the sieves. This powder is then dried and ready for PCT testing.

2.3 Discussion: Lattice Parameter changes and Phase composition changes vs Varying volume fractions of Dual phase systems

There are alternative phases shown to form in the Nd titanate and Ga doped Ba hollandite dual phase systems, such as Ba-Nd-Ti-O phases. However, how does the presence of this alternative phase in the two phase system affect the hollandite and Nd titanate targeted phases? Using Jade software, an estimation of each phase was obtained and compared to SEM images. The $BaNd_2Ti_5O_{14}$ phase however is not in the ICSD database yet and Jade does not have enough information to use this phase for an estimation, so in order to get an estimation of this phase a similar phase, $Ba_{3.75}Pr_{9.5}Ti_{18}O_{54}$, was used. $Ba_{3.75}Pr_{9.5}Ti_{18}O_{54}$ (ICSD# 201534) is another orthorhombic crystal structure with a z value of 1, where $BaNd_2Ti_5O_{14}$ has a z value of 4, and shares and identical XRD spectra to $BaNd_2Ti_5O_{14}$. There is a small difference in peak intensity between the two phases, but the locations of the peaks are almost identical, so this $Ba_{3.75}Pr_{9.5}Ti_{18}O_{54}$ spectra was used as a surrogate for the estimations.

There has been work done on the differences between the two hollandites used in the dual phases systems, comparing the lattice parameter change as the Cs in the single phase hollandite structure

was increased. According to Xu et al[20], As the Cs occupancy in the a site of the hollandite crystal structure is increased, the lattice parameter a increases. This is crucial because Yun et al shows how Cs occupancy changes the microstructure of the hollandite, which can change the properties in the multiphase samples.

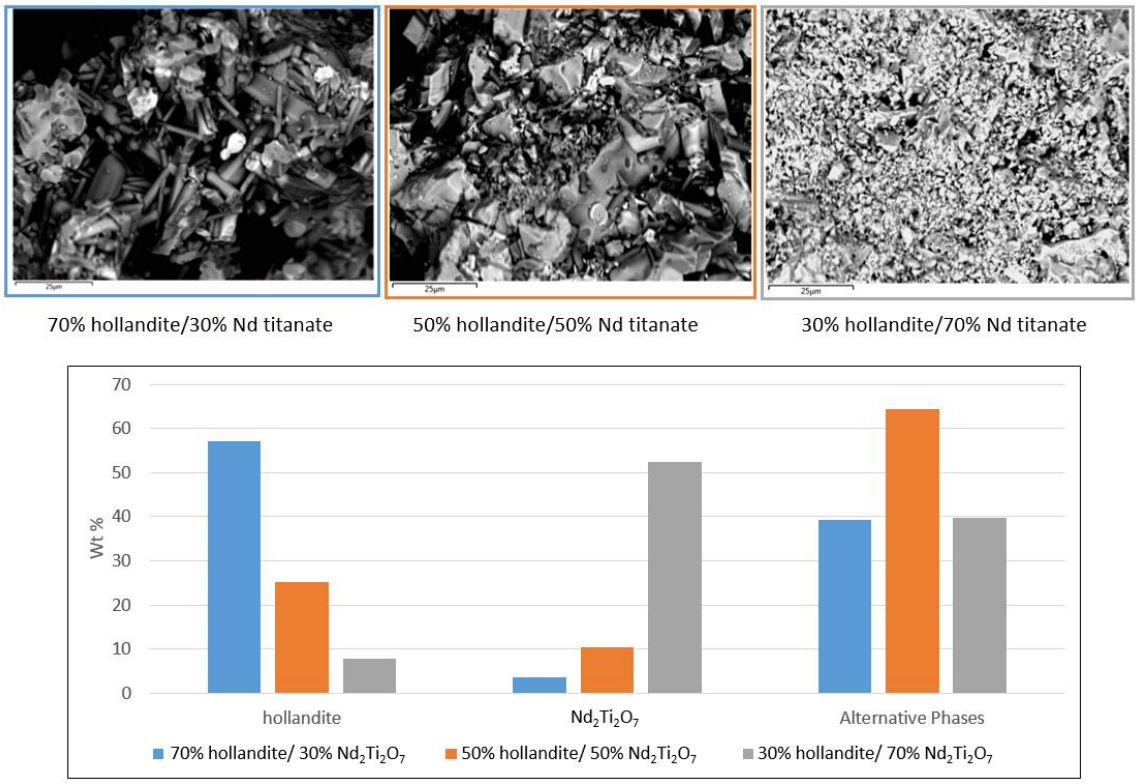

Figure 2-11. Bar graph of estimated phase composition of three samples from PCT testing. These dual phase samples precursors were $Ba_{1.04}Cs_{0.24}Ga_{2.32}Ti_{5.68}O_{16}$ and $Nd_2Ti_2O_7$ in varying volume fractions. These phase compositions are estimates using refinements in Jade software. The SEM images above the graph are images of each of the samples with varying volume fraction.

Shown in Figure 2-11, is the estimated phase composition of the first three PCT samples with varying volume fractions, labeled as HP1, HP2, and HP3 in Table 2-5. The SEM images above the graph show the vast difference in phase formation. In the first SEM image, representing the 70% hollandite and 30% Nd titanate, hollandite is the majority phase in the sample with a few grains

of the Ba-Nd-Ti-O phase, and both Nd titanates. This is supported by the bar graph showing a majority of the phase is estimated to be hollandite, with some $BaNd_2Ti_5O_{14}$ and both Nd titanates.

In the second image, 50% hollandite and 50% Nd titanate, the SEM image shows the majority phase present is a Ba-Nd-Ti-O phase, which is supported by the estimations in the bar graph where approximately 65% alteration phases. Some hollandite remains in this sample as well in the center of the SEM image.

In the third SEM image, the 30% hollandite and 70% Nd titanate sample, shows a majority of the phases present is Nd titanates as a mixture of $Nd_2Ti_2O_7$ and $Nd_4Ti_9O_{24}$. According to the estimations in the bar graph, and confirmed by EDS, the majority of the Nd titanate is present as $Nd_2Ti_2O_7$.

It is important to note the large amount of alternative phases formed in these three dual phase systems. This is important because the PCT test is no longer testing a dual phase system of hollandite and titanate, but rather a multiphase system that is 40 to 65% secondary phases. Even the samples that were primarily hollandite or Nd titanate showed a significant amount of these alternative phases forming, making up approximately a total of 40% of the samples. Alternative phases forming has been reported in similar systems. Lin et al[45] had alteration phases occur in a $Ce_{0.8}Gd_{0.2}O_{2-\delta}$- $CoFe_2O_4$ composite being examined for enhancing grain boundary ionic conductivity.

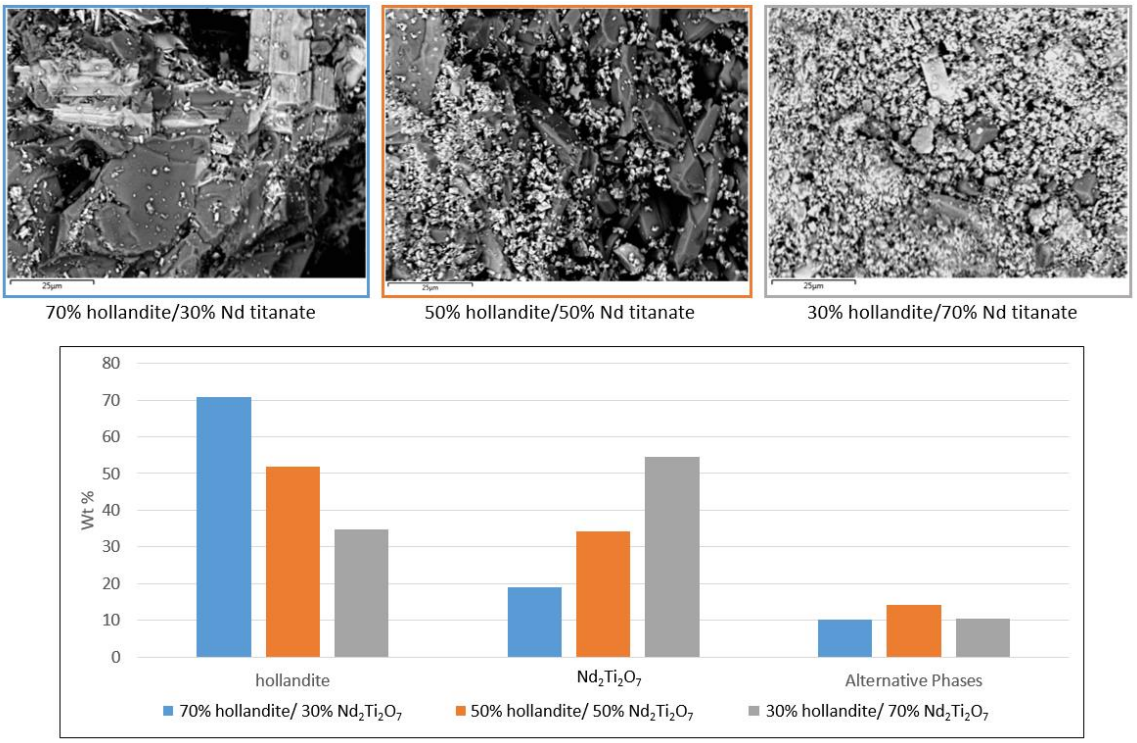

Figure 2-12. Bar graph of estimated phase composition of three samples from PCT testing. These dual phase samples precursors were $Ba_{.667}Cs_{.667}Ga_2Ti_6O_{16}$ and $Nd_2Ti_2O_7$ in varying volume fractions. These phase compositions are estimates using refinements in Jade software. The SEM images above the graph are images of each of the samples with varying volume fraction.

The last three dual phase systems, whose estimated phase composition is shown in Figure 2-12, showed much less alternative phase formation than the $Ba_{1.04}Cs_{0.24}Ga_{2.32}Ti_{5.68}O_{16}$ hollandite systems. These systems correspond to the $Ba_{.667}Cs_{.667}Ga_2Ti_6O_{16}$ and $Nd_2Ti_2O_7$ dual phase systems that are labeled as HP4, HP5, and HP6 in Table 2-5. The SEM images above the graph in Figure 2-12 correspond to each of the systems with changing volume fraction. The first SEM image (right) shows the majority of that system is hollandite, where the second image shows a fairly even mixture of hollandite and Nd titanate, and the third image (left) shows the majority of the sample is Nd titanate.

These $Ba_{.667}Cs_{.667}Ga_2Ti_6O_{16}$ hollandite systems appear to be more stable upon heating, with only a combined estimated 10-15% of Secondary phases forming in all three samples. This is due to the increased stability of the hollandite with the increased Cs in the structure[20]. However, Xu et al[20] show this increase of stability of the hollandite structure also leads to an increase in the tunnel size in the structure of hollandite. This increase of tunnel size allows for greater ion mobility, which could possibly explain why the $Ba_{.667}Cs_{.667}Ga_2Ti_6O_{16}$ hollandite has a larger elemental release compared to the less stabile $Ba_{1.04}Cs_{0.24}Ga_{2.32}Ti_{5.68}O_{16}$ hollandite. This leads to the need to investigate the optimal Cs loading in hollandite to balance stability and resistance to Cs release. These $Ba_{.667}Cs_{.667}Ga_2Ti_6O_{16}$ hollandite systems will be more accurate for PCT testing on the targeted dual phase systems, even though there is some alternative phases forming, the majority of the samples remain to be the hollandite and Nd titanate precursors.

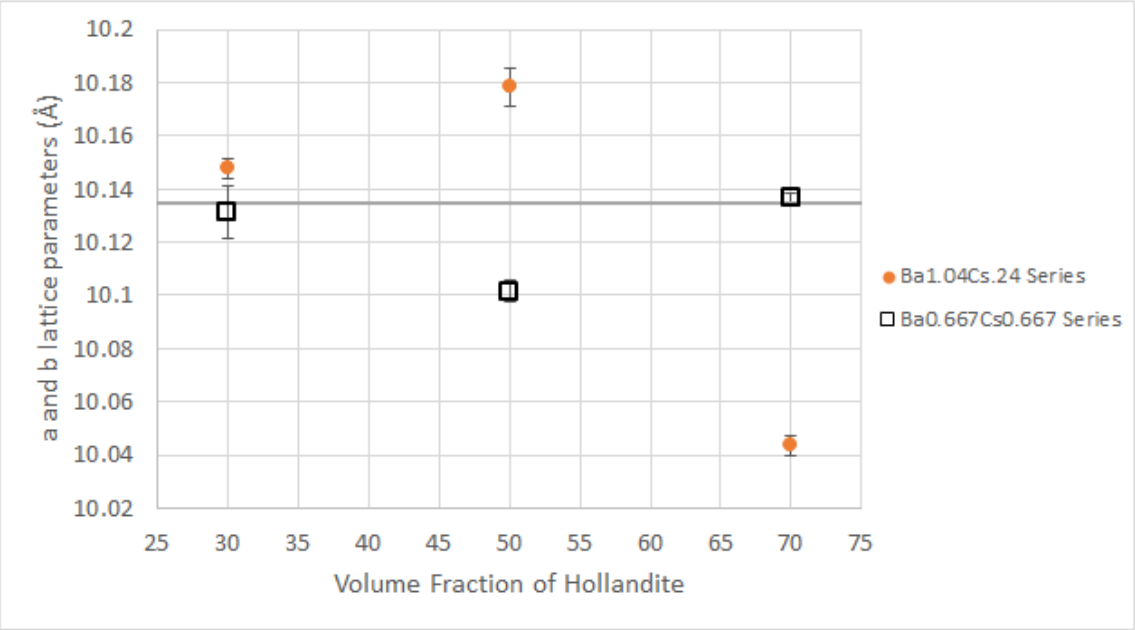

Figure 2-13. Plot of a axis lattice parameters of hollandite as a function of increasing volume fraction in dual phase samples. The grey line across the graph is a literature value for a axis lattice parameter for hollandite (ICSD # 68730).

Figure 2-13 shows a plot of a axis lattice parameters for the two different hollandites in the dual phase systems as volume fraction of hollandite is increased. This plot also represents the b axis lattice parameters of the hollandites due to the tetrahedral crystal structure, where a=b. There is no discernable trend as volume fraction increase with either hollandite composition. However, it does appear that the $Ba_{.667}Cs_{.667}Ga_2Ti_6O_{16}$ hollandite remained consistently closer to the accepted literature value for the a axis lattice parameter. This lattice parameter stability, along with the its ability to remain in the hollandite phase in the dual phase systems well compared to the hollandite with the lower targeted Cs content, seen in Figure 2-12, show that $Ba_{.667}Cs_{.667}Ga_2Ti_6O_{16}$ hollandite is more stable than the $Ba_{1.04}Cs_{0.24}Ga_{2.32}Ti_{5.68}O_{16}$ hollandite.

Chapter 3. Dissolution Studies of Single and Dual Phase Ceramics by Product Consistency Testing

3.1 Motives and Objectives

PCT is a method to examine the quantitative dissolution of elements over time. This is an important test to utilize when examining waste forms for nuclear immobilization due to the many radionuclides they contain. There has been a lot of previous work using PCT to examine glass waste forms, as well as some work examining some ceramic waste forms. However there has been no work examining dual phase samples and how being in contact with other phases could affect these individual phases.

This work will use PCT to examine dissolution of single and dual phase samples. The samples were prepared at Clemson University, but the samples were prepped and the test was carried out at SRNL in July of 2016. The samples are listed previously in Table 2-5. Using the information from PCT on single and dual phase samples, a model can begin to be developed on the leachability of ceramic waste forms inside a repository environment.

The procedure for PCT testing has already been outlined in chapter 1, and the sample preparation has been discussed in chapter 2.

3.2 Results and Discussion

To recall, there were three dual phase samples fabricated using $Ba_{1.04}Cs_{0.24}Ga_{2.32}Ti_{5.68}O_{16}$ hollandite, as well as three samples using $Ba_{.667}Cs_{.667}Ga_2Ti_6O_{16}$ hollandite, shown in Figure 4.1. These hollandites were mixed with Nd titanate, $Nd_2Ti_2O_7$, in varying volume fractions, which were than tested for leachability using PCT.

Table 3-1. List of samples prepared for PCT testing with some basic information about each sample.

Samples	Phase type	Chemical Formula	Volume Fraction H/P	Sample Name
Ga Hollandite 1	Single	$Ba_{1.04}Cs_{0.24}Ga_{2.32}Ti_{5.68}O_{16}$	100/0	H1
Ga Hollandite 2	Single	$Ba_{.667}Cs_{.667}Ga_2Ti_6O_{16}$	100/0	H2
Nd Titanate	Single	$Nd_2Ti_2O_7$	0/100	P1
Ga Hollandite + Nd Titanate		$Ba_{1.04}Cs_{0.24}Ga_{2.32}Ti_{5.68}O_{16}$+ $Nd_2Ti_2O_7$	70/30	HP1
		$Ba_{1.04}Cs_{0.24}Ga_{2.32}Ti_{5.68}O_{16}$+ $Nd_2Ti_2O_7$	50/50	HP2
		$Ba_{1.04}Cs_{0.24}Ga_{2.32}Ti_{5.68}O_{16}$+ $Nd_2Ti_2O_7$	30/70	HP3
		$Ba_{.667}Cs_{.667}Ga_2Ti_6O_{16}$+ $Nd_2Ti_2O_7$	70/30	HP4
		$Ba_{.667}Cs_{.667}Ga_2Ti_6O_{16}$+ $Nd_2Ti_2O_7$	50/50	HP5
		$Ba_{.667}Cs_{.667}Ga_2Ti_6O_{16}$+ $Nd_2Ti_2O_7$	30/70	HP6

To obtain normalized Cs release, the following equations were used[32]:

$$NC_{Cs} = \frac{C_{Cs}}{f_{Cs}} \qquad [1]$$

$$NL_{Cs} = \frac{NC_{Cs}}{SA/V} \qquad [2]$$

where NC_{Cs} is the normalized concentration of Cs (g/L), C_{Cs} is the concentration of Cs in the solution from the PCT test (g/L), f_{Cs} is the mass fraction of Cs in the sample before PCT testing, NL_{Cs} is the normalized Cs release (g/m^2), SA is the surface area of the sample (m^2), and V is the volume of leachate used in the PCT test (L). There were assumptions made to obtain the surface

area used in equation 2. The first assumption was that particles were spherical, and the second assumption was that the average diameter of the particles was based off the sieves used which was +100/-200, equaling an average particle diameter of 112.5 µm

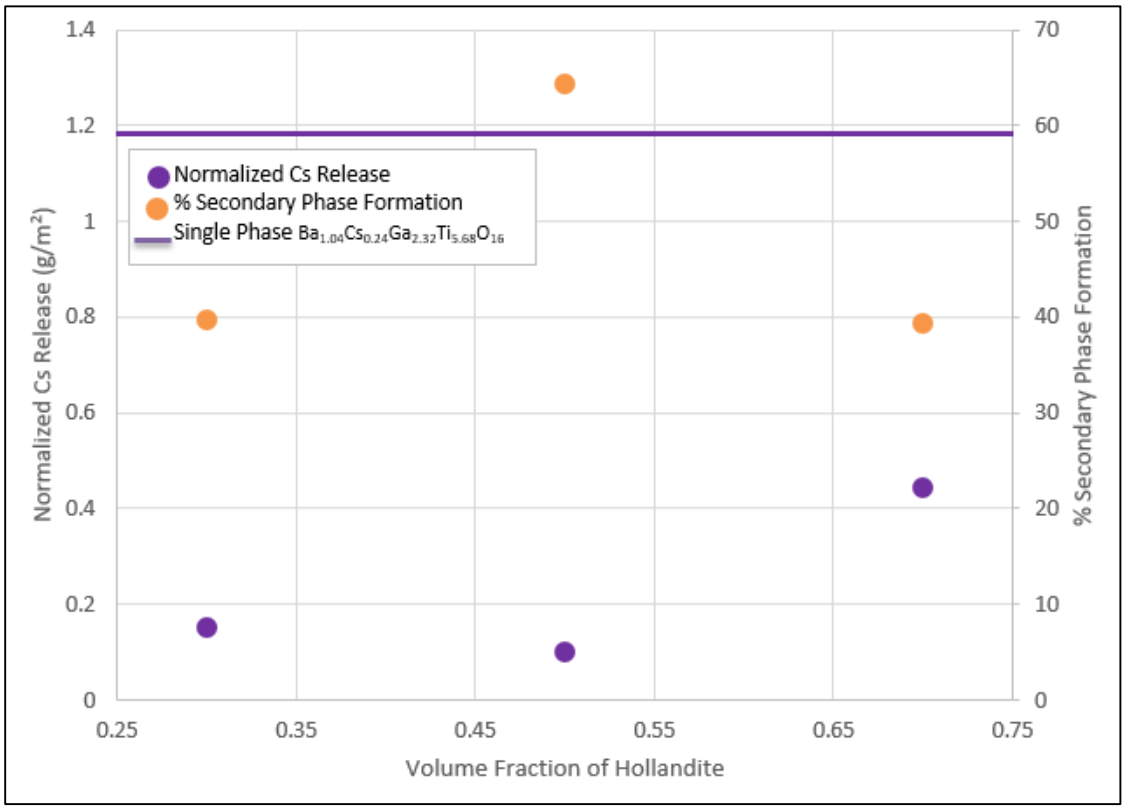

Figure 3-1. Normalized Cs release in the dual phase system as volume fraction of hollandite increases. This data corresponds to samples labeled HP1, HP2, and HP3, fabricated using $Ba_{1.04}Cs_{0.24}Ga_{2.32}Ti_{5.68}O_{16}$ hollandite.

Normalized concentrations of Cs in the leachate from the PCT were calculated from data collected using ICP-MS and reported as volume fraction of hollandite in the systems increased, shown in Figure 3-1. The tests are done in triplicate so a standard deviation can be calculated. The standard deviation for the sample with a hollandite volume fraction of 0.3 are small (+/- 0.002 g/m^2), making them close to the center of the data point and hard to see. The samples with hollandite volume fractions of 0.5 and 0.7 were only ran in duplicate thus not allowing a standard deviation

calculation. However, all the other dual phase systems standard deviation were relatively small, so it is assumed that these values are acceptable.

It appears that the 50/50 volume fraction of $Ba_{1.04}Cs_{0.24}Ga_{2.32}Ti_{5.68}O_{16}$ hollandite and Nd titanate had the best resistance to Cs loss, which was the sample that has the most alternative phases form. This could possibly be due to a shielding effect of the secondary phases that do not contain Cs surrounding the hollandite and preventing aqueous leaching. The Cs in this 50/50 hollandite Nd titanate system appears to remain in the hollandite, however, as the hollandite structure is degraded from secondary phases formed, a Ga titanate forms, which also contains Cs. This phase is not present in the XRD spectra but could be lost due to sharing peaks with other phases in the sample. The pure hollandite phase showed the worse resistance to Cs loss when compared with the dual phase samples, but this could be attributed to having no shielding due to secondary phase formation that is found in the dual phase samples.

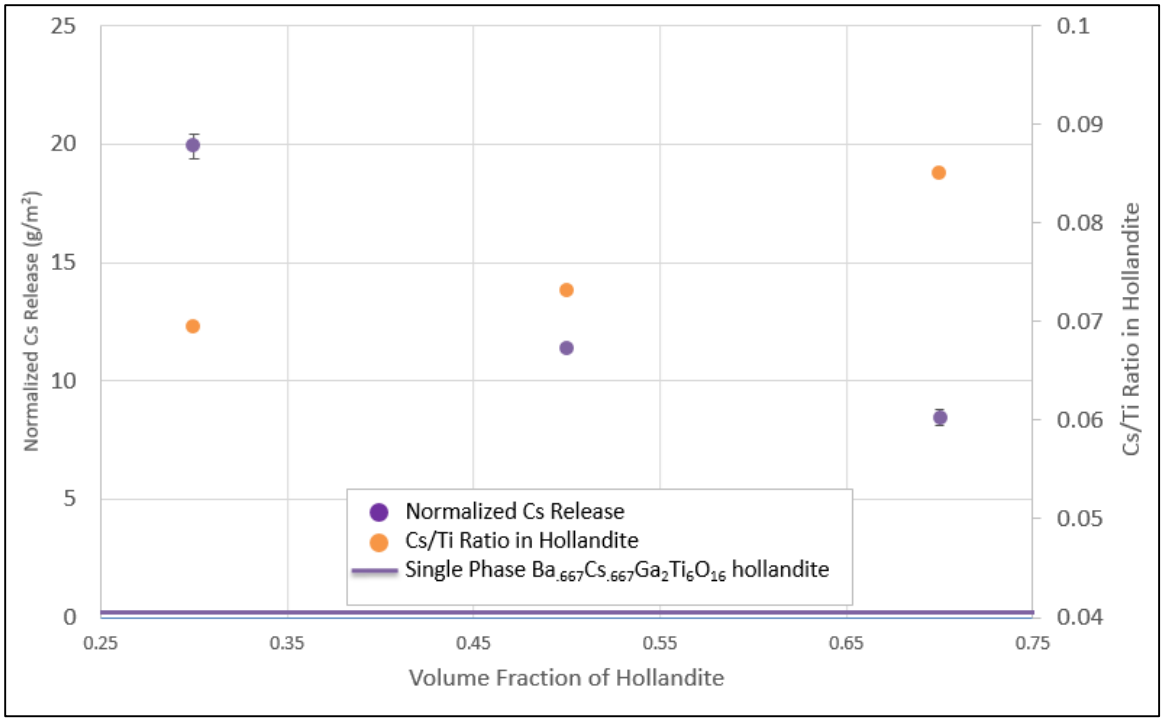

Figure 3-2. Normalized Cs release in the dual phase system as volume fraction of hollandite increases compared to the ratio of Cs to Ti in the hollandites. This data corresponds to samples labeled HP4, HP5, and HP6, fabricated using $Ba_{.667}Cs_{.667}Ga_2Ti_6O_{16}$ hollandite.

Shown in Figure 3-2 is the normalized concentrations of Cs found in leachate as the volume fraction of $Ba_{.667}Cs_{.667}Ga_2Ti_6O_{16}$ hollandite is increased. The standard deviation for the hollandite volume fraction of 0.5 is very small (+/- 0.075 g/m^2), as well as for the pure hollandite sample (+/- 0.006 g/m^2) so they are not visible in the figure. The Cs/Ti ratios shown were calculated using averages of atomic percentages in the hollandites of the samples which were found using EDS.

There is a clear trend that shows the normalized Cs release decreases as the volume fraction of hollandite is increased. The normalized release of Cs also decreases with increasing Cs in the hollandite structure, meaning that the hollandite is more stable with more Cs in the structure, which is supported with work done by Yun et al[20]. However, if you compare the $Ba_{.667}Cs_{.667}Ga_2Ti_6O_{16}$ hollandite systems in Figure 3-2, to the $Ba_{1.04}Cs_{0.24}Ga_{2.32}Ti_{5.68}O_{16}$ hollandite

systems in Figure 3-1, the normalized release of the $Ba_{.667}Cs_{.667}Ga_2Ti_6O_{16}$ hollandite systems is higher. This could be due to the larger amount of alternative phases formed in $Ba_{1.04}Cs_{0.24}Ga_{2.32}Ti_{5.68}O_{16}$ hollandite systems acting as a shield to aqueous dissolution of the hollandite.

The PCT-B results for Cs loss in the dual phase systems are listed in Table 3-2 as both normalized concentration of Cs (NC_{Cs}) as well as normalized Cs release (NL_{Cs}) to easily make comparisons to literature. Some available single, dual, and glass literature values are shown in Table 3-3. Compared to the single phase hollandite, the glass, and the multiphase literature values are all comparable to the Ga doped Ba hollandite and Nd titanate dual phase systems.

Table 3-2. PCT-B results for Cs loss in dual phase systems

Sample	Volume Fraction of hollandite	NCcs (g/L)	NLcs (g/m2)
HP1	0.7	7.81E-01	4.42E-01
HP2	0.5	1.81E-01	1.02E-01
HP3	0.3	2.25E-01	1.51E-01
HP4	0.7	1.31E+01	8.47E+00
HP5	0.5	1.72E+01	1.14E+01
HP6	0.3	2.56E+01	1.99E+01

Table 3-3. PCT-B Results for Cs loss in powdered samples all performed in Deionized Water. Concentrations labeled with *1 next to them are Normalized Mass loss (g/m^2)

Compound	Structure	Temperature (°C)	Time (d)	Normalized Concentration (g/L)	Reference
Single Phase Hollandite	Al-18 Hollandite	90	7	6.20E-01	41
	Al-12 Hollandite	90	7	5.20E-01	
	Mg-18 Hollandite	90	7	1.30E+00	
	Mg-12 Hollandite	90	7	2.80E+00	
Glass Ceramic Composite	5.86% MoO_3	90	3	1.40E-01	40
	6.25% MoO_3	90	3	1.50E-01	
	6.94% MoO_3	90	3	2.70E-01	
	5.86% MoO_3	90	28	1.90E-01	
	6.25% MoO_3	90	28	1.30E-01	
	6.94% MoO_3	90	28	1.80E-01	
Multiphase Ceramic	CSLNTM-02	90	7	2.88E+00 *1	35
	CSLNTM-06	90	7	3.34E+00 *1	
	CSLNTM-11	90	7	9.62E+00 *1	
Multiphase Ceramic	CS/LN-03	90	7	4.41E+01	36
	CS/LN-04	90	7	3.24E+01	
	CS/LN-05	90	7	4.48E+01	
	CS/LN/TM Mo-02	90	7	3.80E+01	
	CS/LN/TM Mo-03	90	7	2.81E+01	
	CS/LN/TM Mo-04	90	7	2.37E+01	
	CS/LN/TM Mo-05	90	7	2.51E+01	

After examining the results from the PCT, it is clear from the results of the dual phase system of $Ba_{.667}Cs_{.667}Ga_2Ti_6O_{16}$ hollandite and Nd titanate that as the volume fraction of hollandite increases in a system, the less dissolution that occurs, meaning the hollandite structure is more stable. The hollandite structure is also stabilized by having more Cs in the structure. The results from the $Ba_{1.04}Cs_{0.24}Ga_{2.32}Ti_{5.68}O_{16}$ and Nd titanate dual phase systems does not show the same trend, however this is possibly due to a shielding effect that the secondary phases is having on the hollandite.

Chapter 4. Accelerated Aging of Ceramic Waste forms by Vapor Hydration Testing

4.1 Motives and Objectives

VHT is useful for examining the alteration phases of waste forms by using a vapor environment to speed up the aging process that occurs in a repository environment. This is important because with a multiphase ceramic system containing very mobile elements, such as Cs, it is important to know all the possible phases that could form and whether they are harmful to the environment. There has been very little previous work with VHT on ceramic waste forms, especially multiphase ceramic waste forms.

This work will use VHT to examine the alteration and aging of single, dual, and multiphase ceramic waste forms, shown in Table 4-1. The samples were all marked using a diamond encrusted blade so the same locations could be examined before and after VHT using XRD, SEM, and EDS. Using these analytical techniques, not only can the phases in the samples be determined before VHT, but a probable idea of what alternative phases, if any, form. This insight into what alternative phases may form is important when planning the long term storage of waste forms in a repository with less than ideal conditions.

Table 4-1. List of samples for VHT

Samples	Phase type	Chemical Formula	Sample Prep	Observations of Samples
Fe Hollandite	Single		Melted in Al_2O_3 crucible received from SRNL	Two different hollandites observed, one higher in Al
Ga Hollandite		$Ba_{1.04}Cs_{0.24}Ga_{2.32}Ti_{5.68}O_{16}$	Melted in Al_2O_3 crucible	Some secondary Cs titanate and Ga titanate
Ga Hollandite		$Ba_{1.04}Cs_{0.24}Ga_{2.32}Ti_{5.68}O_{16}$	Conventionally sintered pellet made through oxide route	
Ga Hollandite		$Ba_{1.04}Cs_{0.24}Ga_{2.32}Ti_{5.68}O_{16}$	Sintered by SPS, made by oxide route	
Ga Hollandite + Nd Pyrochlore	Dual	$Ba_{1.04}Cs_{0.24}Ga_{2.32}Ti_{5.68}O_{16}$+ $Nd_2Ti_2O_7$ (50/50 mix by Volume Fraction)	Sintered pellet made through oxide route	Alternate phases have been observed in these samples
CAF Hollandite	Multiphase		Melted and poured into S.S. Crucible received from SRNL	Pyrochlore, Hollandite, Zirconolite, Al2O3, and Rutile
Fe Analogue Hollandite				

4.2 Single Phase Ceramic Waste Forms

Single phase VHT focused on the single phase hollandites due to Cs being the one of the most mobile and problematic elements trying to be incorporated into the structures of the ceramic waste forms. Cs is also what many researchers have used to measure leaching in ceramic waste forms, whether single or multiphase[46,33,47,48,5,6,36,35].

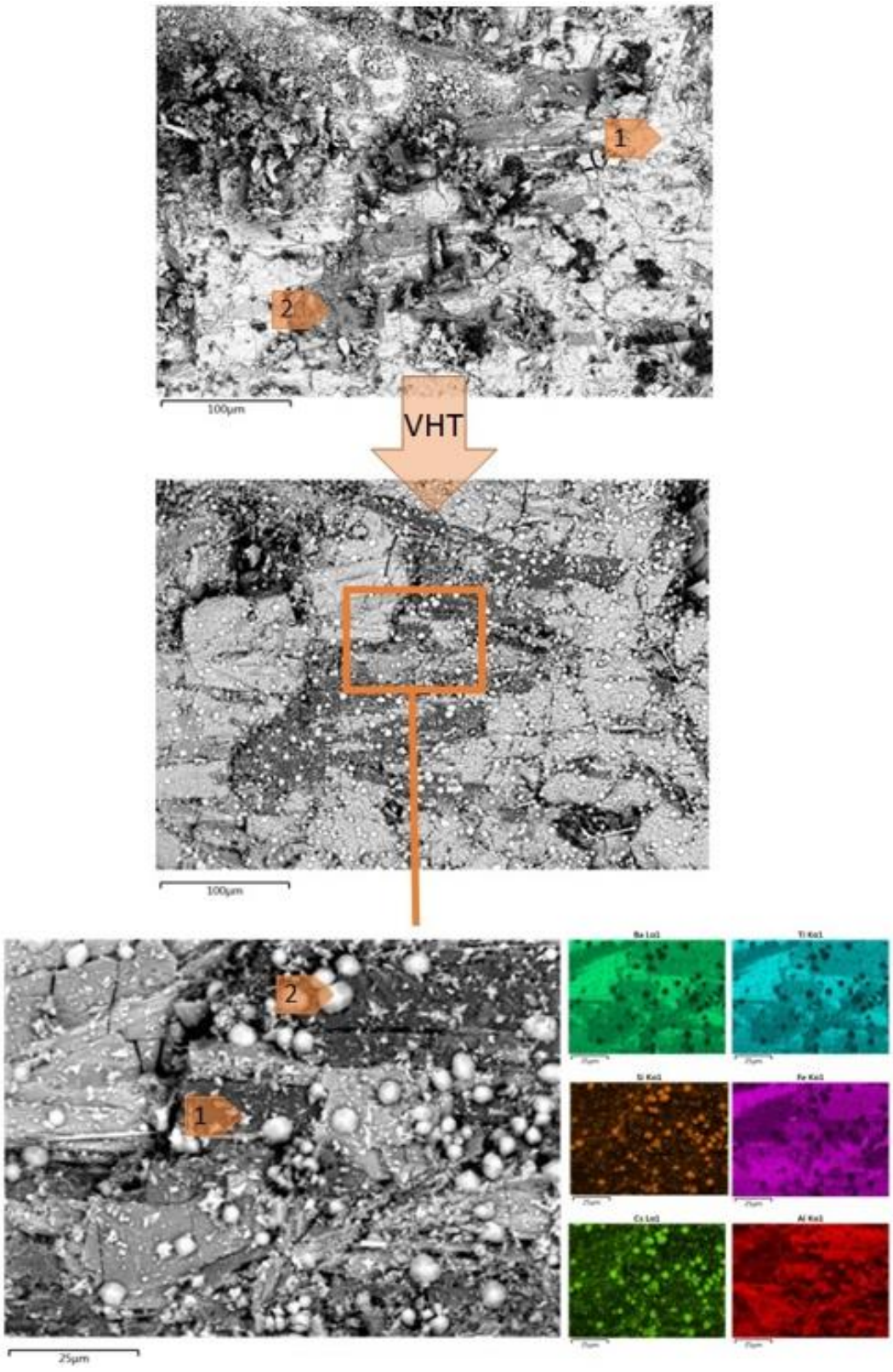
1
2
100µm
VHT
100µm
2
1
25µm
Ba Lα1
Ti Kα1
Si Kα1
Fe Kα1
Cs Lα1
Al Kα1

Figure 4-1. Single phase Fe hollandite melted in an Al_2O_3 crucible, received from SRNL. (A) Sample before VHT where phases are labeled in Table 2 (B) Sample after VHT where phases are labeled in Table 4-2.

Table 4-2. Crystalline phases for SEM images of single phase Fe hollandite in Figure 4-1. (*Crystalline phases determined by XRD results and EDX elemental analysis)

A	Location	Elements	Crystalline Phases*
	1	O, Ti, Fe, Ba, Al, Cs	Hollandite
	2	O, Ti, Fe, Al, Ba, Cs	Hollandite
B	Location	Elements	Crystalline Phases (possible)
	1	O, Cs, Al, Ti	Cs-Ti-Al-O
	2	O, Cs, Al, Ti, Si	Cs-Ti-Al-O

Figure 4-1 shows a single phase Fe hollandite melted in an Al_2O_3 crucible that was received from SRNL, before and after VHT. The hollandite crystal structure was confirmed using XRD and EDX elemental analysis. There were two hollandites observed in the sample, seen in Figure 4-1, one being slightly higher in aluminum, which was determined by EDX elemental analysis.

After VHT, two new phases were found on the surface of the single phase Fe hollandite sample, both phases being a Cs-Ti-Al-O phase. However, the two Cs-Ti-Al-O phases appears to have to different structures, seen in Figure 4-1, where one is spherical, containing small amounts of Si, and one that has an irregular structure, neither of which are confirmed to be crystalline. These Cs-Ti-Al-O phases were speculated only using EDX elemental analysis.

The three single phase Ga doped hollandites that were processed by conventional sintering, melting, and SPS, and the results of their VHT will be discussed in Chapter 5.

4.3 Dual Phase Nd Titanate and $Ba_{1.04}Cs_{0.24}Ga_{2.32}Ti_{5.68}O_{16}$

VHT was conducted on the dual phase sample of $Nd_2Ti_2O_7$ and $Ba_{1.04}Cs_{0.24}Ga_{2.32}Ti_{5.68}O_{16}$ for 30 days. This dual phase system corresponds to PCT sample label HP2, which is a 50/50 volume fraction of Nd titanate and Ga doped Ba hollandite, made by using the crystalline Nd titanate and hollandite as precursors. SEM images of pre VHT and post VHT is shown in Figure 4-2, with phase matches in Table 4-3, where there is no change that occurred from VHT. Note that the EDS mapping for Ba is not shown because the Ti and Ba energies overlap, so the Ti EDS map is identical to the Ba. There are a few reasons that could explain why there was no change due to VHT. The most likely reason no change occurred during VHT is due to not having a good seal on the reaction vessel. Once this test was complete, it was noted that the amount of water in the container was almost completely absent. This could have possibly been caused by a bad gasket on the VHT vessel.

A.

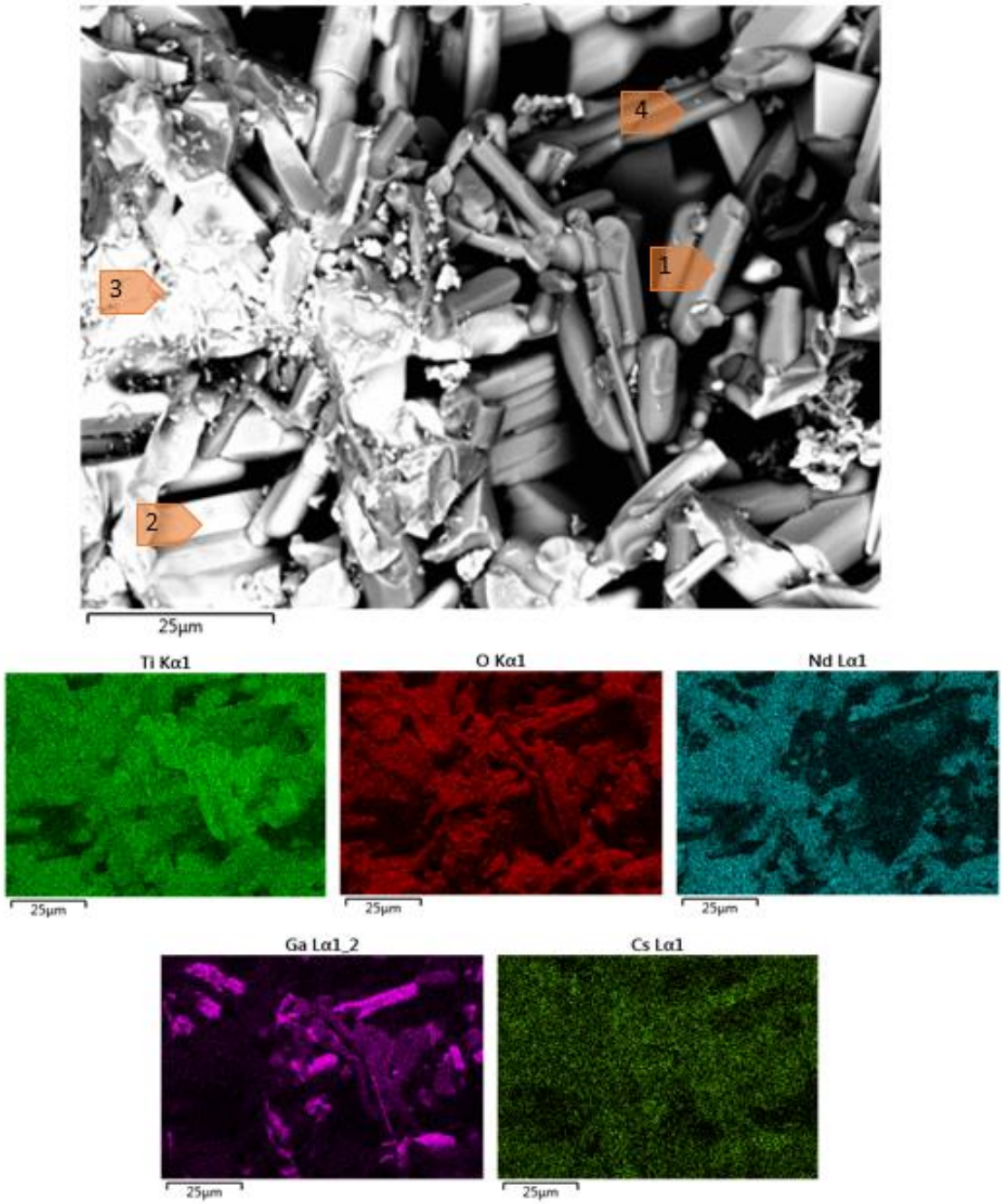
4
1
3
2
25µm
Ti Kα1
25µm
O Kα1
25µm
Nd Lα1
25µm
Ga Lα1_2
25µm
Cs Lα1
25µm

B.

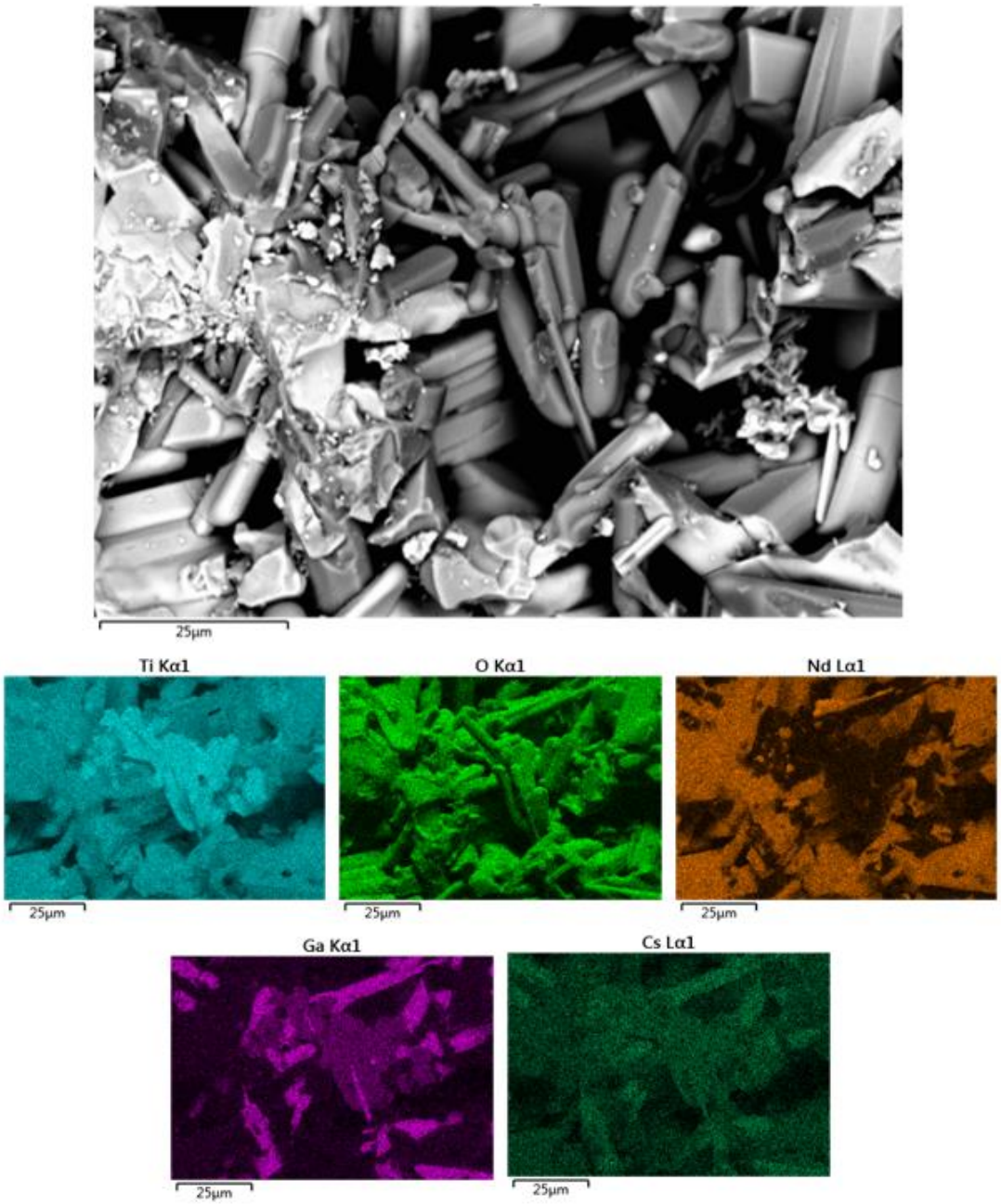

Figure 4-2. Nd titanate and Ga doped Ba hollandite dual phase mixed in 50/50 volume fraction (A) before VHT (B) After VHT.

Table 4-3. Crystalline Phases for SEM images in Figure 4-2(A) and 4-2(B) (*Crystalline phases determined by XRD results and EDX elemental analysis)

	Location	Elements	Crystalline Phases
A	1	O, Ti, Ba, Ga, Cs	Hollandite*
	2	O, Ti, Nd, Ba	$BaNd_2Ti_5O_{14}$*
	3	O, Ti, Nd	Nd titanates*
	4	O, Ti, Ga, Cs	

4.4 Multiphase Ceramic Waste Forms

4.4.1 Cr, Al, Fe doped Hollandite Multiphase

The Cr, Al, Fe (CAF) doped hollandite multiphase samples were melted and poured into a stainless steel crucible at SRNL. VHT results for the CAF hollandite multiphase are shown in Figure 4-3 and 4-4, with phases shown in Tables 4-4 and 4-5, respectively. The phases of the multiphase ceramic waste forms were confirmed by XRD analysis EDX elemental analysis, with the aid of previous work done on this particular multiphase waste form[39]. However, the alternative phases shown after VHT are possible phases only determined by SEM/EDS. Note that the EDS mapping for Ba is not shown because the Ti and Ba energies overlap, so the Ti EDS map is identical to the Ba.

A.

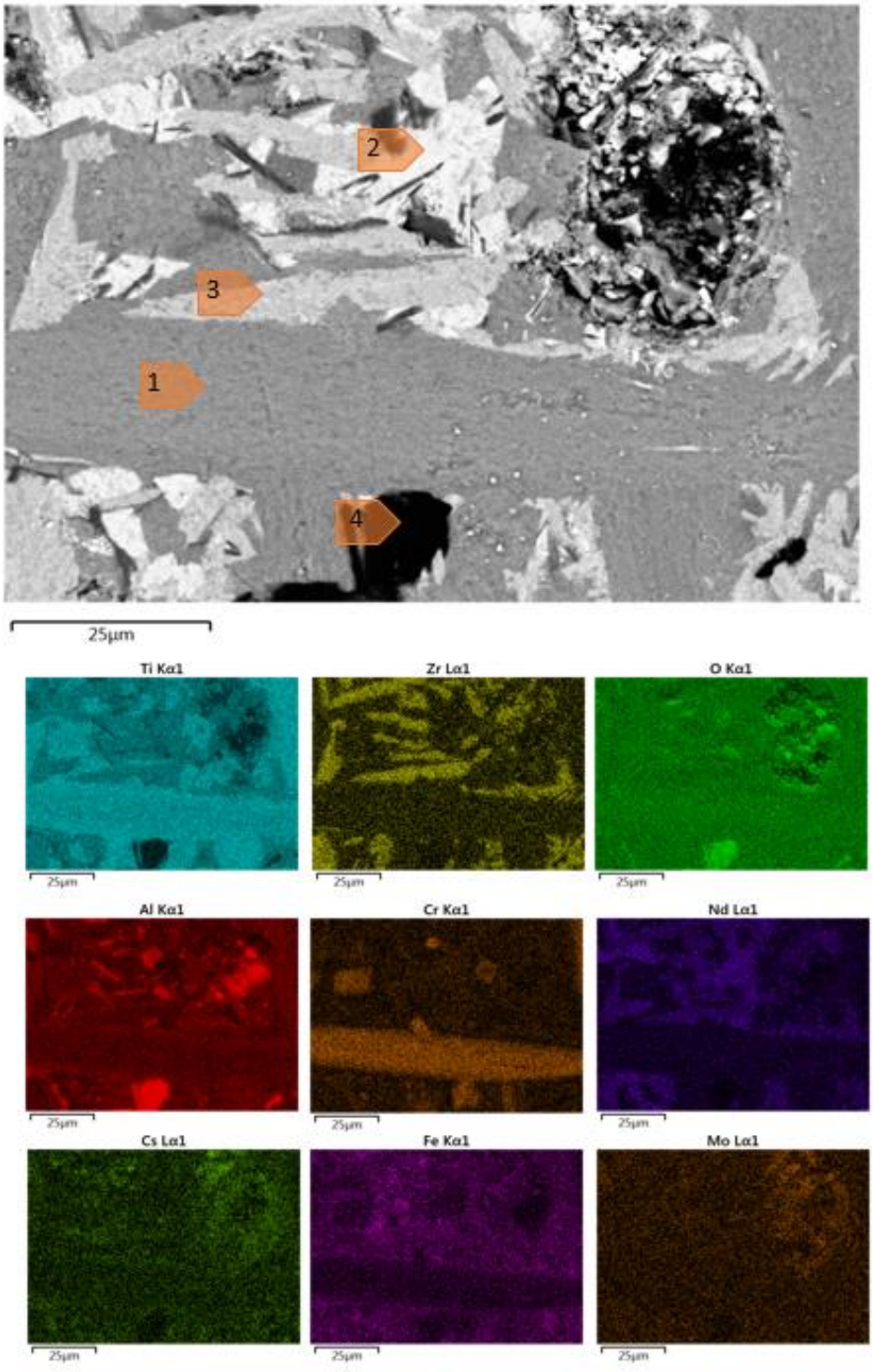
2
3
1
4
25µm
Ti Kα1
Zr Lα1
O Kα1
Al Kα1
Cr Kα1
Nd Lα1
Cs Lα1
Fe Kα1
Mo Lα1

B.

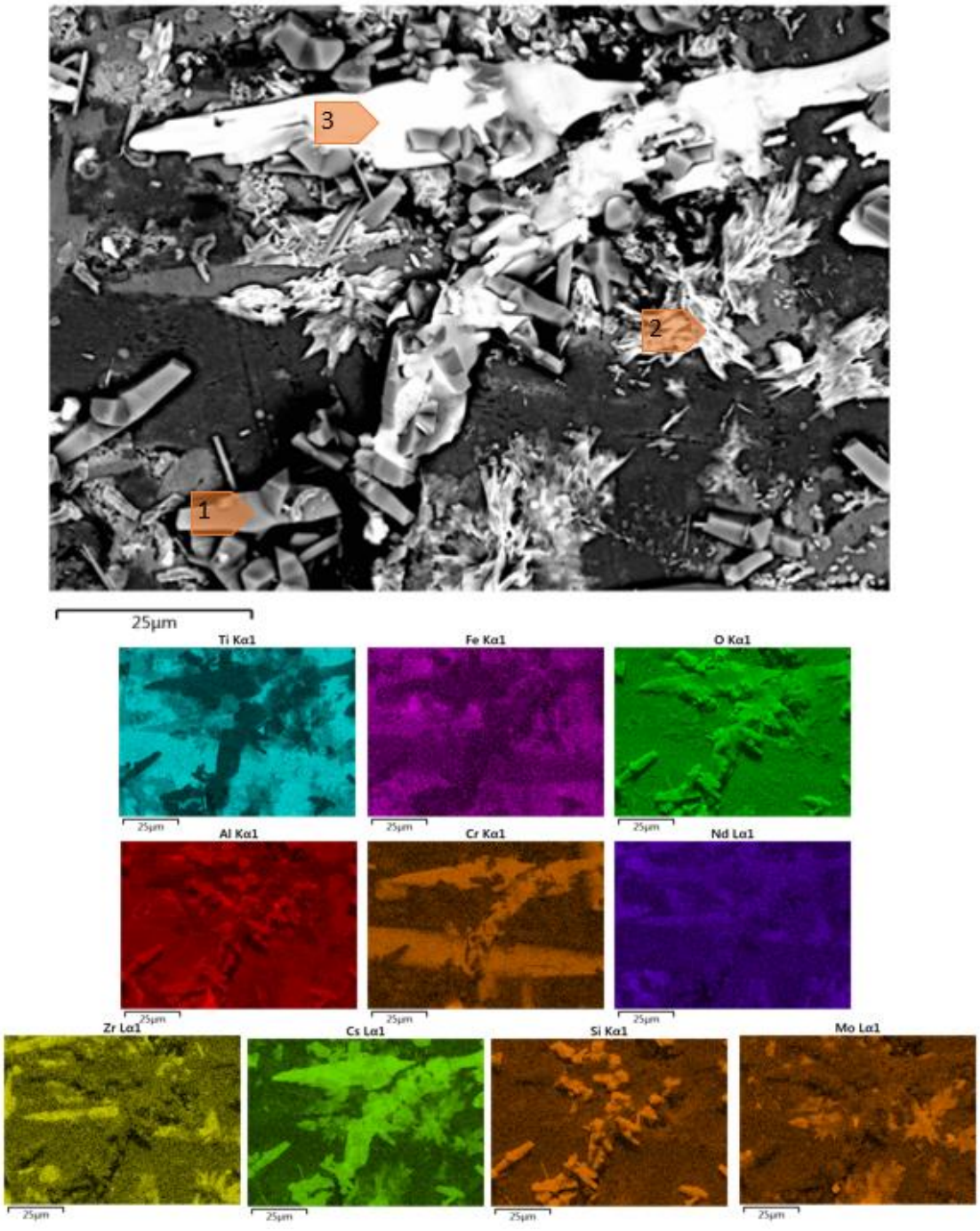
3
2
1
25µm
Ti Kα1
Fe Kα1
O Kα1
Al Kα1
Cr Kα1
Nd Lα1
Zr Lα1
Cs Lα1
Si Kα1
Mo Lα1

Figure 4-3. Cr, Al, Fe (CAF) doped hollandite multiphase sample taken from the side of a bulk sample very close to the stainless steel crucible. (A) Sample before VHT where phases are labeled in Table 4-4 (B) Sample after VHT where phases are labeled in Table 4-4.

Table 4-4. Crystalline Phases for SEM images in Figure 4-3(A) and 4-3(B) (*Crystalline phases determined by XRD results and EDX elemental analysis)

	Location	Elements	Crystalline Phases*
A	1	O, Ti, Ba, Cr, Al, Fe, Cs	Hollandite
	2	O, Ti, Nd, Ce	Pyrochlore
	3	O, Ti, Zr, Ca	Zirconolite
	4	O, Al	Al_2O_3
B	Location	Elements	Crystalline Phases (possible)
	1	O, Cs, Al, Ti	Cs-Ti-Al-O
	2	O, Ti, Cs, Mo	Cs_2MoO_4
	3	O, Cs, Cr,	Cs_2CrO_4

A.

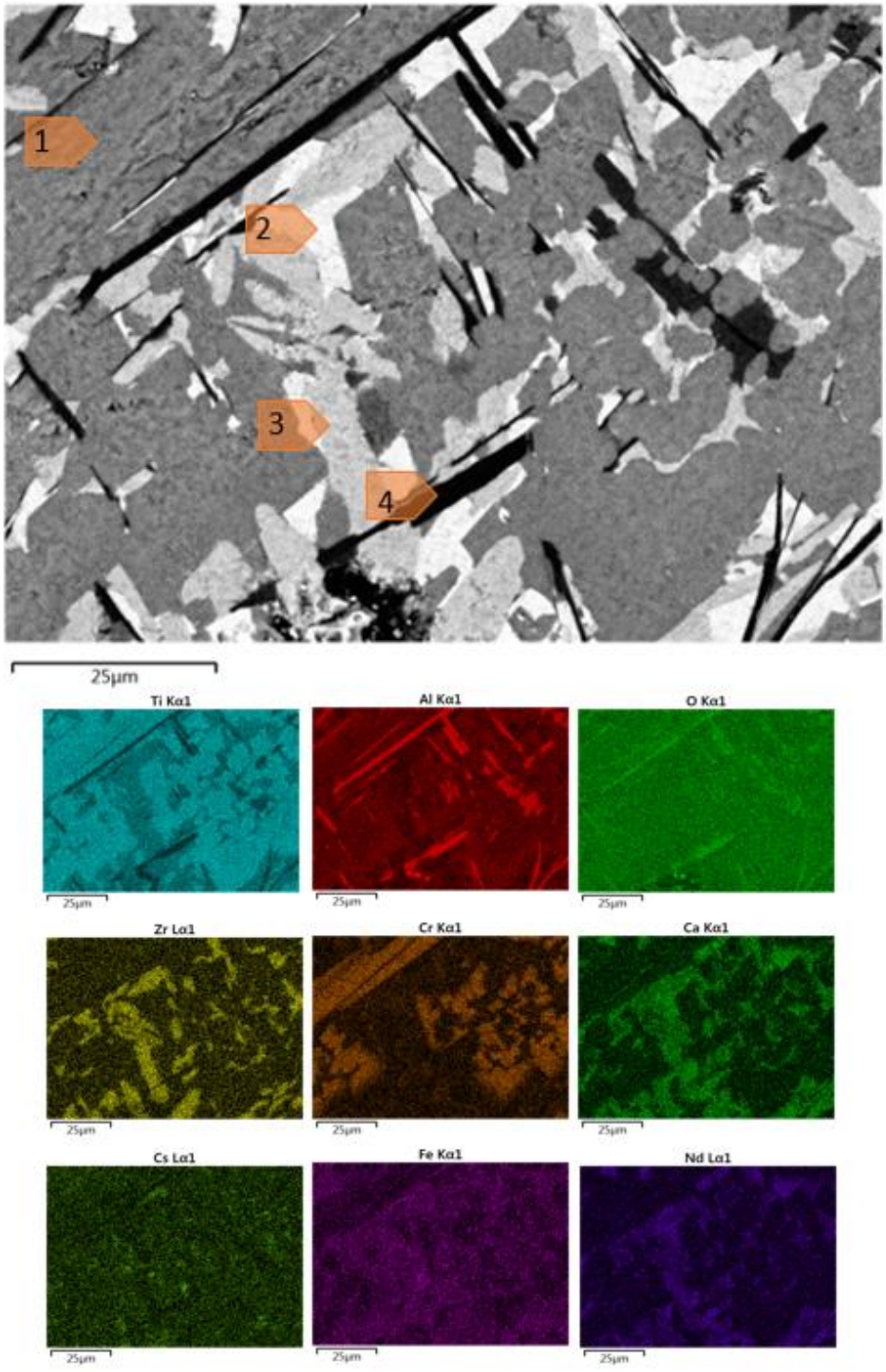
1
2
3
4
25µm
Ti Kα1
Al Kα1
O Kα1
Zr Lα1
Cr Kα1
Ca Kα1
Cs Lα1
Fe Kα1
Nd Lα1

B.

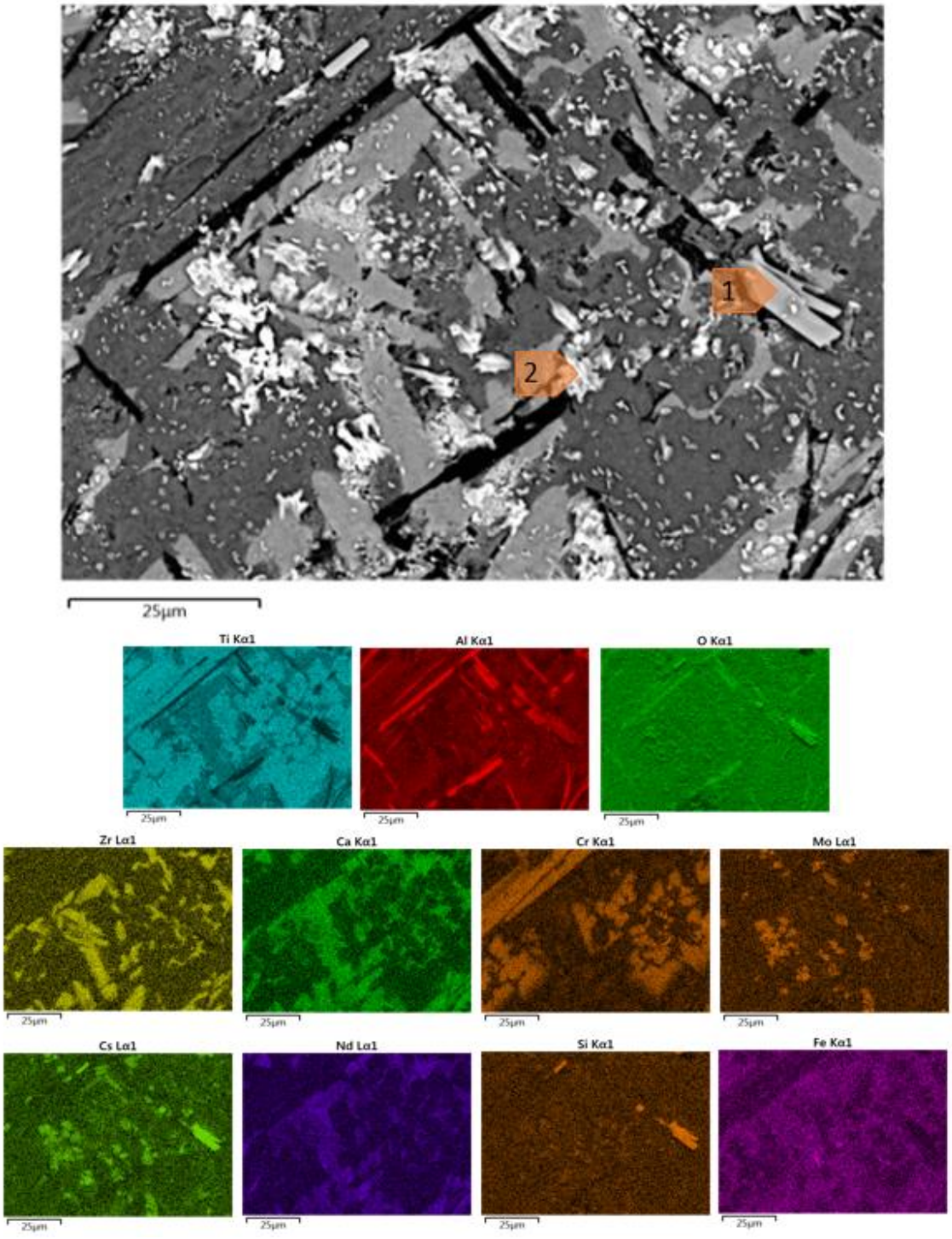
1
2
25µm
Ti Kα1
Al Kα1
O Kα1
Zr Lα1
Ca Kα1
Cr Kα1
Mo Lα1
Cs Lα1
Nd Lα1
Si Kα1
Fe Kα1

Figure 4-4. Cr, Al, Fe (CAF) doped hollandite multiphase sample taken from the top of the bulk sample (A) Sample before VHT where phases are labeled in Table 4-5 (B) Sample after VHT where phases are labeled in Table 4-5.

Table 4-5. Crystalline Phases for SEM images in Figure 4-4(A) and 4-4(B). (*Crystalline phases determined by XRD results and EDX elemental analysis)

	Location	Elements	Crystalline Phases*
A	1	O, Ti, Ba, Cr, Al, Fe, Cs	Hollandite
	2	O, Ti, Nd, Ce	Pyrochlore
	3	O, Ti, Zr, Nd,Ca	Zirconolite
	4	O, Al	Al_2O_3
B	Location	Elements	Crystalline Phases (possible)
	1	O, Cs, Al, Ti	Cs-Ti-Al-O
	2	O, Ti, Cs, Mo	Cs2MoO4

Both of these multiphase samples contained the same four phase before VHT: hollandite, pyrochlore, zirconolite, and alumina. After VHT, the formation of some new phases are shown, one being the Cs-Ti-Al-O phase previously seen forming on the surface of the single phase hollandite samples which occurs on both of the CAF hollandite multiphase samples. On the first CAF hollandite multiphase, Figure 4-3 and Table 4-4, some other water soluble phases where observed such as a possible Cs molybdate and Cs chromate. The second CAF hollandite multiphase also shows possible formation of Cs molybdate on its surface. This shows that the location these samples were taken from in a large bulk sample had an impact on the phase formation from VHT as well as the amount of phases formed when comparing the two samples.

4.4.2 Fe-Analogue Hollandite Multiphase

Fe-analogue hollandite multiphase was melted and poured into a stainless steel crucible by SRNL, from which the samples were received. SEM images, along with EDX elemental analysis from

before and after VHT are shown in Figure 4-4, and Table 4-5. Using SEM, EDX, and XRD the phases found present in the Fe analogue multiphase are hollandite, pyrochlore, zirconolite, alumina, and in this particular sample a small amount of a possible Cs-Ti-Al-O phase. After VHT, however, this small amount of Cs-Ti-Al-O phase was washed away, and instead the same small spherical particles of a Cs-Ti-Al-O phase that has been seen previously in single and multiphase samples. There is also an unknown phase that has appeared on the surface of the Fe-analogue hollandite multiphase after VHT that contains high levels of Ca, and small amounts of Ti, and Fe. Note that the EDS mapping for Ba is not shown because the Ti and Ba energies overlap, so the Ti EDS map is identical to the Ba.

A.

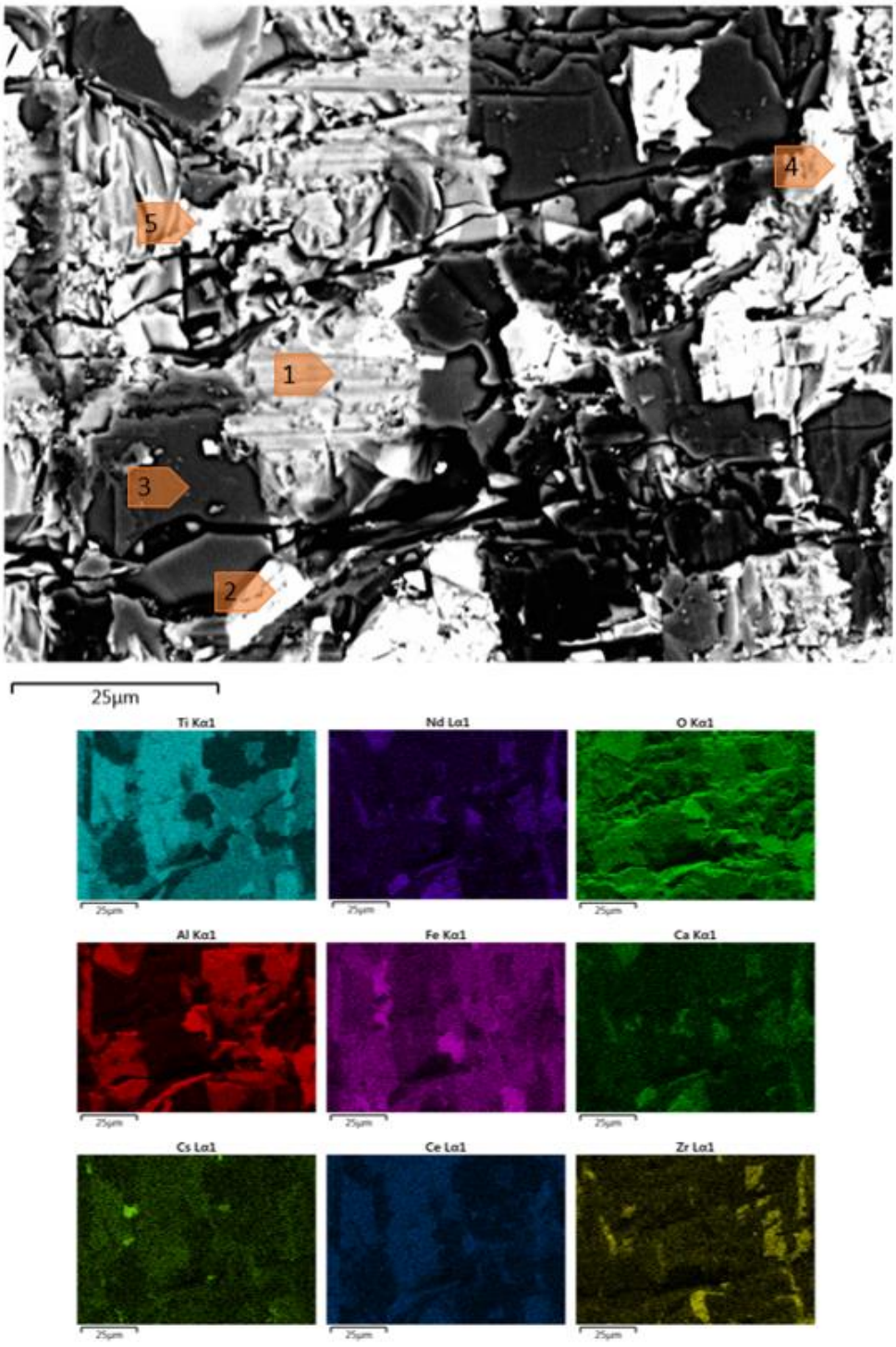
5
4
1
3
2
25µm
Ti Kα1
Nd Lα1
O Kα1
Al Kα1
Fe Kα1
Ca Kα1
Cs Lα1
Ce Lα1
Zr Lα1

B.

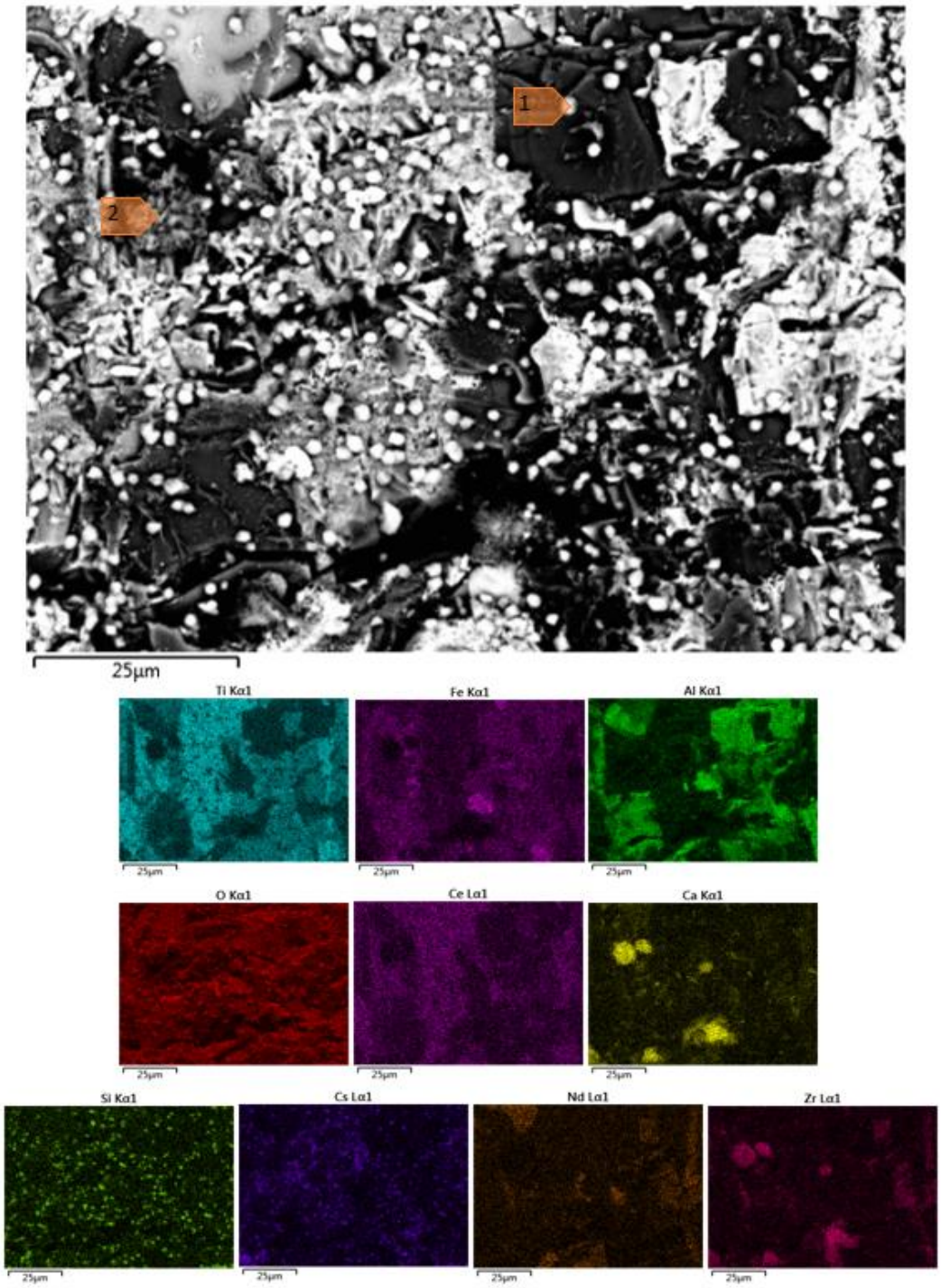
1
2
25µm
Ti Kα1
Fe Kα1
Al Kα1
O Kα1
Ce Lα1
Ca Kα1
Si Kα1
Cs Lα1
Nd Lα1
Zr Lα1

Figure 4-5. Fe Analogue Hollandite Multiphase (A) Sample before VHT where phases are labeled in Table 4-6 (B) Sample after VHT where phases are labeled in Table 4-6.

Table 4-6. Crystalline Phases for SEM images in Figure 4-5(A) and 4-5(B). (*Crystalline phases determined by XRD results and EDX elemental analysis)

	Location	Elements	Crystalline Phases
A	1	O, Ti, Fe, Al, Ba, Cs	Hollandite*
	2	O, Ti, Nd, Ca	Pyrochlore*
	3	O, Al, small amounts Fe	Al_2O_3*
	4	O, Ti, Zr, Ca,	Zirconolite*
	5	O, Ti, Al, Cs, small amounts Fe and Si	Cs-Ti-Al-O
B	Location	Elements	Crystalline Phases (possible)
	1	O, Cs, Al, Ti	Cs-Ti-Al-O
	2	O, Ca, Zr, small amounts Al, Ti	

4.5 Environmental Corrosion Studies on Single and Multi-Phase Ceramic Waste Forms

There are multiple tests that are useful for advancing the aging or dissolution of crystalline ceramic waste forms, but how would they compare to really being in contact with soil or metal in a real repository? Four samples were placed into a lysimeter, and placed into the ground at AMRL by Brian Powell in April of 2016 where they will remain for approximately 6 months. The purpose of this experiment is to examine surface alteration in real conditions with soil, rain water, temperature variation, etc.

All four samples were placed in the same lysimeter to ensure similar conditions. The different samples are found in Table 4-7. Each monolithic sample was characterized using SEM, EDS, and XRD in certain marked locations on each side of the sample. One side of each sample was against soil, while the other side was in contact with 302 stainless steel sheets.

Once the samples were removed from the lysimeter, they were rinsed very lightly with a small amount of water to remove the very large amounts of soil on the samples to perform any SEM or EDS. No mechanical scrubbing or strong flowing water was used in hope of not removing any possible deposited phases.

Table 4-7. Lysimeter samples along with information about where the samples are from, how they were made, and the phases that were observed in the samples.

Sample		Sample Information	Process	Phases
L1	"CAF-MP-Top"	Cr, Al, Fe hollandite multiphase sample received from SRNL	melted and poured into stainless steel crucible - sample from top of bulk sample	hollandite, pyrochlores/perovskites, zirconolite, rutile, and Al_2O_3.
L2	"Fe-Analogue Multiphase"	Fe analogue hollandite multiphase sample received from SRNL	melted and poured into stainless steel crucible - sample from top of bulk sample	hollandite, pyrochlores/perovskites, zirconolite, rutile, and possibly $FeAl_2O_4$
L3	"E-Bottom"	Fe analogue hollandite multiphase sample received from SRNL	bottom of the container of a multiphase bulk sample that was a 1kg demo run made by Cold crucible induction	hollandite, pyrochlores/perovskites, zirconolite, rutile, possibly $FeAl_2O_4$, and areas rich in Cs
L4	"Fe-SP-Pour"	Fe hollandite single phase received from SRNL	melted and poured into alumina crucible	two different hollandites, one being higher in Fe, as well as rutile, and Cs rich areas

A.

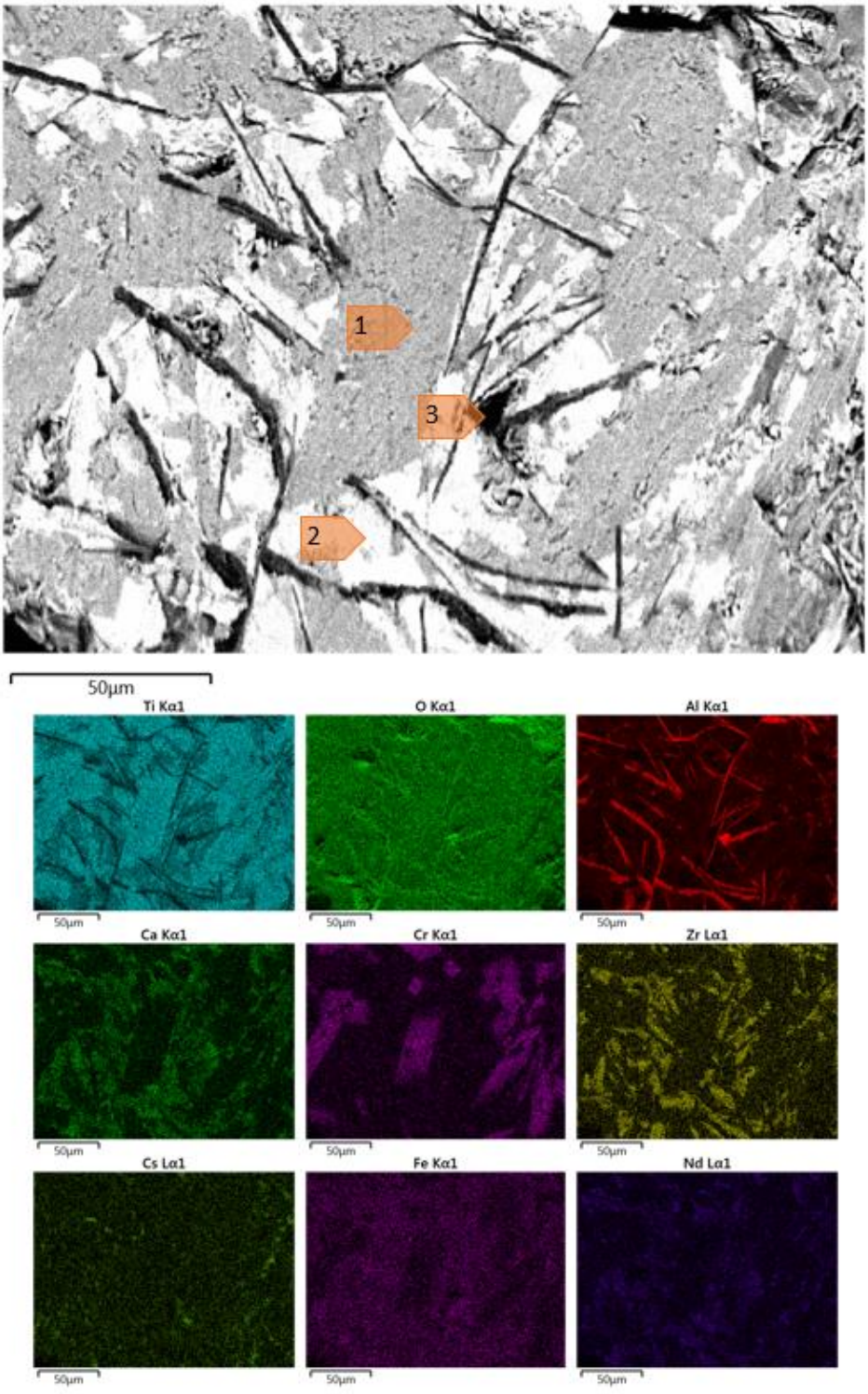
1
3
2
50µm
Ti Kα1
O Kα1
Al Kα1
Ca Kα1
Cr Kα1
Zr Lα1
Cs Lα1
Fe Kα1
Nd Lα1

B.

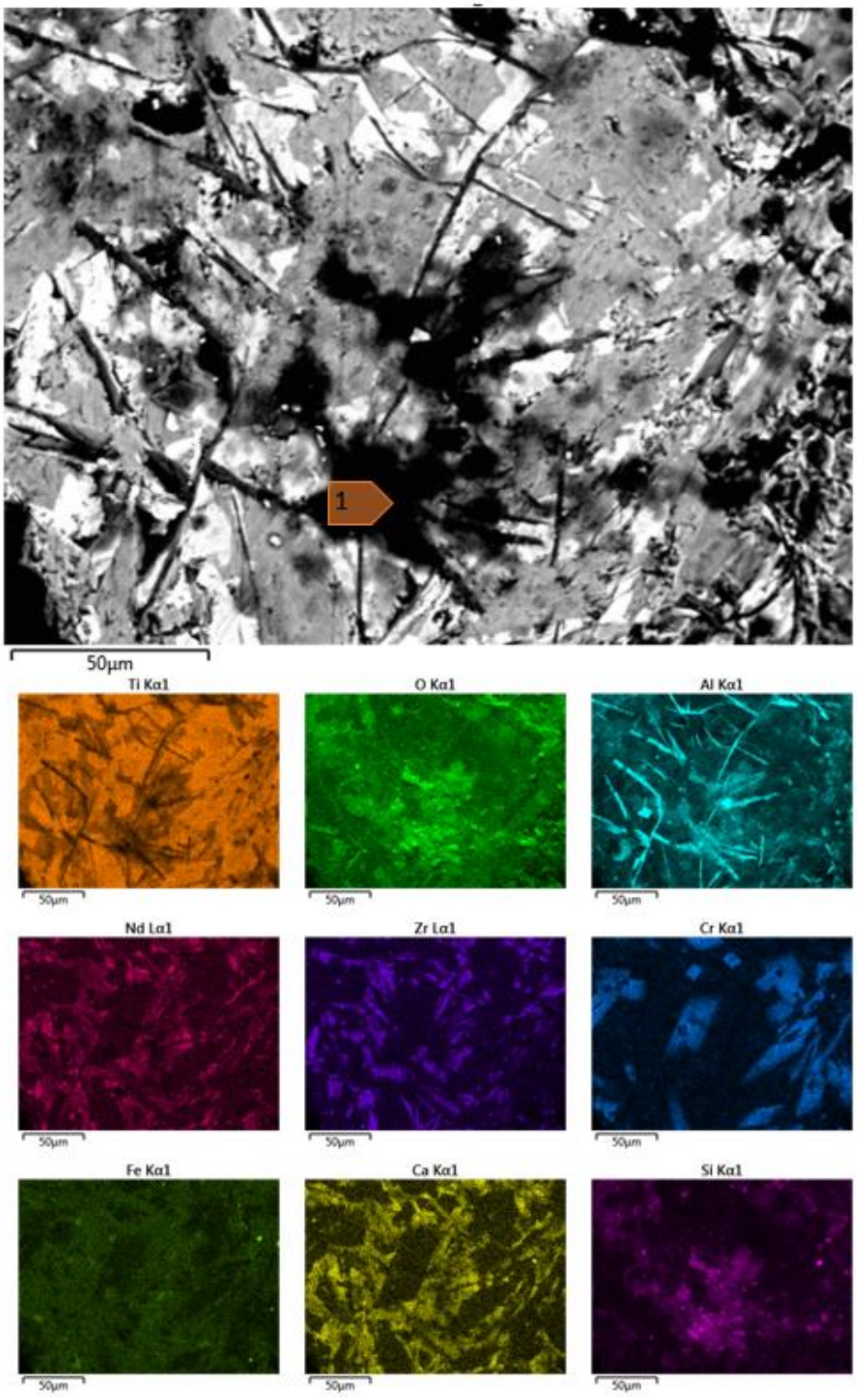

Figure 4-6. Cr, Al, Fe doped hollandite multiphase that was in contact with the soil inside of the lysimeter (A) Sample before VHT where phases are labeled in Table 4-8 (B) Sample after VHT where phases are labeled in Table 4-8.

Table 4-8 Crystalline Phases for SEM images in Figure 4-6(A) and 4-6(B). (*Crystalline phases determined by XRD results and EDX elemental analysis)

A	Location	Elements	Crystalline Phases
	1	O, Ti, Fe, Al, Ba, Cs	Hollandite*
	2	O, Ti, Nd, Ca	Pyrochlore/Zirconolite*
	3	O, Al, small amounts Fe	Al_2O_3*
B	Location	Elements	Phases
	1	O, Si	Soil from lysimeter

A.

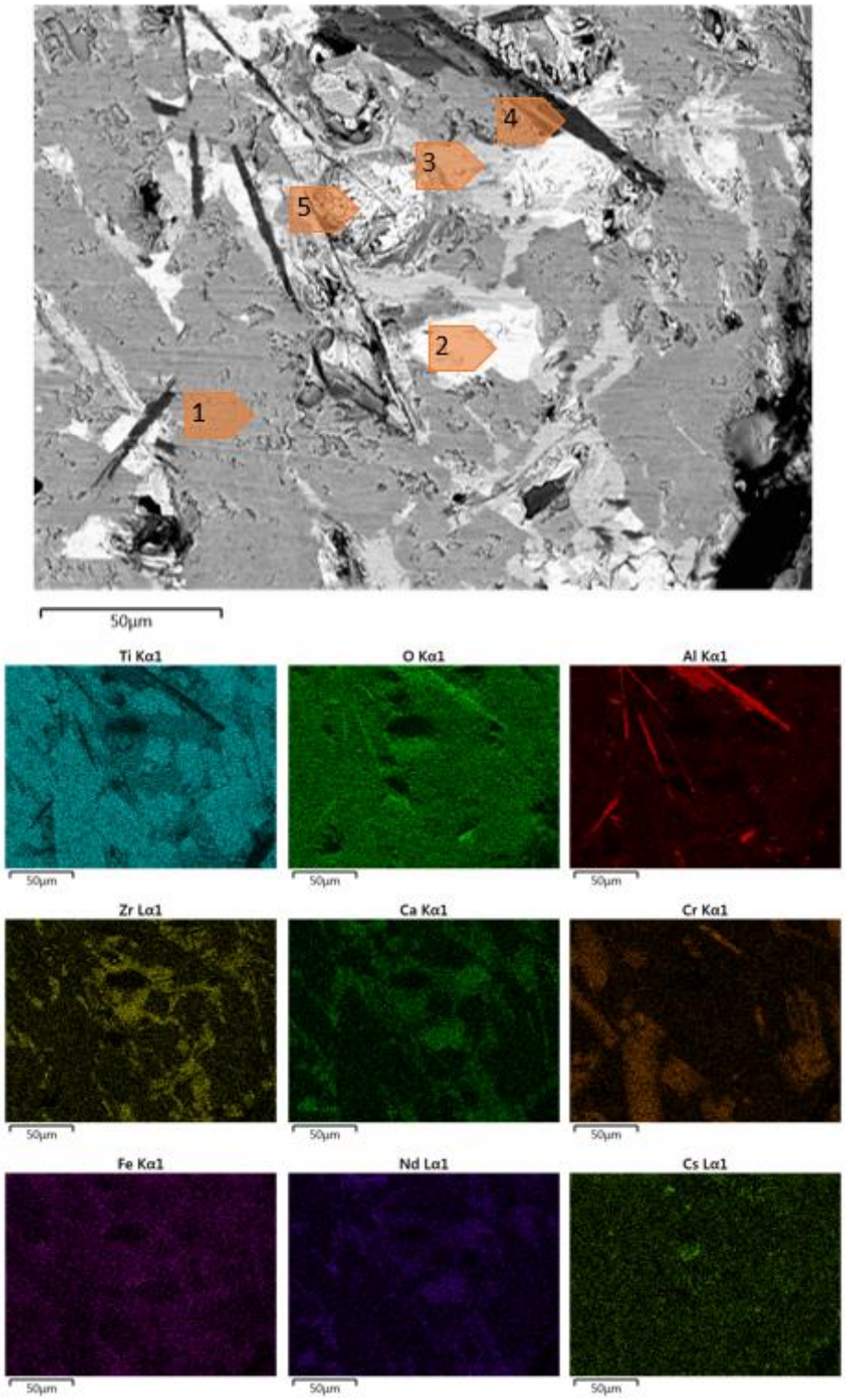
1
2
3
4
5
50µm
Ti Kα1
O Kα1
Al Kα1
Zr Lα1
Ca Kα1
Cr Kα1
Fe Kα1
Nd Lα1
Cs Lα1

B.

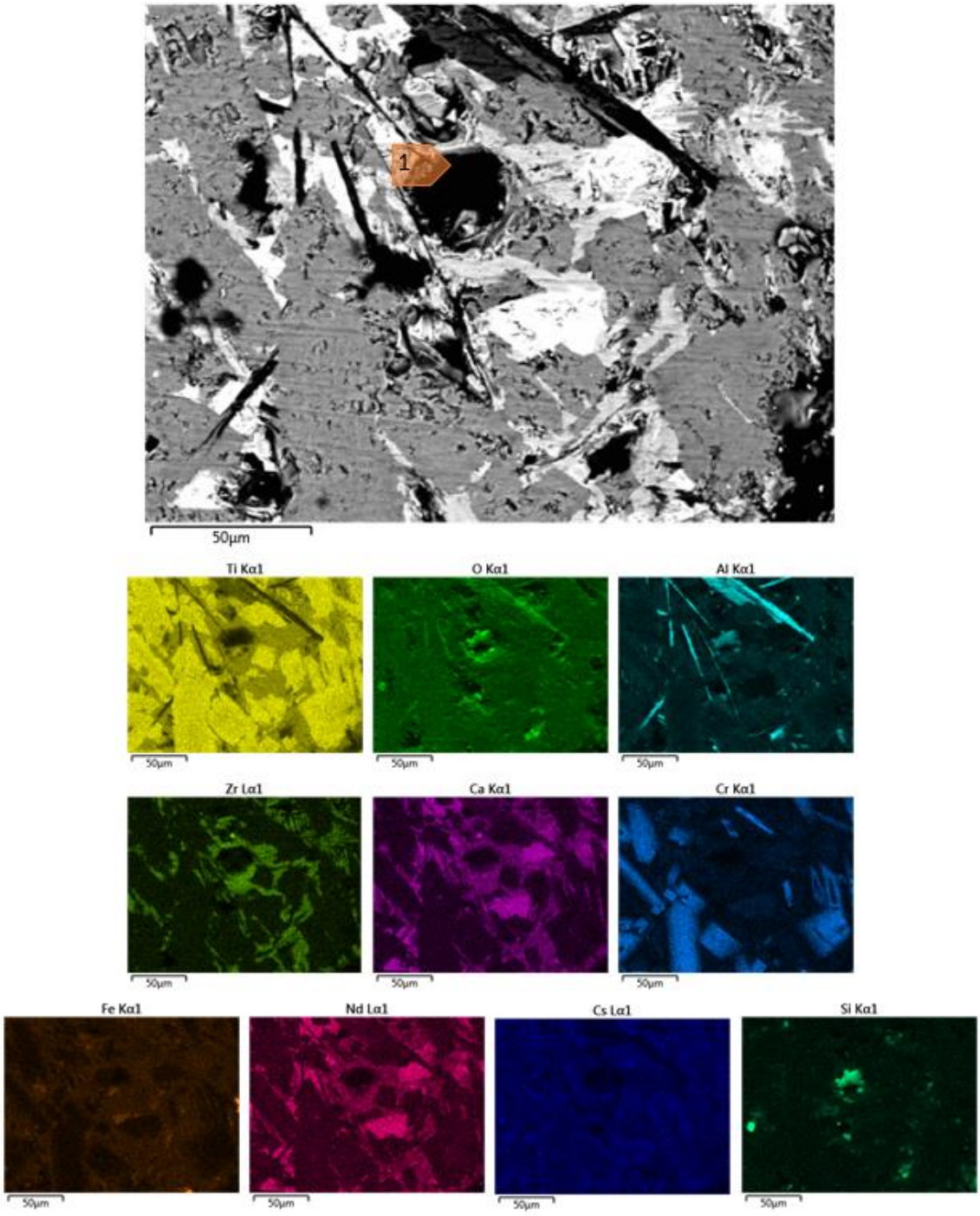
1
50µm
Ti Kα1
O Kα1
Al Kα1
Zr Lα1
Ca Kα1
Cr Kα1
Fe Kα1
Nd Lα1
Cs Lα1
Si Kα1

Figure 4-7 Cr, Al, Fe doped hollandite multiphase that was in contact with stainless steel inside of the lysimeter (A) Sample before VHT where phases are labeled in Table 4-8 (B) Sample after VHT where phases are labeled in Table 4-8.

Table 4-9 Crystalline Phases for SEM images in Figure 4-7(A) and 4-7(B). (*Crystalline phases determined by XRD results and EDX elemental analysis)

	Location	Elements	Crystalline Phases
A	1	O, Ti, Fe, Al, Ba, Cs	Hollandite*
	2	O, Ti, Nd, Ca	Pyrochlore*
	3	O, Ti, Zr, Ca,	Zirconolite*
	4	O, Al,	Al_2O_3*
	5	O, Ti, Al, Cs, small amounts Fe and Si	
B	Location	Elements	Crystalline Phases (possible)
	1	Si	Soil from lysimeter

Seen in Figures 4-6 and 4-7 is SEM images for the two sides of a monolith sample of Cr, Al, Fe doped hollandite multiphase that was one of the four monoliths put into the lysimeter for six months for an environmental corrosion test. Tables 4-8 and 4-9 show the phases found before and after the 6 month corrosion test corresponding to Figures 4-6 and 4-7. Note that the EDS mapping for Ba is not shown because the Ti and Ba energies overlap, so the Ti EDS map is identical to the Ba.

To begin, examining the SEM images in Figures 4-6 and 4-7, it appears that the same phases found in the Cr, Al, and Fe doped hollandite multiphase remain consistent with previous samples used for VHT. The same phase assemblage of hollandite, pyrochlore, zirconolite, and Al_2O_3 is observed on both sides of the monolith. However, in Figure 4-7 there appears to be a small amount of Cs-Al-Ti-O phase before the samples were placed in the lysimeter for the 6 month environmental corrosion test.

In Figures 4-7 and 4-8, examining the SEM images after the 6 month environmental corrosion the samples seem relatively unchanged. In both samples there is some residual sand leftover from being inside the lysimeter which is listed in Tables 4-8 and 4-9. The only noticeable difference is seen in Figure 4-8 was where the Cs-Ti-Al-O phase was located prior to the 6 month test, is now replaced with sand. This phase is known to be easily leachable, even seen in prior VHT. However unlike the VHT, this Cs rich phase was not leached and deposited on the surface of the sample.

Very similar results were seen on the other samples placed into the lysimeter, so they have been omitted. The lack of alteration of the samples, such as what has been seen in VHT, is due to the shot test time of only 6 months. If the test was allowed to continue for years, there is a higher chance of seeing some possible deposited phases or grain boundary leaching. It is important to note that these samples are also not being introduced to extreme conditions as the VHT samples were, such as high temperatures.

4.6 Conclusions: comparing Vapor Hydrations Tests

Similar phases and results were seen in the single and multiphase samples. The most notable phase was a Cs-Ti-Al-O phase which appeared in every system, except the dual phase samples. Once again, it should be noted that the dual phase sample showed no clear alteration phases, but this is most likely due to a bad gasket resulting in water loss during the test, leaving the environment with much lower humidity. However, the single phase Fe hollandite showed significant amounts of a Cs-Ti-Al-O phase on its surface. The multiphase samples, the Cr, Al, Fe, hollandite multiphase and the Fe analogue hollandite multiphase, also showed a Cs-Ti-Al-O phase as one of the main alteration phases deposited on the surface after VHT. The multiphase samples

did show other phases depositing as well, such as a possible Cs molybdate and Cs chromate, which are important to note as well.

With the deposited phases being so similar in samples after VHT, it does appear that Cs retention in the waste forms are similar, regardless of whether they appear in single or multiphase systems. Future work should focus on more VHT on dual phase sample, being a large gap in current work. With Cs retention appearing to be similar in single and multiphase systems, it would also be important to perform VHT on single, dual, and multiphase systems with varying Cs loading in the hollandite.

Chapter 5. The Effect of Grain Size on Alternative Phase formation of Hollandite

5.1 Motives and Objectives

The motivation of this experiment comes from a multiphase VHT. Seen in Figure 5-1, is a multiphase sample made with Cr, Al, Fe doped hollandite before and after a 30 day VHT. Figure 5-1a shows the multiphase before VHT, Figure 5-1b shows the multiphase after VHT, and Figure 5-1c shows the multiphase after VHT after being rinsed with a small amount of deionized water. There are many alternative phases formed during VHT, however they are either water soluble or loose on the surface and washed away with ease. Notice, the large grains seen before VHT and after being rinsed with deionized water are largely unaltered. This leads to the idea that the leaching that is occurring for these alternative phases to form is coming from the grain boundaries. If this is true, then the larger the grains, the less grain boundaries, and the less leaching and alternative phase formation will occur.

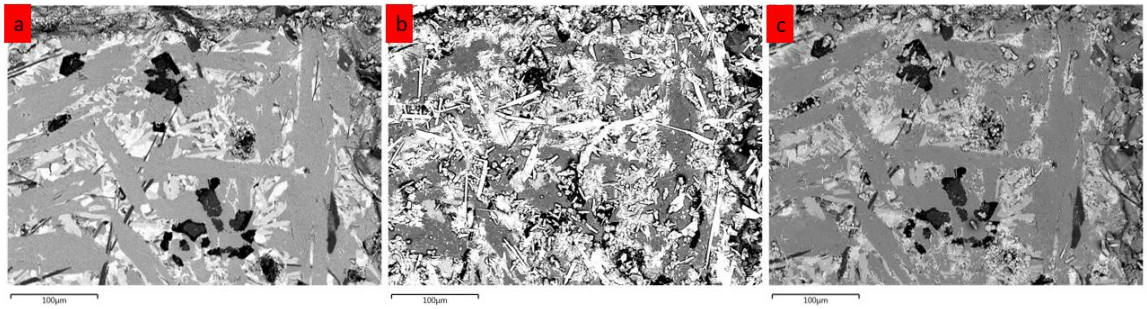

Figure 5-1. Cr, Al, and Fe, doped hollandite multiphase: a) before 30 day VHT, b) after 30 day VHT, c) after 30 day VHT after rinsed with a small amount of D.I. water

To examine this possible effect of grain size on the durability of ceramic waste forms, samples of $Ba_{1.04}Cs_{.24}Ga_{2.32}Ti_{5.68}O_{16}$ made with different grain sizes will be tested using VHT to see the extent of alternative phase formation. Seen in Figure 5-2 is a cartoon depicting how the grain size affects

the leaching and alternative phase formation. These differences in grain sizes were made by sintering the hollandite in three different ways: by melting, conventional sintering, and spark plasma sintering (SPS). These samples were then taken and VHT was performed on them for 14 days.

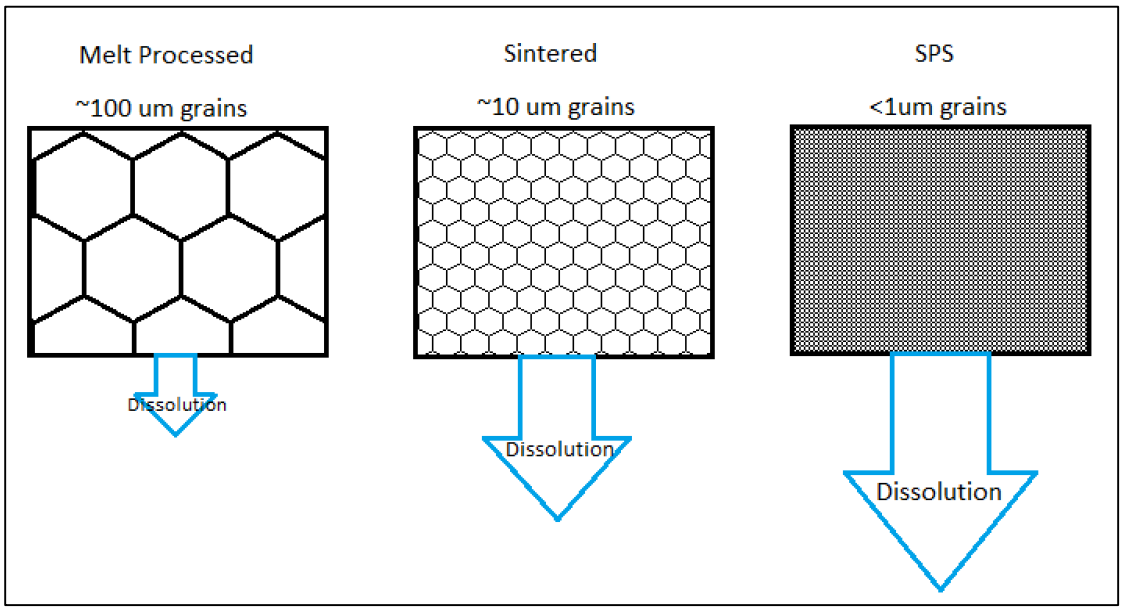

Figure 5-2. Depiction of how grain size could affect leaching and alternative phase formation.

5.2 Sintering Techniques

To test the different sintering techniques, the same batch of hollandite was used for to make the samples regardless of densifying method. This hollandite was prepared by heating at 1200 °C for 20 hours, then crushed, milled, and made into pellets for another heating of 1250 °C for 4 hours. This powder was confirmed by XRD to be tetrahedral hollandite. It should be noted that the scale bars are different for SEM images of grains of the three different sintering methods, making it easier to see the size of the grains.

Melt Processing

The first densification method is to melt process the hollandite. This was achieved by taking approximately 30 g of the hollandite powder and placing them into a large crucible. This crucible was then placed inside of another crucible as a secondary containment for the hollandite if it leaches through the first crucible. This second crucible was sealed and put in the furnace and ramped to 1525 °C for a 30 minute hold time. Once cooled the crucible was broken with a hammer to obtain pieces of the melted sample, which were then polished into small monoliths.

SEM images and EDS elemental mapping is shown in Figure 5-3. While the large grains were achieved and the majority of the sample is hollandite, there are three distinct phases present, listed in Table 5-1. The sample does appear to have a small amount of aluminum in all of the phases present, which could have come from the alumina crucible the sample was melted in. The melt processed hollandite was the only sample found containing Al. It should be noted that the Ba and Ti energies overlap making the EDS maps identical, so Ba is not shown.

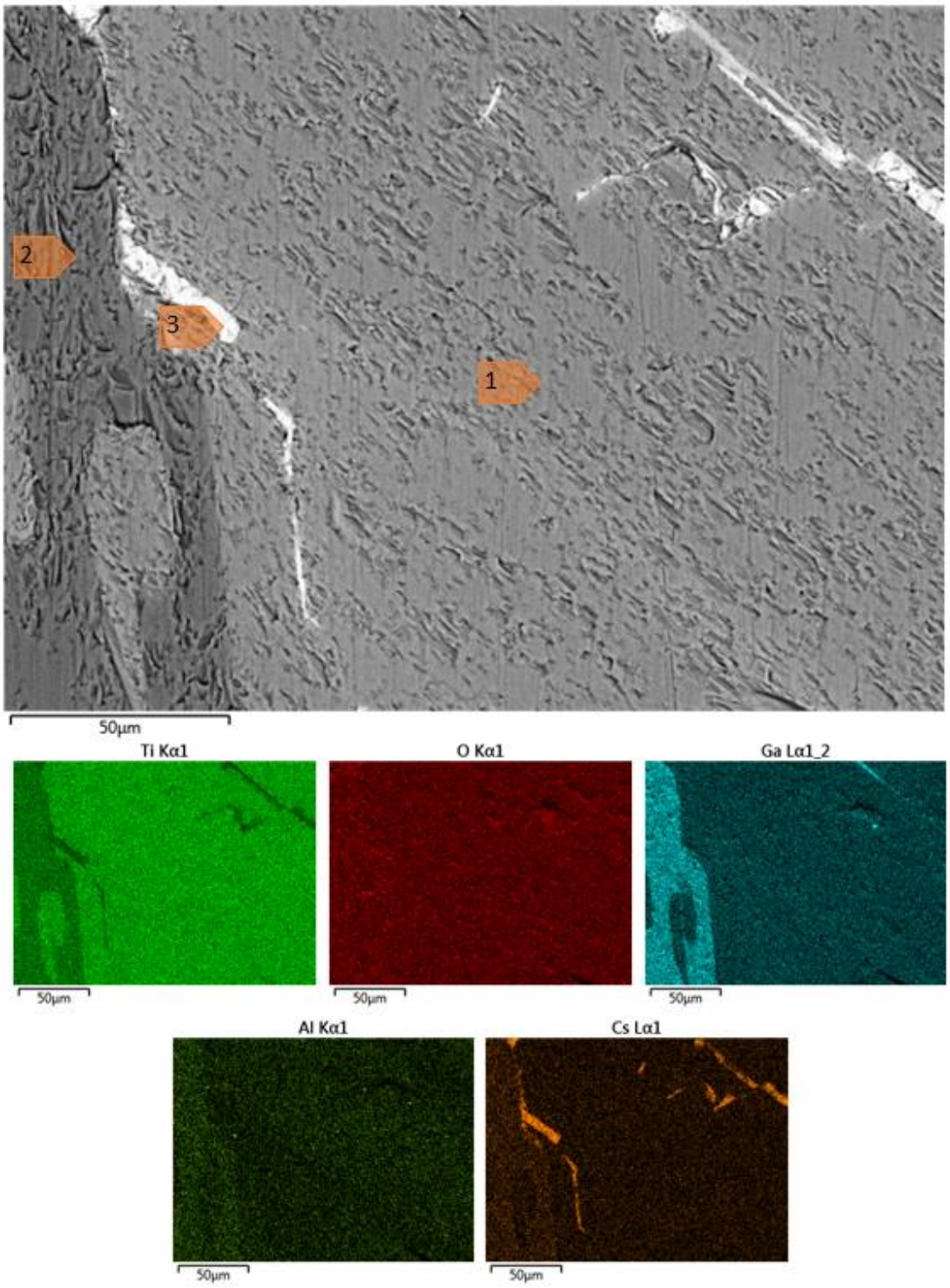

Figure 5-3. SEM image with EDS elemental maps of the melt processed hollandite.

Table 5-1.Phases present in the melt processed hollandite in Figure 5-3. (*Crystalline phases determined by XRD results and EDX elemental analysis)

Location	Elements	Crystalline Phases
1	O, Ti, Ga, Ba, Cs, small amounts of Al	hollandite*
2	O, Ti, Ga, small amounts of Cs and Al	Ga titanate
3	O, Ti, Cs	Cs titanate

Conventional Sintering

To densify the hollandite by conventional sintering methods, the hollandite was first pressed into pellets and then heated in the furnace. Temperature was slowly brought up to 1250 °C and held for four hours.

The SEM and EDS elemental maps of the conventional sintered sample, seen in Figure 5-4, show that the majority of the sample is hollandite, however there are a few grains with much higher in gallium and slightly higher in Cs. This is similar to the same Ga titanate that was seen in the melted hollandite. The conventional sintered hollandite also appears to still be slightly porous, which could lead to increased leaching due to increased surface area.

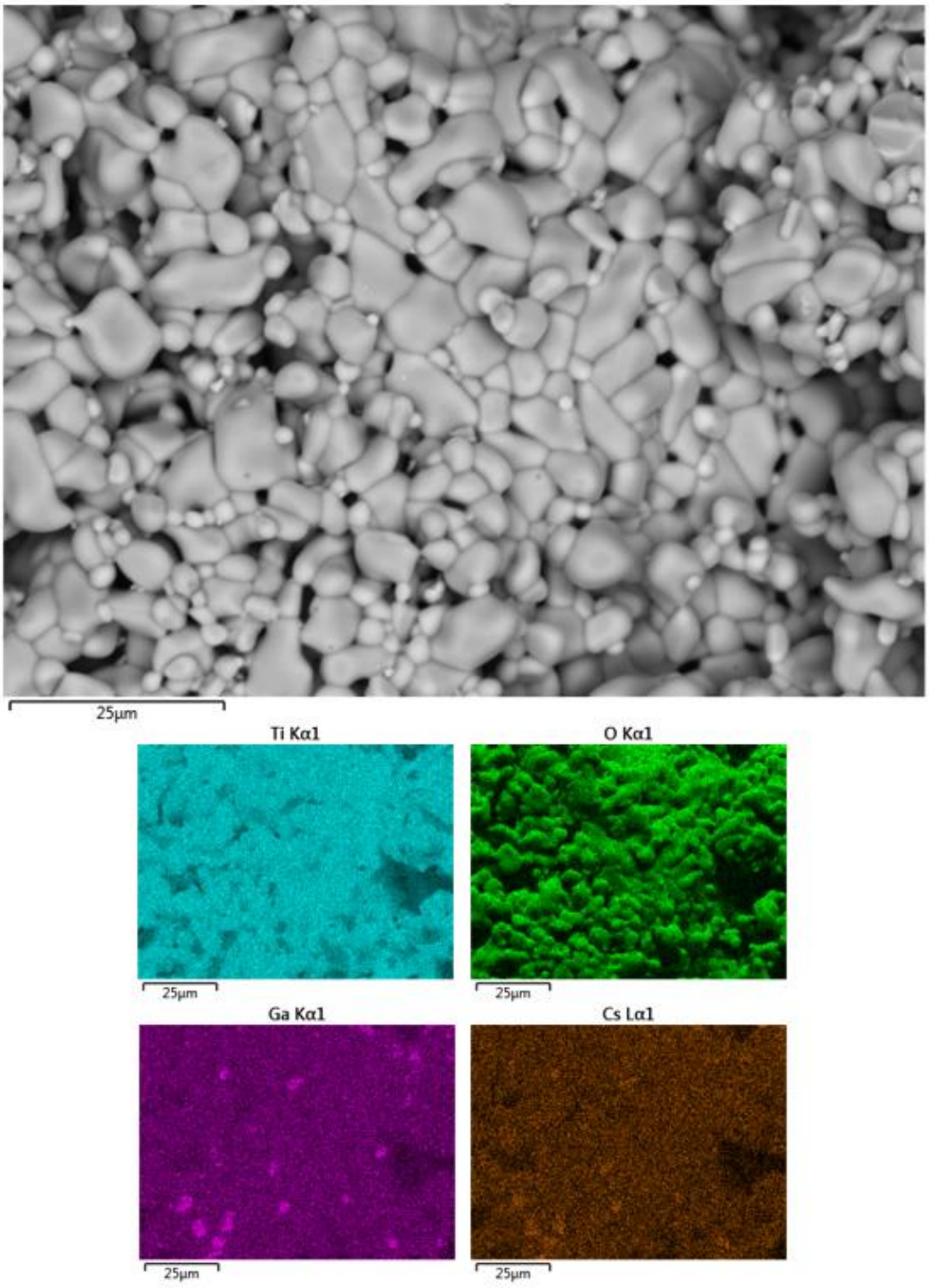

Figure 5-4. SEM image with EDS elemental maps of hollandite densified by conventional sintering.

Spark Plasma Sintering

Spark plasma sintering (SPS) is a method of sintering using an electric current. The hollandite powder was put into a graphite die, which has a higher conductivity than the powder, and pulses of electricity starting with 100 amps and increasing to 500 amps over time. This current goes through the powder, leading to heating. This SPS sample achieved a sintering temperature of approximately 1250 °C and held at this temperature is held there for about 5 minutes, achieving a densified hollandite.

Figure 5-5 shows an SEM image of the grain size of the SPS hollandite used. However the SEM used to take this image was not able to take EDS measurements. Figure 5-6 shows the sample at a lower magnification, where the grain size is not visible but EDS for the sample is available. There are 3 phases present in the SPS samples, which are listed in Table 5-2. The major phase is the targeted hollandite, the second phase appears to be a Ga titanate that was seen in all samples, and the third phase appears to be Ga oxide, one of the precursors used to form hollandite.

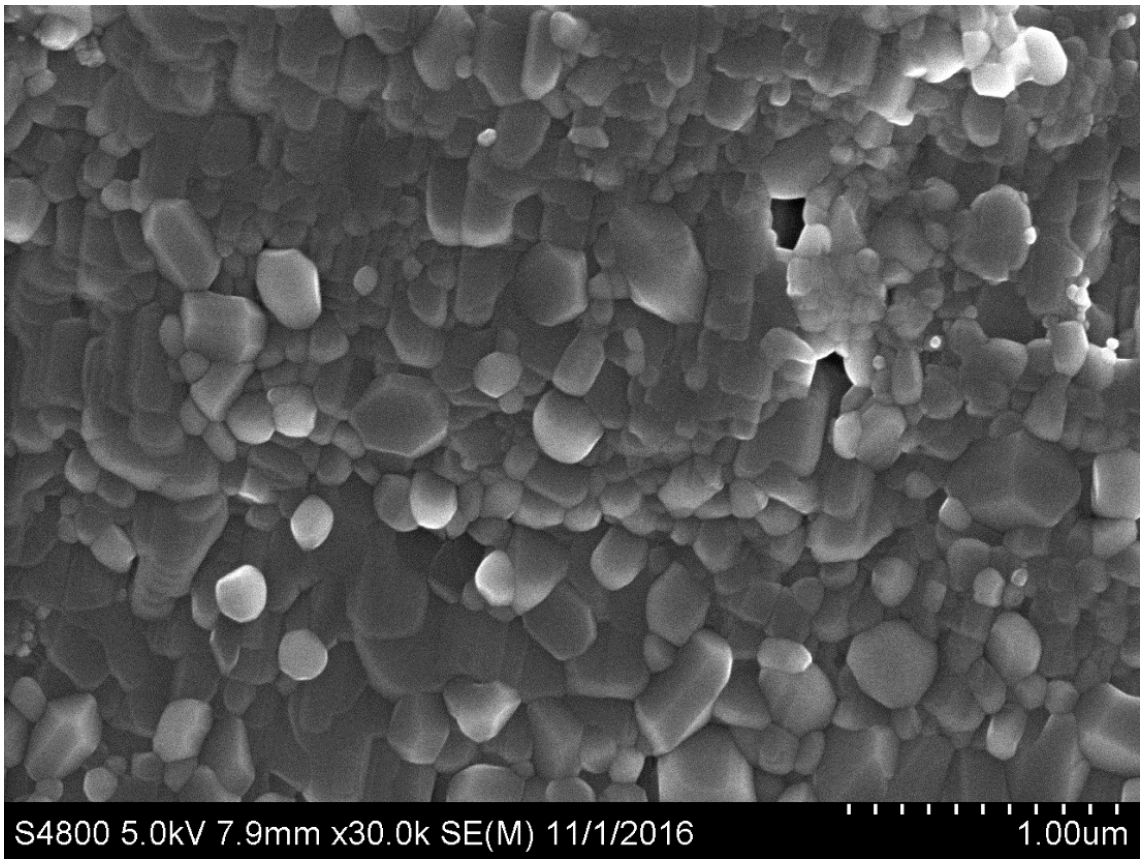

Figure 5-5. Low voltage SEM image of SPS hollandite, showing submicron gains achieved by SPS sintering.

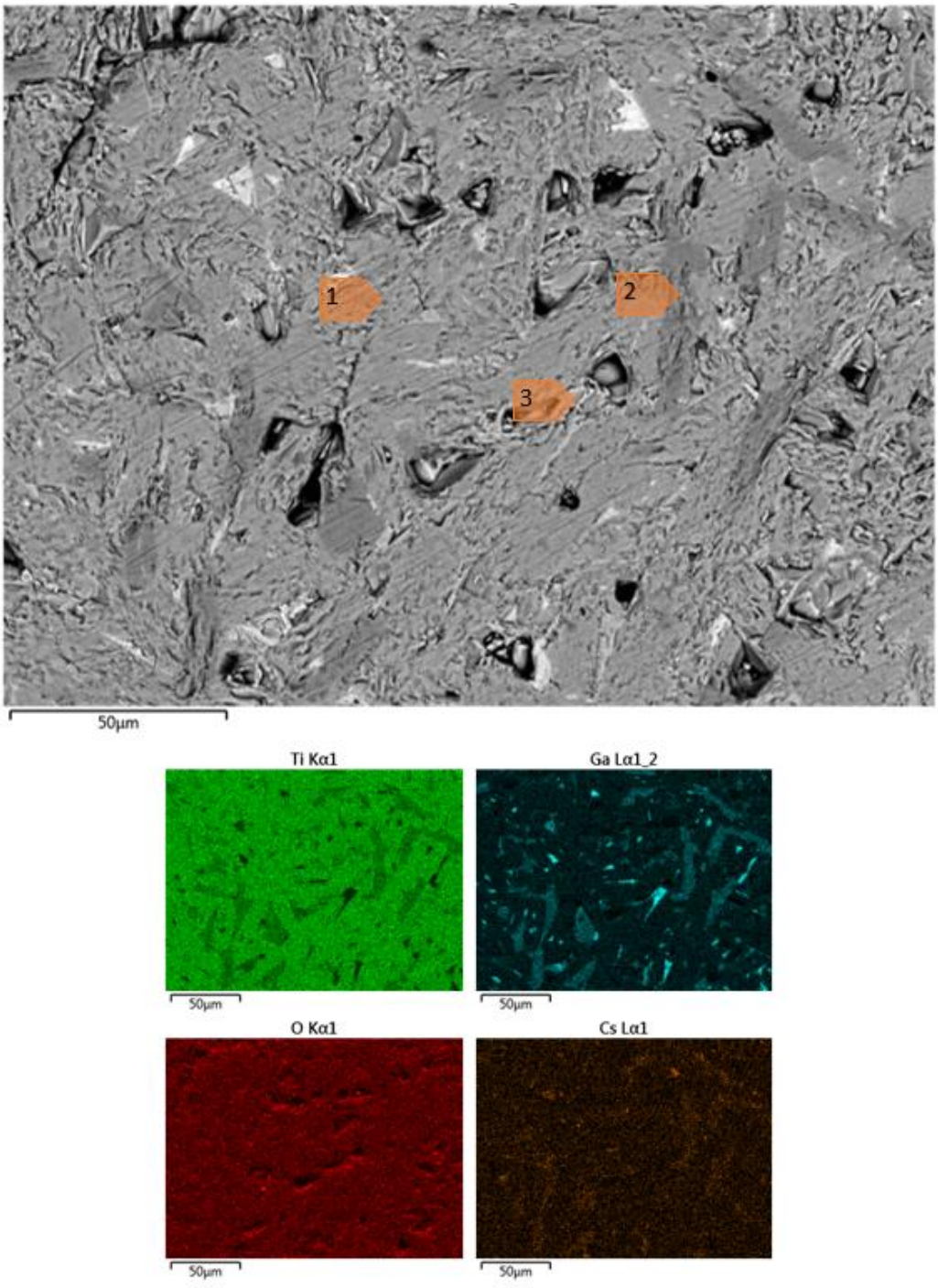

Figure 5-6. SEM image with EDS elemental maps of hollandite densified by spark plasma sintering (SPS).

Table 5-2.Phases present in the SPS hollandite in Figure 5-6. (*Crystalline phases determined by XRD results and EDX elemental analysis)

Location	Elements	Crystalline Phases
1	O, Ti, Ga, Ba, Cs,	hollandite*
2	O, Ti, Ga, trace amounts Ba, Cs	Ga titanate
3	O, Ga	Ga oxide

5.3 Results and Discussion

After the 14 day VHT the samples were removed and SEM and EDS were used to examine the surface of each sample. The SEM images for the melt processed hollandite, the conventional sintered hollandite, and the SPS hollandite are shown in images 5-7, 5-8, and 5-9 respectively. It should be noted that images 5-7 and 5-8 correspond the same locations on the samples previously shown in Figures 5-3 and 5-4. However, the SPS hollandite shown in Figure 5-6 before VHT does not correspond to the same location in Figure 5-9. The location before VHT on the SPS hollandite in Figure 5-6 appeared to be mechanical damaged after VHT, most likely due to fastening the Pt wire around the sample before VHT. Therefore, Figure 5-9 is on another location on the sample after VHT.

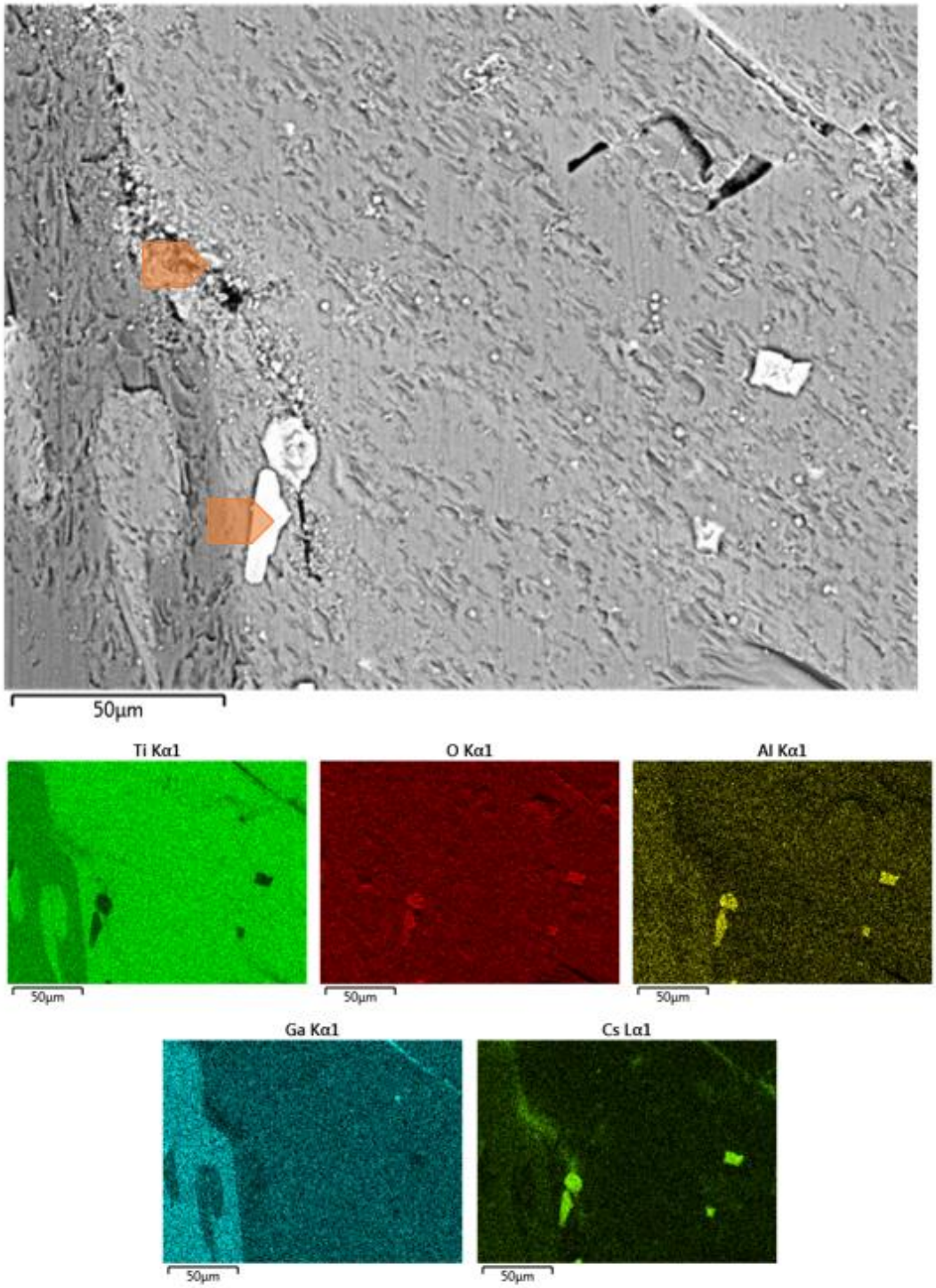

Figure 5-7. SEM image with EDS elemental maps of the melt processed hollandite post VHT.

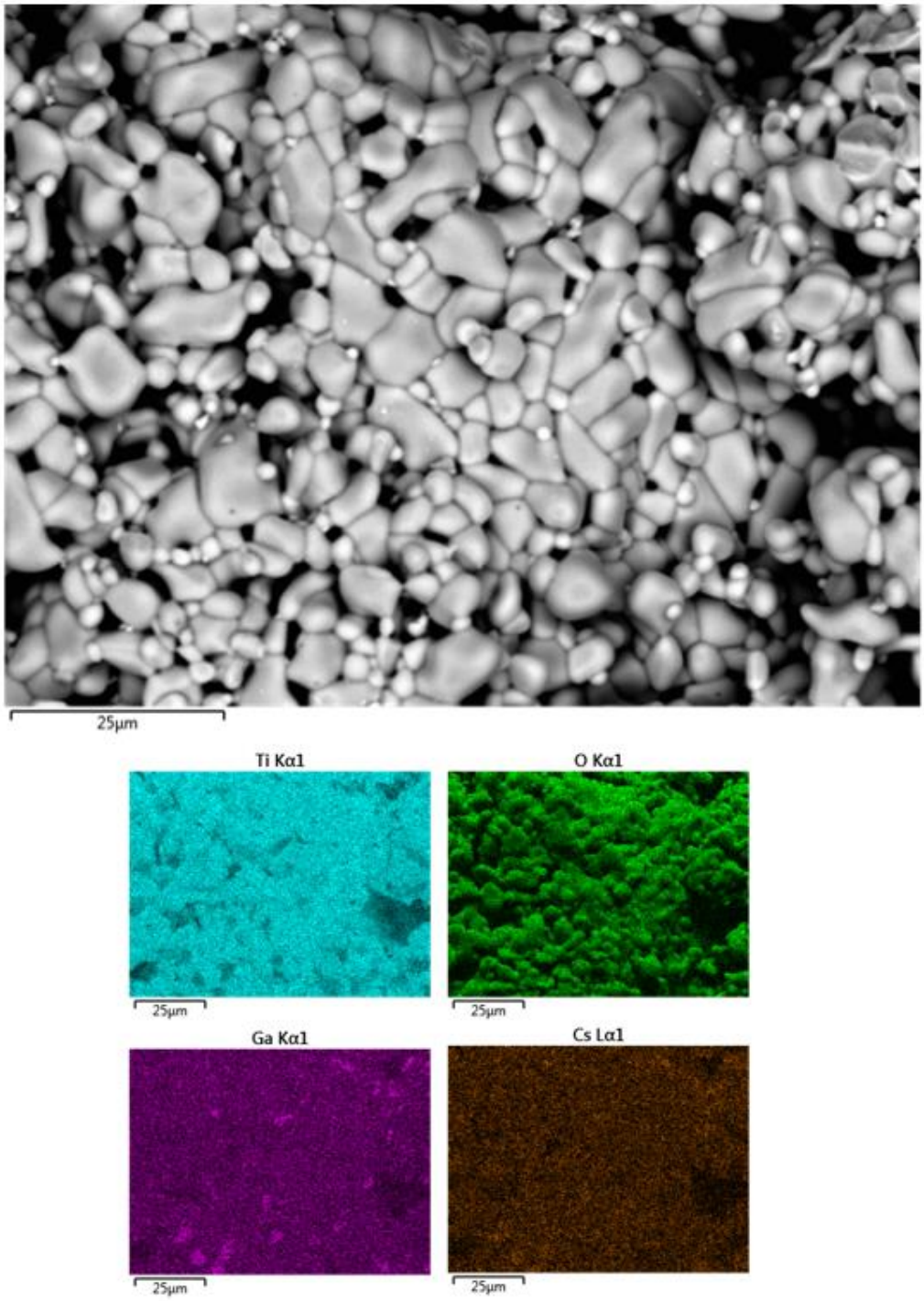

Figure 5-8. SEM image with EDS elemental maps of hollandite densified by conventional sintering post VHT.

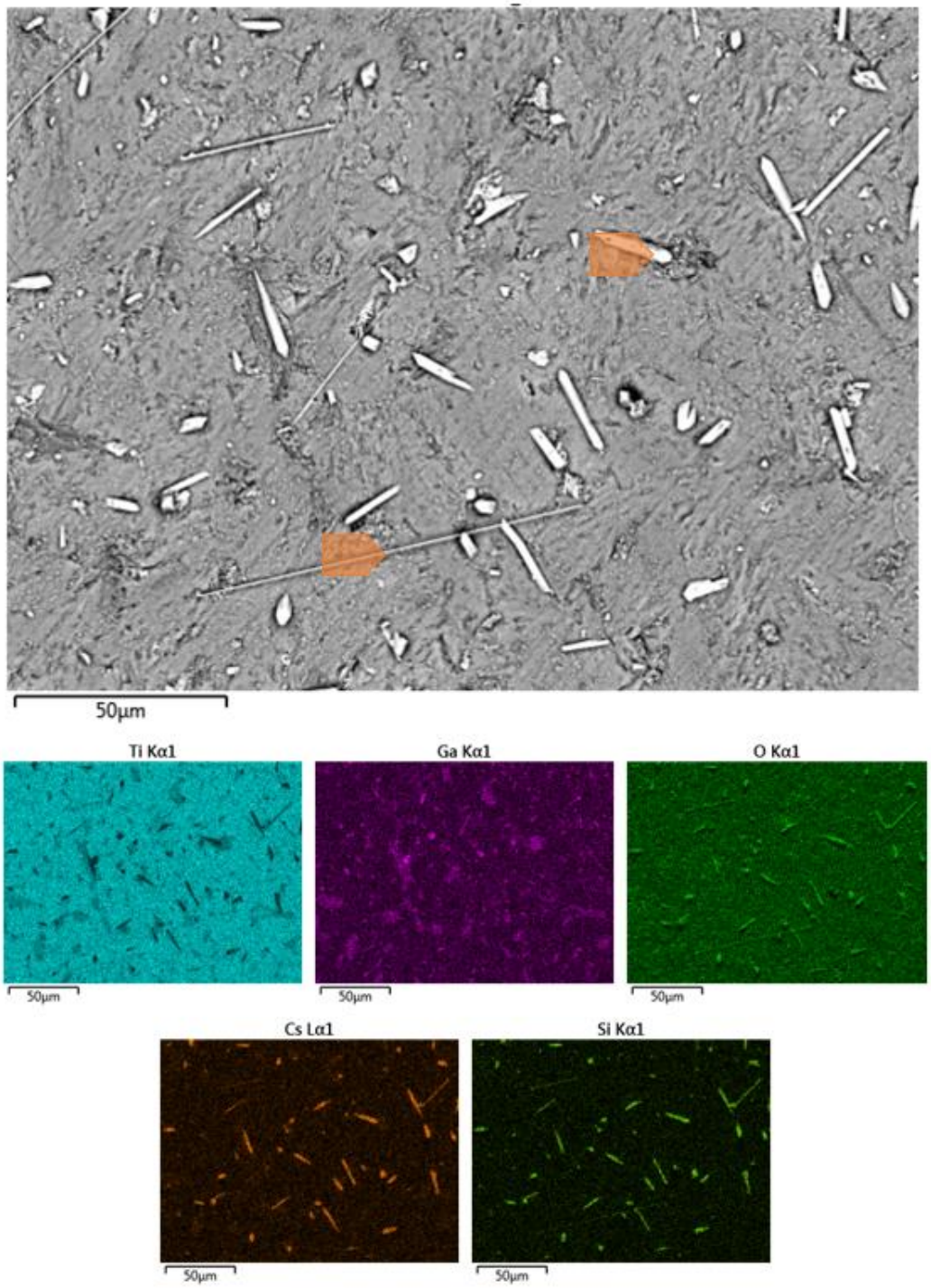

Figure 5-9. SEM image with EDS elemental maps of hollandite densified by spark plasma sintering (SPS) post VHT.

The melt processed hollandite showed some significant alteration on the surface, indicated by the arrows in Figure 5-7. However, it seems this phase is nearly identical to the phase numbered 3 in Figure 5-3. Since this phase was seen on the surface before VHT, it is very likely this phase dissociated and reformed on the surface of the melt processed hollandite. Which doesn't necessarily indicate the leaching for this phase occurred from the grain boundaries but rather directly from the phase on the surface that is no longer seen.

The conventional sintered sample showed absolutely no alteration from the VHT. Comparing images in Figure 5-4 to images in Figure 5-8 show no change

The SPS hollandite sample however showed the most alteration on the surface, seen in Figure 5-9. After VHT a Cs-Ti-O phase was deposited on the surface that has not yet been determined. The grains in the sample also appear to be relatively unchanged, unlike in the melt processed hollandite.

After reviewing the results of the VHT for the three different densifying methods for hollandite, it does appear the SPS hollandite sample, having the smallest grain size, did show the most leaching and alternative phase formation. The conventional sintered sample, with the medium grain size, showed no change. The melted hollandite did show a Cs phase on the surface, it more than likely came from the Cs titanate phase on the surface before VHT, instead of actually leaching from the grain boundaries. Therefore, as grain size decreases, the amount of leaching during VHT increases, however large amounts of secondary phases in the sample can significantly affect the leachability of hollandite as well.

Chapter 6. Conclusions and Future Work

6.1 Dual Phase Studies

In the dual phase systems there were some possible new phases that were witnessed. In the Nd titanate and hollandite dual phase systems there was the phase $BaNd_2Ti_5O_{14}$ that was identified using SEM, EDS, and XRD. Very little literature is available on this phase and none that show it appearing as a secondary phase in multiphase waste forms. Accompanying this $BaNd_2Ti_5O_{14}$ phase was a $Nd_4Ti_9O_{24}$ and a possible Ga titanate, the later only being seen in SEM and EDS. These two phase explain what happens as the Hollandite structure is degraded, causing $Nd_2Ti_2O_7$ to transition to $Nd_4Ti_9O_{24}$, and Cs and Ga are forming another titanate. It was also determined that depending on the composition of the Ga hollandite, heavily effected the amount of phase alteration upon heating systems of crystallized Nd titanate and Ga doped Ba hollandite. The larger amount of Cs substituted into the A site of the hollandite structure led to less secondary phases forming when in the dual phase systems, meaning the hollandite structure is more stable with the more Cs substitution.

In the La titanate and hollandite systems, similar phases seen in the Nd titanate systems were observed in the raw powder precursor. However, not seen in the Nd titanate samples was the La titanates in the dual phase system actually reducing into a perovskite structure, which is one of the actual targeted phases in the multiphase titanate waste forms. This shows how favorable this perovskite is to form.

The Ce brannerite and hollandite systems showed absolutely no reaction, which was expected from the single phase studies. Ce brannerite was favorable to form at only a very specific temperature range, which below did not form, and above melted.

There is still a large gap in dual phase model systems as this is just examined a few possible systems. In order to make the ideal ceramic multiphase waste form it is important to understand the single phases, the dual phase systems, and then the multiphase systems. Continued work on dual phase systems with varying Cs content in the hollandite structure and investigating dual phase systems with different hollandite dopants, such as Fe, Zn, Cr, etc… Varying the titanate used in the systems as well is paramount, not only different lanthanide titanates, but structures as well, $Nd_2Ti_2O_7$ is the absolute simplest system, where the multiphase targets pyrochlore, which would require doping of the Nd titanate. Investigating these dopants to form pyrochlore would also lead to investigating zirconolite which is related to the pyrochlore structure.

6.2 Vapor Hydration Testing / Environmental Corrosion Studies

Using VHT, many different single, dual, and multiphase systems were investigated. To begin, in almost all systems, except the dual phase system that had an experimental error, saw Cs rich phases leached out and deposited onto the surface of the samples. The most commonly seen was a Cs-Ti-Al-O phase after VHT, in single and multiphase samples. In conclusion, it appears that regardless of single or multiphase systems, Cs retention in waste forms are similar. It could also be deduced that even different compositions of hollandites produce similar Cs phases, seen in the multiphase and even when comparing the single phase Fe hollandites to the single phase Ga hollandites.

Future work for VHT includes more work on dual phase systems, being a large gap in the available literature. The idea that Cs retention is similar in single and multiphase systems should also be further tested by performing VHT on systems with varying Ba to Cs ratios.

6.3 Product Consistency Testing

The results from PCT of the dual phase system of $Ba_{.667}Cs_{.667}Ga_2Ti_6O_{16}$ hollandite and Nd titanate show as the volume fraction of hollandite increases, the less dissolution that occurs. This means that as the volume fraction of hollandite in a multiphase is decreased, the stability of the hollandite is increased. The results from the $Ba_{1.04}Cs_{0.24}Ga_{2.32}Ti_{5.68}O_{16}$ and Nd titanate dual phase systems does not show the same trend, however it is difficult to make any conclusions from this data due to the large amounts of secondary phases that formed in these systems.

Future work with PCT includes more testing with different dual phase systems with varying Cs content in the hollandite structure and dual phase systems with different hollandite dopants, such as Fe, Zn, Cr, etc… Varying the different dual phase systems, such as doped pyrochlores and zirconolites would be important as hollandite is constantly in contact with them in the multiphase systems.

REFERENCES

[1] *South Carolina: State Profile and Energy Estimates*, *U.S. Energy Inf. Adm.*, (2016).

[2] *On Site Storage of Nuclear Waste*, *N.E.I.*, (n.d.).

[3] L. Lerner, *Nuclear fuel recycling could offer plentiful energy*, *Argonne Natl. Lab.*, (2012).

[4] L. Brasse (INL), E.W. May (INL), and INL Systems Analyses, *Material Recovery & Waste Form Development 2015 Accomplishments*. 2015.

[5] C. Kim, J. Park, and T. Hwang, "Analysis of Leaching Behavior of Simulated LILW Glasses by Using the MCC-1 Test Method," *J. Nucl. Sci. Technol.*, **48** [7] 1108–1114 (2011).

[6] J. Marra (WSRC/SRTC) and W. Ebert (ANL), *Accounting for a Witrified Plutonium Waste Form in the YUCCA Mountain Repository Total System Performance Assessment (TSPA)*. 2003.

[7] J.H. Christian, *Crystallization in High-Level Waste Glass : A Review of Glass Theory and Noteworthy Literature*. 2015.

[8] K.L. Smith, G.R. Lumpkin, M.G. Blackford, R.A. Day, and K.P. Hart, *The durability of synroc*, *J. Nucl. Mater.*, **190** 287–294 (1992).

[9] B.M. Clark, P. Tumurugoti, S.K. Sundaram, J.W. Amoroso, J.C. Marra, and K.S. Brinkman, "Microstructures of Melt Processed and Spark Plasma Sintered Ceramic Waste Forms," *Metall. Mater. Trans.*, **1E** [Number 4] 341–348 (2014).

[10] A.E. Ringwood, V.M. Oversby, and S.E. Kesson, *Immobilization of high-level nuclear reactor wastes in SYNROC: A current appraisal*, *Nucl. Chem. Waste Manag.*, **2** [4] 287–305 (1981).

[11] K.S. Brinkman, K.M. Fox, J.C. Marra, and M. Tang, *Crystalline Ceramic Waste Forms : Reference Formulation Report*. 2012.

[12] L.H. Brixner, "Preparation + Properties of Ln2ti2o7-Type Rare Earth Titanates," *Inorg. Chem.*, **3** [7] 1065- (1964).

[13] G.C. Lau, B.D. Muegge, T.M. McQueen, E.L. Duncan, and R.J. Cava, "Stuffed rare earth pyrochlore solid solutions," *J. Solid State Chem.*, **179** [10] 3126–3135 (2006).

[14] L.G. Shcherbakova, L.G. Mamsurova, and G.E. Sukhanova, "Lanthanide Titanates," *Russ. Chem. Rev.*, **48** [3] 228–242 (2007).

[15] T.T. Zhang, K.W. Li, J. Zeng, Y.L. Wang, X.M. Song, and H. Wang, "Synthesis and structural characterization of a series of lanthanide stannate pyrochlores," *J. Phys. Chem. Solids*, **69** [11] 2845–2851 (2008).

[16] J.M. Farmer, L.A. Boatner, B.C. Chakoumakos, M.H. Du, M.J. Lance, C.J. Rawn, and J.C. Bryan, "Structural and crystal chemical properties of rare-earth titanate pyrochlores," *J. Alloys Compd.*, **605** 63–70 (2014).

[17] D.R. Modeshia and R.I. Walton, "Solvothermal synthesis of perovskites and pyrochlores: crystallisation of functional oxides under mild conditions.," *Chem. Soc. Rev.*, **39** [11] 4303–4325 (2010).

[18] D.A. Crandles, "The Optical Properties of RTiO3 Perovskites (R=LA, CE, PR, ND, SM,GD);" McMaster University, 1992.

[19] V. Aubin-Chevaldonnet, D. Caurant, a. Dannoux, D. Gourier, T. Charpentier, L. Mazerolles, and T. Advocat, "Preparation and characterization of (Ba,Cs)(M,Ti)8O16 (M = Al3+, Fe3+, Ga3+, Cr3+, Sc3+, Mg2+) hollandite ceramics developed for radioactive cesium immobilization," *J. Nucl. Mater.*, **366** [1–2] 137–160 (2007).

[20] Y. Xu, Y. Wen, R. Grote, J. Amoroso, L.S. Nickles, and K.S. Brinkman, "A-site compositional effects in Ga-doped hollandite materials of the form Ba x Cs y Ga 2x + y Ti 8 − 2x − y O 16 : implications for Cs immobilization in crystalline ceramic waste forms," *Nat. Publ. Gr.*, [May] 1–8 (2016).

[21] S.E. Kesson, W.J. Sinclair, and a. E. Ringwood, "Solid solution limits in SYNROC zirconolite," *Nucl. Chem. Waste Manag.*, **4** [3] 259–265 (1983).

[22] E.C. Buck, B. Ebbinghaus, A.J. Bakel, and J.K. Bates, *Characterization of a Pu-Bearing Zirconolite-Rich SYNROC*. Boston, MA, 1996.

[23] E.R. Vance and D.K. Agrawal, "Incorporation in Crystalline of Radionuclides Titanates," **3** 229–234 (1983).

[24] M.A. Subramanian, G. Aravamudan, and G.V. Subba Rao, *Oxide pyrochlores — A review*, *Prog. Solid State Chem.*, **15** [2] 55–143 (1983).

[25] a. Jiřička, J.D. Vienna, P. Hrma, and D.M. Strachan, "The effect of experimental conditions and evaluation techniques on the alteration of low activity glasses by vapor hydration," *J. Non. Cryst. Solids*, **292** [1–3] 25–43 (2001).

[26] J.S. Luo, W.L. Ebert, J.J. Mazer, and J.K. Bates, *Simulation of Natural Corrosion by Vapor Hydration test: Seven-year Results*. Argonne, IL, 1996.

[27] T.E. Kiess and S.H. Hanauer, "Yucca Mountain Project Status," *MRS Proc.*, **757** (2002).

[28] R.L. Schulz, K.G. Brown, T.H. Lorier, and J.D.V.B.M. Jorgensen, "Hanford Immobilized LAW Product Acceptance : Tanks Focus Area Testing Data Package II," [September] (2000).

[29] J. Neeway, A. Abdelouas, B. Grambow, S. Schumacher, C. Martin, M. Kogawa, S. Utsunomiya, S. Gin, *et al.*, "Vapor hydration of SON68 glass from 90 °c to 200 °c: A kinetic study and corrosion products investigation," *J. Non. Cryst. Solids*, **358** [21] 2894–2905 (2012).

[30] V.H. Test, "Standard Test Method for Measuring Waste Glass or Glass Ceramic Durability by Vapor Hydration Test 1," *ASTM Int.*, **C1663**-**9** 1–16 (2014).

[31] W.L. Bourcier, "Interim Report on Development of a Model to Predict Dissolution Behavior of the Titanate Waste Form in a Repository and Compilation of Data from SPFT

Ceramic Dissolution Tests," (1999).

[32] ASTM C1285-02, "Standard Test Methods for Determining Chemical Durability of Nuclear, Hazardous , and Mixed Waste Glasses and Multiphase Glass Ceramics : The Product Consistency Test (PCT)1," *ASTM, Conshohocken, USA, 2002*, **15** 1–26 (2002).

[33] M.L. Carter, E.R. Vance, D.R.G. Mitchell, J. V. Hanna, Z. Zhang, and E. Loi, "Fabrication, characterization, and leach testing of hollandite, (Ba,Cs)(Al,Ti)$_2$Ti$_6$O16," *J. Mater. Res.*, **17** [January] 2578–2589 (2002).

[34] M. James, M.L. Carter, Z. Zhang, Y. Zhang, K.S. Wallwork, M. Avdeev, and E.R. Vancez, "Crystal chemistry and structures of (Ca,U)titanate pyrochlores," *J. Am. Ceram. Soc.*, **93** [10] 3464–3473 (2010).

[35] K.S. Brinkman, K.M. Fox, and M. Tang, *Development of Crystalline Ceramics for Immobilization of Advanced Fuel Cycle Reprocessing Wastes*. 2011.

[36] A.L. Billings, K.S. Brinkman, K.M. Fox, J.C. Marra, M. Tang, and K.E. Sickafus, *Preliminary Study of Ceramics for Immobilization of Advanced Fuel Cycle Reprocessing Wastes*. 2010.

[37] K.S. Brinkman, J.W. Amoroso, J.C. Marra, and M. Tang, "Crystalline Ceramic Waste Forms : Comparison of Reference Process for Ceramic Waste Form Fabrication," (2013).

[38] J.W. Amoroso, J.C. Marra, S.D. Conradson, M. Tang, and K.S. Brinkman, "Melt Processed Single Phase Hollandite Waste forms for Nuclear Waste Immobilization: Ba1.0Cs0.3A2.3Ti5.7O16; A = Cr, Fe, Al," *J. Alloys Compd.*, **584** 590–599 (2014).

[39] J.W. Amoroso, J.C. Marra, M. Tang, Y. Lin, F. Chen, D. Su, and K.S. Brinkman, "Melt Processed Multiphase Ceramic Waste forms for Nuclear Waste Immobilization," *J. Nucl. Mater.*, **454** [1–3] 12–21 (2014).

[40] J.V. Crum, B.J. Riley, L.R. Turo, M. Tang, and A. Kossoy, *Summary Report : Glass-Ceramic Waste Forms for Combined Fission Products*. 2011.

[41] M.L. Carter, A.L. Gillen, K. Olufson, and E.R. Vance, "HIPed Tailored Hollandite Waste Forms for the Immobilization of Radioactive Cs and Sr," *J. Am. Ceram. Soc.*, **92** 1112–1117 (2009).

[42] A. Preuss and R. Gruehn, *Preparation and Structure of Cerium Titanates Ce2TiO5, Ce2TiO7, and Ce4Ti9O24*, *J. Solid State Chem.*, **110** [2] 363–369 (1994).

[43] R.S. Roth, T. Negas, H.S. Parker, D.B. Minor, and C. Jones, "Crystal Chemistry of Cerium Titanates, Tantalates and Niobates," *Mat. Res. Bull.*, **12** [2] 1173–1182 (1977).

[44] V. Valeš, L. Matějová, Z. Matěj, T. Brunátová, and V. Holý, "Crystallization kinetics study of cerium titanate CeTi2O6," *J. Phys. Chem. Solids*, **75** [2] 265–270 (2014).

[45] Y. Lin, S. Fang, D. Su, K.S. Brinkman, and F. Chen, "Enhancing grain boundary ionic conductivity in mixed ionic-electronic conductors," *Nat. Commun.*, **6** 1–9 (2015).

[46] T. Suzuki-Muresan, J. Vandenborre, a. Abdelouas, B. Grambow, and S. Utsunomiya,

"Studies of (Cs,Ba)-hollandite dissolution under gamma irradiation at 95°C and at pH 2.5, 4.4 and 8.6," *J. Nucl. Mater.*, **419** [1–3] 281–290 (2011).

47 F. Angeli, P. McGlinn, and P. Frugier, "Chemical durability of hollandite ceramic for conditioning cesium," *J. Nucl. Mater.*, **380** [1–3] 59–69 (2008).

48 L.L. Hench, D.E. Clark, and J. Campbell, "High Level Waste Immobilization Forms," *Nucl. Chem. Waste Manag.*, 149–173 (1984).